Title

Mechanosensitive β-Catenin Signaling Modulates Mesenchymal Stem Cell Chondrogenesis

Permalink

https://escholarship.org/uc/item/26z9t3fg

Author

Statman, Lauren Yael

Publication Date

2012

Peer reviewed|Thesis/dissertation

Mechanosensitive β-Catenin Signaling

Modulates Mesenchymal Stem Cell Chondrogenesis

by

Lauren Yael Statman

DISSERTATION

Submitted in partial satisfaction of the requirements for the degree of

DOCTOR OF PHILOSOPHY

in

Bioengineering

in the

GRADUATE DIVISION

of the

UNIVERSITY OF CALIFORNIA, SAN FRANCISCO

AND

UNIVERSITY OF CALIFORNIA, BERKELEY

Mechanosensitive β-Catenin Signaling

Modulates Mesenchymal Stem Cell Chondrogenesis

Lauren Yael Statman

Abstract

Bone marrow-derived mesenchymal stem cells are a promising source of cells for cartilage regeneration therapies due to their ease of isolation and capacity to differentiate into cells resembling articular chondrocytes. However, the current differentiation protocols result in the development of additional phenotypic features, common to hypertrophic and osteoarthritic chondrocytes, which are undesirable in the context of articular cartilage repair. In this work we investigated the roles of cyclic hydrostatic pressure and canonical Wnt/β-catenin signaling in regulating the phenotype of chondrogenic MSCs. We used a standard chemically defined medium containing TGF-β to induce chondrogenic differentiation in pellets of human MSCs. Hydrostatic pressure was applied using a custom-built loading chamber. β-catenin signaling was modified using small molecules; XAV939 for inhibition and CHIR99021 for stimulation. The chondrogenic MSCs in this culture system resembled osteoarthritic chondrocytes, co-expressing features of both articular and hypertrophic chondrocytes. Cyclic hydrostatic pressure favored a modest shift in the phenotypic balance away from hypertrophy and toward chondrogenesis. In addition, cyclic hydrostatic pressure inhibited intracellular signaling via the ERK1/2 and canonical Wnt/β-catenin pathways. Inhibition of β-catenin signaling with XAV939 significantly augmented chondrogenesis and inhibited hypertrophy, suggesting that this may be a potential mechanism by which hydrostatic

pressure is transduced in MSCs. Stimulation of β-catenin with CHIR99021, inhibited both types of chondrogenic differentiation. Our results indicate that β-catenin is an attractive target for phenotypic modulation of chondrogenic MSCs, and has potential applications in cartilage regeneration therapies from tissue engineering to targeted drug delivery to gene therapy.

Table of Contents

<u>List of Tables</u>

List of Figures

Chapter 1 Introduction

1.1 Mesenchymal Stem Cells and Potential Applications in Cartilage Repair Therapies

Mesenchymal stem cells (MSCs), like other stem cell types, have tremendous promise in tissue engineering and regenerative medicine applications. Due to their ability to differentiate into cells of different skeletal lineages, they represent an abundant cell source for repair of skeletal tissues ravaged by disease. MSCs are tissue culture plastic-adherent cells capable of differentiation into osteoblasts, adipocytes, and chondrocytes [1, 2]. MSCs were first isolated from bone marrow as cells that form fibroblastic colonies (CFU-Fs) and have osteogenic potential [3]. Later, the osteogenic, adipogenic, and chondrogenic differentiation capacities of MSCs were definitively demonstrated [2]. Since their initial discovery, MSCs have been isolated from a variety of tissues including adipose tissue [4], skeletal muscle [5], synovium [6], dental pulp [7], and umbilical cord [8], and have been reported to differentiate into cells of smooth muscle, skeletal muscle, tendon, endothelial, epithelial, and neural lineages [9]. Many cell surface antigens have been proposed for purifying MSCs from various tissues including different combinations of Stro-1, SH2, SH3, SH4, CD29, CD44, CD71, CD73, CD90, CD105, CD106, CD120a, CD124, CD146, CD200, and CD271 [1, 2, 9, 10]. Negative markers include endothelial and hematopoietic markers such as CD45, CD34, CD14, CD79α, or HLA-DR [1, 2, 9, 11]. Unfortunately, there is no consensus as to which combination of markers represents a true MSC, or which tissue might contain the best MSC population. In this work MSCs

were isolated from bone marrow, selected by tissue culture plastic adherence, and validated by demonstration of trilineage differentiation capacity.

Characterization of bone marrow-derived MSCs demonstrates population heterogeneity with both undifferentiated progenitors and lineage-committed precursors among the plastic adherent cells. While groups of plastic adherent cells are capable of osteogenesis, adipogenesis, and chondrogenesis, individual MSCs may or may not be capable of trilineage differentiation. In one study, when cells from individual CFU-Fs were assessed for their differentiation capacity, most were capable of osteogenic and adipogenic differentiation, and only a small portion were capable of chondrogenic differentiation [2]. Another study showed that while nearly all MSC clones could go differentiate into osteoblasts, 60-80% could become either osteoblasts or chondrocytes, and only about 30% demonstrated trilineage potential [12]. MSC heterogeneity is, therefore, a significant limitation of this and other MSC-based research. In addition to the heterogeneous character of MSC populations, MSCs possess some degree of differentiation plasticity. MSC-derived osteoblasts can be transdifferentiated into adipocytes and chondrocytes under specific culture conditions [13]. MSC-derived adipocytes and chondrocytes can transdifferentiate to the other two lineages as well [13]. Thus, another limitation of MSCs is the instability of their differentiated phenotype. While MSCs are capable of some degree of self-renewal, these other characteristics distinguish MSCs from true stem cells. Other names have been proposed including "mesenchymal stromal cells," "multipotent stromal cells," "mesenchymal progenitor cells," and "skeletal stem cells," although "mesenchymal stem cell" continues to be the most widely used [9].

Despite the limitations of MSCs, these cells are important for their potential to repair tissue damage caused by trauma or disease. Since MSCs can differentiate into chondrocytes, they may be able to contribute to articular cartilage regeneration. However, while endogenous MSCs reside in nearby connective tissues *in vivo*, cartilage has a limited healing capacity. Instead, damage caused by wear or traumatic injury nearly always progresses to osteoarthritis (OA). The Centers for Disease Control and Prevention reports that arthritis afflicts nearly 50 million individuals over the age of 18, and costs upwards of 128 billion dollars annually [14, 15]. OA accounts for more than 50% of all diagnosed cases of arthritis [16]. End-stage OA is typically treated with total joint replacement, which has a limited lifetime and does not fully restore joint function [17]. Focal cartilage defects can be treated with microfracture of the subchondral bone, osteochondral grafts, or autologous chondrocyte implantation aimed at regenerating tissue at the site of injury. Such therapies provide some measure of pain relief, although the tissue formed tends to be inferior fibrocartilage rather than true articular cartilage, and successes come at the expense of the subchondral bone or donor cartilage [18].

If the chondrogenic capacity of MSCs could be channeled to engineer cartilage grafts *in vitro* or regenerate cartilage *in vivo*, it would address many of the drawbacks linked to the current treatments. In addition to their chondrogenic potential, MSCs can be expanded *in vitro*, providing high cell numbers with limited donor site morbidity, although their differentiation capacity decreases with increasing passage number. MSCs also lack MHC class II cell surface markers, making them virtually undetectable by the immune system, and they secrete factors that support wound healing [19]. Therefore, MSCs are an attractive cell candidate for cell-based cartilage regeneration strategies. The

success of such repair strategies will depend on the quality of tissue generated by the MSCs. In the next section, the structure and function of articular cartilage will be discussed and compared with the tissue obtained through MSC chondrogenesis.

1.2 Articular Cartilage and MSC Chondrogenesis

Articular cartilage is the tissue covering the articulating surfaces in diarthrodial joints. It is a smooth, glistening tissue that supports near frictionless motion and mechanical loads within the joint [20]. Articular cartilage is avascular and aneural, and its major components are water, collagen, proteoglycans (PGs), and cells; water accounts for 60-85% of tissue wet weight, collagen for 10-30%, PGs for 3-10%, and cells for less than 5%. The main type of collagen in articular cartilage is type II collagen (Col2). Col2 is a homotrimer of three α1(II) protein chains that form a helix, and many Col2 molecules polymerize to form a fibril network with the assistance of cartilage oligomeric matrix protein (COMP) and type XI collagen (Col11). Minor collagens in the fibril network include types III (Col3), VI (Col6), IX (Col9), XII (Col12), and XIV (Col14). The primary PG in articular cartilage is aggrecan, which consists of a core protein modified along its length with the sulfated glycosaminoglycans (GAGs) chondroitin sulfate and keratan sulfate. Many aggrecan molecules bind to hyaluronan with link protein to form large aggregates embedded with Col2 fibrils. Other matrix PGs include biglycan, decorin, fibromodulin, lumican, perlecan, and versican. The cells in articular cartilage are chondrocytes, which are isolated from each other in lacunae throughout the tissue and are responsible for maintenance of the surrounding tissue. Adult chondrocytes are relatively inactive metabolically, but they produce and secrete the collagens and PGs of the

4

extracellular matrix and the enzymes required to remodel healthy tissue and degrade damaged tissue.

The organization of its various matrix components varies through the depth of articular cartilage [21, 22]. Col2 content decreases from the superficial zone at the joint surface through the middle zone and deep zone, while aggrecan increases through these layers. In the superficial zone, thin collagen fibrils are arranged parallel to the joint surface with very little aggrecan and higher levels of Col1. The chondrocytes in this zone are flattened with a fibroblastic appearance and secrete lubricin to facilitate joint articulation. In the middle zone, round chondrocytes are sparsely embedded in the extracellular matrix. Aggrecan content is increased and the Col2 fibrils are thicker and randomly oriented. In the deep zone, aggrecan content increases even more and the thickest Col2 fibrils are oriented perpendicular to the articular surface. The chondrocytes are still round and are arranged in columns. Below the deep zone, the tidemark delineates the beginning of the calcified cartilage. In the calcified cartilage the structural organization remains the same, but with depleted aggrecan levels and with a mineral content of 65% [23]. The chondrocytes in the calcified cartilage exist in uncalcified lacunae and express type X collagen (Col10) and alkaline phosphatase (ALP) [23-25]. Blood vessels from the subchondral bone invade the calcified cartilage, but the mineral prevents diffusion of soluble factors from the subchondral bone across the tidemark [23, 26].

When it is said that MSCs are able to differentiate into chondrocytes, it means that MSCs can develop into the kind of cells that populate articular cartilage. The degree of MSC chondrogenesis depends on the culture conditions. It has long been known that

5

maintenance of the chondrocyte phenotype requires a three dimensional culture system [27]. Not only do chondrocytes dedifferentiate in monolayer culture, but they largely lose their chondrocyte differentiation capacity, suggesting that physical factors such as cell shape are essential to regulating the chondrocyte phenotype [18, 27]. Therefore, MSC chondrogenesis commonly employs 3D culture configurations to promote differentiation. In the "pellet" culture system, suspensions of MSCs are centrifuged to form cellular aggregates [28-31]. MSCs have also been suspended in various polymer solutions and polymerized to yield a gel laden with MSCs, or seeded directly onto fibrous polymer scaffolds [32-37]. Choosing a 3D culture system involves consideration of other factors that might regulate chondrogenesis. For example, pellet cultures have high numbers of cell-cell contacts as in developing cartilage, whereas gels isolate individual cells as in adult cartilage. Gels allow for high oxygen and nutrient diffusion which is important for cell metabolism and is more limited in dense pellet culture, but hypoxic conditions might favor chondrogenesis [38]. With a scaffold, the initial mechanical properties can be controlled, and substrate stiffness has been shown to influence cell fate [39]. Thus, selecting a culture configuration involves prioritizing these factors. In this work we employed a pellet culture system, which recapitulates the high cell density essential to developmental chondrogenesis.

Three dimensional culture alone is not sufficient to induce MSC chondrogenesis. In the above culture systems, chondrogenesis is induced by culturing the MSCs in chemically defined medium containing growth factors that promote differentiation. Chondrogenic medium (CM) formulations vary slightly, but typically consist of basal medium supplemented with insulin/transferrin/selenium (ITS), ascorbate, pyruvate,

6

proline, dexamethasone, and a transforming growth factor (TGF)-β-family growth factor [40]. Unlike other differentiation media, CM is well defined because it is typically serum-free. Finally, extrinsic mechanical conditioning has been used to enhance chondrogenesis by mimicking the physical environment of native cartilage [41].

Successful chondrogenic induction of MSCs is characterized by the presence of an extracellular matrix rich in aggrecan and Col2. Histological staining with toluidine blue [28-30], Alcian blue [31, 36, 37, 42], and Safranin O [30, 33, 42, 43] has demonstrated extensive GAG deposition in sections of MSC-derived chondrogenic tissue. Immunohistochemistry using Col2 antibodies has revealed Col2 accumulation as well [28, 31, 35, 43]. GAG and collagen increases have been quantified by enzymatically digesting the MSC tissue and measuring radio-labeled sulfate incorporation [29, 36], dimethylmethylene blue dye binding [29, 32, 33, 36], and hydroxyproline content [33, 42]. Other matrix molecules including versican, biglycan, decorin, link protein, fibromodulin, and COMP are present in MSC-derived cartilage [29, 36]. In addition to the similar extracellular matrix composition, when MSCs differentiate into chondrocytes, they assume a transcriptional profile similar to that of articular chondrocytes. Increases in cartilage specific genes encoding the cartilage specific transcription factor Sox9 (*Sox9*) [30, 35, 37], and matrix proteins Col2 (*Col2a1*) [28-30, 32, 33, 35-37], aggrecan (*Acan*) [29, 30, 33, 35-37], Col9 [30, 33, 36], Col11 [30, 36] and COMP (*COMP*) [29, 30, 33, 35] have been demonstrated in quantitative real time reverse transcription-polymerase chain reaction, microarray analyses, and by *in situ* hybridization. While numerous cartilage components have been found in chondrogenic MSC tissue, the benchmark for confirming chondrogenesis in this work is the presence of GAG by dye-binding and Col2

by immunohistochemistry, and increased expression of *Sox9*, *Col2*, and *Acan* via quantitative RT-PCR.

Chondrogenic MSCs also exhibit additional features that are not found in articular cartilage, but rather during endochondral ossification and osteoarthritic degradation. MSCs have trilineage differentiation capacity, but under chondrogenic conditions do not mineralize or accumulate lipids, markers of osteogenic and adipogenic differentiation, respectively [2, 37]. However, chondrogenic MSC cultures do exhibit increased deposition of Col10 [29, 44-47], increased secretion of matrix metalloproteinase 13 (MMP13) [48], and increased ALP activity [28, 44-48]. *Col10* [28-32, 37, 44, 46], *MMP13* [44, 46, 48], and *ALP* transcription are increased as well [2]. Further, upon subcutaneous implantation in immunodeficient mice, these chondrogenic MSCs undergo vascular invasion and calcification [44-46]. Though these are decidedly un-articular features, they are not foreign to chondrocytes having been described above in the calcified cartilage. In addition, when articular cartilage becomes osteoarthritic, inflammation and tissue degradation is accompanied by vascularization and tissue mineralization [49, 50]. Even healthy cartilage is subject to such changes. In addition to the permanent chondrocytes that populate articular cartilage, temporary chondrocytes in the growth plate mature during the process of endochondral ossification in service of long bone growth. These chondrocytes express markers of terminal differentiation—Col10, MMP13, and ALP—before they undergo matrix mineralization, vascular invasion, and programmed cell death. The phenotype observed in osteoarthritic chondrocytes may result from an aberrant endochondral ossification program.

While markers of terminal differentiation, the endpoint of endochondral ossification, are expressed in the natural course of development, they are undesirable in the context of articular cartilage repair, which necessitates the elimination of a terminal and/or osteoarthritic phenotype. In order to optimize the phenotype of chondrogenic MSCs, it is necessary to manipulate the chondrogenic culture conditions. However, it is unknown how various intrinsic and environmental factors interact to control MSC differentiation and which ones might be the best targets. Biology serves as a rich source of inspiration in this case. Since chondrogenic MSCs at times resemble developing chondrocytes, articular chondrocytes, maturing growth plate chondrocytes, and osteoarthritic chondrocytes, the mechanisms governing these processes are essential to understanding regulation of the MSC-derived chondrocyte phenotype and identifying opportunities for manipulation. In the next section, mechanical regulation of articular chondrocytes will be discussed. Following that, the molecular mechanisms regulating developmental chondrogenesis, chondrocyte maturation and endochondral ossification, and OA will be surveyed in search of common pathways that are potential targets for intervention.

1.3 Chondrocyte Mechanotransduction

Articular chondrocyte function is regulated by mechanical forces. The matrix composition and structure of articular cartilage dictates its mechanical properties. Physical forces and the mechanical properties of the tissue together define the mechanical environment of the chondrocytes within the tissue. In turn, the chondrocytes remodel the tissue in order to adapt to applied mechanical loads. The collagen and PG content of the

tissue is increased in areas of greater loading to support those loads [51, 52]. The chondrocytes in load bearing regions sense the higher loads and respond by synthesizing more matrix molecules [53-55]. In damaged osteoarthritic cartilage not only do the altered tissue mechanics render the tissue unable to support loads, but may contribute to chondrocyte deregulation by decoupling the chondrocytes from their normal loading environment. As described earlier, articular cartilage is composed primarily of water, Col2, aggrecan, and chondrocytes. This can be thought of as chondrocytes dwelling in a biphasic matrix with a fluid phase and solid phase, which together give rise to cartilage's viscoelastic behavior [56].

The solid phase of cartilage is composed of sulfated PGs and collagen. Aggrecan and other sulfated PGs are responsible for regulating tissue swelling due to their high density of negative charges known as the fixed charge density (FCD) of cartilage [20]. The negative charges on the sulfated GAG chains are spaced closely enough to give rise to repulsion forces, pushing the PGs away from each other. Furthermore, the negative FCD attracts positive counter ions to restore tissue electroneutrality. The counter ions mitigate swelling due to repulsion forces, but they increase the osmolarity relative to the surrounding fluid, which draws in more water to maintain osmotic equilibrium. The stable triple helix structure of Col2 has great tensile strength and traps the PGs in its network. The boundaries of the tissue are thus defined by the balance between the swelling forces of the PGs and the tensile resistance of Col2. At rest, these opposing forces gives rise to a basal hydrostatic pressure in the tissue is about 0.2 MPa due to these forces [57].

Both the solid and fluid phases determine how cartilage responds to joint loading. Compressive forces and fluid shear in cartilage arise from contact between opposing joint surfaces. Matrix compression causes fluid to flow out of the cartilage surface resulting in direct and lateral deformation of the superficial zone of cartilage as the solid matrix is compacted. However, only 1-5% of the fluid is lost during normal gait while the rest remains in the tissue [57]. Rapid deformation of the solid phase during normal gait lowers the permeability of cartilage, resisting fluid flow. The trapped fluid in the middle and deep zones of cartilage becomes pressurized at 5-15 MPa [58, 59]. Because the fluid phase is virtually incompressible, the solid phase is not deformed under hydrostatic pressure. When the compressive force is removed, the hydrostatic pressure in the lower zones of cartilage is relieved, the superficial zone resumes its original shape, and the fluid returns to the tissue. If, however, a static load is sustained, a larger volume of fluid would be exuded from the tissue over time leading to deformation in these lower cartilage zones as forces are transferred to the solid matrix. This behavior is the typical creep behavior of a viscoelastic material.

In addition to basal swelling pressure, chondrocytes embedded in the cartilage matrix experience deformation, fluid flow, and high levels of hydrostatic pressure during joint loading. In the superficial layer, the chondrocytes are exposed to fluid flow upon fluid exudation, and when the solid matrix is compacted the chondrocytes are exposed to compressive, tensile, and shear forces [59]. Under compression and tension, the chondrocytes experience changes in shape and volume, while shear causes deformation, but no volume change. In the middle and deep zones, hydrostatic pressure predominates and shields those chondrocytes from both deformation and volume changes. All of these

forces have been shown to alter chondrocyte metabolism, and some examples are listed in Table 1-1. Notably, static or excessively high loads decrease matrix synthesis, but physiological levels of dynamic loads favor synthesis of cartilage-specific extracellular matrix components [59-61]. Thus, these mechanical cues are an additional factor that regulates chondrogenesis. Physiological levels of the forces found in cartilage promote chondrogenesis of MSCs [62], so in this work we focused on the effects of physiological levels of hydrostatic pressure.

The conversion of physical forces into biological signals occurs through the process of mechanotransduction. The exact mechanism by which this occurs is not entirely resolved, but likely involves the cytoskeleton. The microfilaments, intermediate filaments, and microtubules that compose the cytoskeleton are coupled to their external environment by adhesion molecules [63]. These focal adhesions are home to signaling proteins including focal adhesion kinases and extracellular signal-regulated protein kinases, and the downstream effectors Rho, caveolin-1, G-proteins, and protein kinase A [64]. In addition, other intracellular regulatory proteins can be immobilized along the length of a cytoskeletal filament. Application of mechanical stresses results in rearrangement of the cytoskeletal components and alters the connections between the cytoskeleton and associated molecules. Affected molecules may be activated by their release or shape change and initiate a signaling response. The importance of the cytoskeleton as a regulator of chondrocyte phenotype is best illustrated in monolayer culture. When chondrocytes spread out in monolayer culture they dedifferentiate, but disruption of the actin cytoskeleton causes them to round up and resume production of Col2 and GAGs [65]. The actin cytoskeleton in flattened cells may repress pro-

Table 1-1: Effects of Mechanical Loading on Chondrocytes

Cells	Force	Loading Regime	Effect	Reference
Cartilage explants	Compression	50% strain, 24 hours	Decreased *Acan*, *Col2a1*, Decreased [^{35}S]sulfate and [^{3}H]proline incorporation	[66]
Cartilage explants	Compression	30-50% strain, 5 minutes	Increased apoptosis, sGAG release	[67]
Chondrocytes in collagen gels	Compression	Up to 50% strain, 24 hours	Decreased [^{35}S]sulfate and [^{3}H]proline incorporation	[68]
Cartilage explants	Compression	1-20% strain, 0.01-1 Hz	Increased [^{35}S]sulfate and [^{3}H]proline incorporation	[53]
Chondrocytes in agarose	Compression	15% strain, 1 Hz, 48 hours	Increased GAG synthesis; Increased [^{3}H]thymidine incorporation	[69]
Chondrocytes in agarose	Compression	10% strain, 1 Hz, 5 hours/day, 28 days	Increased sGAG and hydroxyproline content	[70]
Chondrocytes in agarose	Compression	10% strain, 1-3 Hz, 1-3 hours	Increased Aggrecan promoter acitivity; Decrased Col2a1 promoter activity	[71]
High density chondrocyte construct	Fluid shear	1 dyne/cm^2, 3 days	Increased Col2	[72]
Cartilage explants	Fluid shear	150 mm Hg, 2.5 Hz, 10 days	Increased [^{35}S]sulfate incorporation and sGAG deposition	[73]
Monolayer chondrocytes	Fluid shear	1.6 Pa rotating, 24-72 hours	Increased sGAG	[74]
Monolayer chondrocytes	Fluid shear	1.6 Pa rotating, 1 day	Decreased Col2a1, Increased apoptosis	[75]
Chondrocytes in agarose	Hydrostatic pressure	5 MPa, 4 hours	Increased *Acan* and *Col2a1*	[76]
Cartilage explants	Hydrostatic pressure	5 MPa, 0.5 Hz, 1.5 hours	Increased [^{35}S]sulfate incorporation; Inhibition at lower frequencies	[77]
Monolayer chondrocytes or pellets	Hydrostatic pressure	10 MPa, 1 Hz, 4 hours/day	Increased *Acan* and *Col2a1* after 4 days	[78]
Monolayer chondrocytes	Hydrostatic pressure	5-10 MPa, 1 Hz, 4 hours	Increased *Acan* and *Col2a1* after 4 days	[79]
Monolayer chondrocytes	Hydrostatic pressure	5/10 MPa, 1 Hz, 4 hours, 4 days	Increased *Acan*, *Col2a1*, Aggrecan, Col2	[75]

chondrogenic signals, while the rounded cytoskeleton supports them. Many mechanosensitive elements have been described in chondrocytes that interact with the regulatory transcription factors and signaling pathways that will be discussed below [80], and the mechanotransduction of hydrostatic pressure will be discussed in more detail in Chapter 4.

1.4 Developmental Chondrogenesis

Chondrocytes first appear during embryonic skeletal development. Limb formation begins with the clustering of prechondrogenic mesenchymal cells into a precartilage mesenchymal condensation with high numbers of cell-cell contacts [81-87]. The mesenchymal cells then differentiate into chondrocytes secreting the characteristic extracellular matrix of Col2 and aggrecan [88, 89]. As the matrix is elaborated around them, individual chondrocytes are pushed away from each other to yield the skeletal anlagen, a cartilaginous structure containing discrete chondrocytes that serves as a template for the developing skeleton [81-86]. Ultimately, the anlagen is lengthened by chondrocyte maturation and turned into bone through the process of endochondral ossification. Chondrocytes remain only in the articulating surfaces at the ends of the bone and, temporarily, in the growth plate where they continue the process of skeletal elongation until the growth plate fuses during puberty. While most of the chondrocytes in the anlagen die during the process of endochondral ossification, the mechanisms that control their initial differentiation are essential to understanding chondrocyte regulation and MSC chondrogenesis.

Developmental chondrogenesis is characterized by alterations in cellular morphology, extracellular matrix content, and the gene expression profiles of the differentiating mesenchymal cells. Morphologically, undifferentiated cells display multiple cellular processes [85], and produce a matrix of type I collagen (Col1) [89, 90], fibronectin [90, 91], hyaluronic acid [92], and mesenchyme-specific PGs [93]. During condensation, the cells become rounded and cluster together, while the extracellular matrix is pushed outward. The condensed cells begin expressing *Col2a1* [94] and *Acan*

[89], and decrease expression of *Col1* [94], which becomes confined to the perichondrium. These transcriptional changes correspond spatially and temporally with increased deposition of a cartilage-specific extracellular matrix containing Col2 [90, 95] and aggrecan [89]. Other matrix components produced by neo-chondrogenic cells include Col9, Col11, COMP, link protein, and other PGs, which are also found in mature articular cartilage [21, 96-98].

The role of mesenchymal condensation in the subsequent chondrogenesis of mesenchymal cells has been studied in micromass cultures of embryonic limb bud cells that recapitulate the condensation-chondrogenesis sequence observed *in vivo* [99, 100]. Increasing the density of the micromass correlates with greater overall chondrogenesis [95, 99-102]. Enhancement or disruption of micromass condensation via modulation of cell adhesion proteins results in improved or inhibited chondrogenesis, respectively [103-108]. The simplest explanation is that a larger condensation represents a greater number of cells committed to a chondrogenic lineage, but condensation may also aid lineage commitment and/or chondrogenic differentiation by allowing cells to directly communicate with each other. Gap junctions, membrane-bound channels that directly link neighboring cells, increase during mesenchymal condensation and persist through chondrogenesis until the cells detach from one another and accumulate extracellular matrix between them [87, 109]. In micromass culture, transfer of gap junction-permeable dye is observed exclusively in regions of chondrogenic differentiation, suggesting a role for cell coupling in the spatial coordination of chondrogenesis [110], whereas blocking gap junction communication inhibits chondrogenesis [108, 111].

Lineage commitment and condensation alone are not sufficient to initiate chondrogenic differentiation [107]. Extracellular matrix interactions, cell-cell interactions, secreted factors, and transcription factors have all been implicated as factors that regulate developmental chondrogenesis following condensation. Since MSCs in pellet culture physically recapitulate the dense packing of the precartilage condensation, the factors regulating MSC chondrogenesis are likely to overlap with those that are known to regulate developmental chondrogenesis. Some of the key regulators of developmental chondrogenesis will be explored in more detail below to clarify which signals might be involved in the regulation of MSC chondrogenesis.

Fibronectin

Fibronectin (FN) is a dimeric glycoprotein found in the extracellular matrix of various tissues including the mesenchyme, the precartilage condensation, and mature cartilage [90, 91]. FN is present throughout the mesenchyme, but becomes highly concentrated in the precartilage condensation before assuming a diffuse distribution pattern in mature cartilage [91]. FN interacts with other extracellular matrix proteins via collagen, fibrin, and heparin binding domains, and with cells via its heparin binding and integrin-binding arginine-glycine-aspartate (RGD) domains [112]-[113]. FN may aid condensation of chondroprogenitors by using these sites of cellular attachment to incorporate them into the condensation.

FN is produced in various isoforms as a result of alternative mRNA splicing. Alternative splicing of *FN* over the course of developmental chondrogenesis suggests a role in mediating differentiation. Between condensation and differentiation, the splicing

pattern of *FN* changes from B^+A^+ to B^+A^-; exon IIIA, which is required for condensation and normal chondrogenesis, is spliced out [114]. In micromass culture, the B^+A^+ "mesenchymal" isoform of FN enhances condensation and supports chondrogenesis, while other isoforms of FN inhibit condensation and compromise chondrogenesis [112]. The B^+A^+ isoform has been shown to discourage cell spreading in mesenchymal cells *in vitro* [112], so it could serve as a signal to promote cell rounding and thereby enhance cell packing. The switch to the B^+A^- "differentiated" isoform of FN, which provides no apparent pro-chondrogenic benefit, suggests that the role of FN in regulating chondrogenesis occurs at the level of condensation.

Tenascin-C

Tenascin (TN)-C is a glycoprotein of the cartilage extracellular matrix first observed during mesenchymal condensation [115]. TN-C is selectively localized to prechondrogenic regions of the condensed mesenchyme, but progressively disappears from the anlagen as the chondrocytes mature, although it persists in the perichondrium and articular cartilage [115-117]. This expression pattern suggests a role in promoting early chondrogenesis. Indeed, limb bud mesenchyme micromasses cultured on TN substrates demonstrate enhanced chondrogenesis [115, 118, 119], while TN-C antibodies inhibit chondrogenesis [119]. In addition, TN-C inhibits attachment to FN [36], so the transition from binding to FN during the condensation phase to binding to TN-C may be a signal to begin differentiation.

Like *FN*, *TN-C* is subject to alternative splicing that changes over the course of chondrogenesis. TN-C is made up of six monomers each containing a series of epidermal

growth factor (EGF)-like repeats, a series of FN type III repeats, and a fibrinogen-like domain [115, 117, 118]. Splice variants of TN-C differ as to the number of extra FN type III repeats [117, 118]. As mesenchymal cells differentiate into chondrocytes they express TN-C splice variants with fewer and fewer extra FN type III repeats [117], until fully differentiated chondrocytes express TN-C with no extra repeats as their primary isoform [118]. Attachment of undifferentiated cells to "mesenchymal" TN-C containing the maximum number of FN type III repeats is decreased compared to other TN-C isoforms [118], suggesting that binding to TN-C binding improves with advancing differentiation state. Cells grown on TN-C form attachments, but remain rounded rather than spread out [120]. Since the cells are better able to attach to TN-C as they differentiate, TN-C may support chondrogenesis by promoting continued cell rounding.

N-Cadherin

N-cadherin, a member of the calcium-dependent classical cadherin family of cellular adhesion glycoproteins, is highly expressed during mesenchymal condensation [103, 104]. Cadherins are membrane bound proteins that associate with each other via their extracellular cadherin domains to form adherens junctions between neighboring cells. The intracellular domain is linked to the actin cytoskeleton by interactions with β-catenin and α-catenin, and this association can modulate both cell adhesion and intracellular signaling [121]. Adhesion via N-cadherin is one means by which pre-chondrogenic mesenchymal cells are able to selectively draw themselves into the condensation [122]. Since only prechondrogenic cells express N-cadherin, its diffuse distribution seen in the mesenchyme becomes considerably concentrated in the

condensation as the lineage committed cells aggregate [103, 104]. However, following condensation, N-cadherin expression is lost from the chondrogenic cells and persists only in the perichondrium.

The importance of N-cadherin in regulating chondrogenesis has been demonstrated by perturbing its activity. Injecting an anti-N-cadherin antibody, NCD-2, into the developing chick limb bud inhibits chondrogenesis *in vivo* [103]. In micromass culture, overexpression of loss-of-function N-cadherin mutants results in decreased capacity for condensation and subsequent chondrogenic differentiation [106, 107]. Even though this suggests a role in driving chondrogenesis, N-cadherin is conspicuously absent from differentiating cartilage. In fact, sustained expression of N-cadherin after micromass condensation prevents chondrogenic differentiation [107, 123]. Coupled with its expression pattern, the inhibitory effect of N-cadherin on differentiation indicates that though N-cadherin may be required for lineage committed cells to condense, it negatively regulates chondrogenesis.

NCAM

Neural cell adhesion molecule (NCAM) is a cell surface glycoprotein involved in calcium-independent adhesion and is observed during chondrogenesis. Like N-cadherin, NCAM is weakly present in mesenchymal cells and is enhanced in the precartilage condensation [119, 124]. As the cells become more differentiated NCAM disappears from the condensation, but remains in the perichondrium. Treatment with anti-NCAM antibodies inhibits micromass aggregation and chondrogenesis, while overexpression of NCAM increases condensation [119, 124]. However, unlike N-cadherin, overexpression

of NCAM in the micromass condensation does not inhibit chondrogenesis, but increases it [124]. Thus, while its expression profile suggests a role in condensation rather than chondrogenesis, NCAM may serve as an early differentiation signal as well.

Sox9

Sox9 is a transcription factor that is strongly expressed in committed chondroprogenitors [125, 126], and its expression is maintained during chondrogenic differentiation [127] and in articular cartilage [125]. Sox9 is a member of the SRY-related high mobility group (HMG) box (Sox) family of proteins, and contains a DNA-binding HMG box [45] and a transcription activation domain [127]. Binding of the HMG box to consensus sequences on the minor groove of DNA induces a sharp bend to allow for assembly of transcriptional regulatory complexes at nearby DNA sites [128]. Heterozygous mutations in *Sox9* result in campomelic dysplasia, a disorder characterized by skeletal bowing and other defects, respiratory distress, and XY sex reversal. *Sox9$^{+/-}$* mice also exhibit symptoms of campomelic dysplasia, and their skeletal and respiratory defects have been traced to impaired cartilage formation during development [129]. Sox9 is thus involved in normal chondrogenesis, and additional studies have demonstrated that Sox9 exerts its effects at both the levels of condensation and differentiation.

Sox9 is a marker of chondrogenic lineage commitment expressed by mesenchymal chondroprogenitors even before condensation [125, 126]. In a *Sox9$^{flox/flox}$;Prx1-Cre* mouse, which does not express *Sox9* in its mesenchymal cells, there are no condensations [130]. Mesenchymal cells without *Sox9* are excluded from condensations in *Sox9* chimeras [131]. Conversely, overexpression of *Sox9* accelerates

aggregation in micromass cultures, and in mice, $Sox9^{-/-}$ cells near the condensation become segregated before overt chondrogenesis. Together, this suggests that Sox9 may regulate adhesion molecules that enhance condensation [126, 131].

Sox9 is a true chondrogenic differentiation factor, being both necessary and sufficient to induce chondrogenesis. Limb bud cells from $Sox9^{flox/flox}$;Prx1-Cre mice exhibit no cartilage differentiation in micromass culture [130]. Even when surrounded by $Sox9$-expressing cells in the mesenchymal condensation, $Sox9^{-/-}$ cells do not differentiate into chondrocytes [131]. In $Sox9^{fl/fl}$;Col2a1-Cre mice, in which Sox9 is knocked out of early chondrocytes, chondrogenesis is impaired and the cells remain condensed [130]. When Sox9 is knocked out of more mature chondrocytes, they halt their differentiation program [132]. These studies illustrate that Sox9 is required for chondrogenesis to proceed at every stage of differentiation. Meanwhile, overexpression of Sox9 enhances chondrogenesis, even under conditions where chondrogenic differentiation should be impaired [126, 133, 134]. Sox9 can cause ectopic cartilage formation [126, 133] and switch non-chondrogenic cells to a chondrogenic program [126], indicating that Sox9 is both necessary and sufficient to drive chondrogenesis.

Sox9 drives expression of the primary extracellular matrix components of cartilage and is aided by transcription co-factors. The HMG domain of Sox9 binds to a sequence in the *Col2a1* enhancer and the transcription activation domain activates the *Col2a1* promoter [135]. Even non-chondrogenic cells overexpressing *Sox9* display an increase in *Col2a1* mRNA [136]. Sox9 also binds the A1 enhancer sequence in the *Acan* gene leading to activation of A1-driven reporters [80, 137]. Since *Sox9* is also expressed in the developing central nervous system [125], heart [125], kidney [138], and gonads

21

[138], specificity for activating transcription of *Col2a1* and *Acan* in chondrogenic cells is conferred by cartilage-specific cofactors such as L-Sox5 and Sox6 [139], and PGC-1α [133]. Each of these factors can form a complex with Sox9, and co-expression of *Sox9* with either *L-Sox5*, *Sox6*, or *PGC-1α* leads to increased activation of the *Col2a1* promoter relative to expression of Sox9 alone [133, 136]. Co-expression of *Sox9* with *L-Sox5* and *Sox6* led to an increase in *aggrecan* compared to *Sox9* alone [136], and co-expression of *Sox9* with *PGC-1α* led to an increase in *COMP* and *link protein* relative to expression of *Sox9* alone [133]. These and likely other cofactors coordinate the degree to which Sox9 activates chondrogenesis in various cell types.

The TGF-β Superfamily

Members of the transforming growth factor (TGF)-β family are secreted proteins that activate signaling responses through structurally related receptors. These growth factors contain a highly conserved C-terminal domain, and in their mature form, exist as homodimers linked by disulfide bridges at their cysteine rich domain [140]. The two main subclasses are the TGF-β (and activin) molecules and the bone morphogenetic proteins (BMPs), which signal to unique receptors [141]. All TGF-β family receptors form a stable tetramer of two type I receptors and two type II receptors upon ligand binding, allowing for phosphorylation of the type I receptors by the type II receptors, followed by autophosphorylation of the type I receptors [140]. Receptor activation leads to downstream Smad signaling. In general TGF-βs bind to the ALK4, ALK5, and ALK7 type I receptors and activate Smads 2 and 3, and BMPs bind to the ALK2, ALK3, and ALK6 type I receptors and activate Smads 1, 5, and 8 [141]. However, there are

exceptions to this general pattern as TGF-β can bind to ALK1 and activate Smad1/5/8 [142]. In addition, activated type I receptors can phosphorylate proteins that activate non-Smad signaling cascades including several of the MAP kinases and the β-catenin pathway. The affinity of the TGF-β family molecules for a particular combination of receptors determines in part the specificity of the signal transduced. These Smads couple with Smad4 to effect transcriptional activation.

TGF-β activity is found in prechondrogenic mesenchymal cells and chondrocytes, and after condensation its expression is confined primarily to the surrounding perichondrium. TGF-βs have redundant functions as indicated by the mild skeletal phenotype in TGF-β1 and TGF-β3 null mutants [141] and the activation of common Smads. Smad3 (and Smad2 to a lesser extent) are the primary mediators of the TGF-β signal in chondrogenesis [143, 144]. Treatment of micromass cultures with various TGF-βs enhances condensation and chondrogenesis (Table 1-2), and this effect depends on downstream Smad signaling. Overexpression of the inhibitory Smad, Smad7, inhibits condensation and chondrogenesis [145]. These studies demonstrate that TGF-β promotes the commitment of undifferentiated cells to a chondrocytic lineage by promoting condensation as well as their subsequent differentiation. Conditional deletion of the TGF-β type II receptor in chondrogenic precursors following mesenchymal condensation does not affect subsequent chondrogenesis, suggesting that other factors can maintain chondrogenesis in the absence of TGF-β signaling [146].

Several BMPs, BMP receptors, and their target Smads are found in the precartilage condensation and can enhance chondrogenesis [141, 147]. Treatment of micromass cultures with BMP-2 or activation of BMP signaling in the limb bud with

Table 1-2: Effects of TGF-β Superfamily in Developmental Chondrogenesis

Molecule	System	Effects on Chondrogenesis	Other Effects	Reference
TGF-β1	GF treatment of micromass cultures of chick limb mesenchymal cells	Enhanced condensation		[148]
TGF-β1	GF treatment of micromass cultures of mouse limb mesenchymal cells	Enhanced chondrogenesis		[149]
TGF-β1	GF treatment of micromass cultures of chick limb mesenchymal cells	Enhanced chondrogenesis		[150]
TGF-β1	GF treatment of interdigital space in chick limb bud	Ectopic chondrogenesis		[151]
TGF-β3	GF treatment of micromass cultures of chick limb mesenchymal cells	Enhanced chondrogenesis	Greatest effects pre-condensation	[152]
TGF-β type II receptor	*Tgfβr2$^{fl/fl}$;Col2a1-Cre* mouse	No effect on chondrogenesis		[146]
BMP-2	GF treatment of micromass cultures of chick limb mesenchymal cells	Enhanced chondrogenesis	Greatest effects post-condensation	[152]
BMP2	Expression of RCAS-BMP2 in micromass cultures of chick limb mesenchymal cells	Enhanced chondrogenesis		[153]
BMP-2	GF treatment of micromass cultures of chick limb mesenchymal cells	Enhanced chondrogenesis	Reversed by LiCl treatment	[154]
BMP-2	GF treatment of micromass cultures of chick limb mesenchymal cells	Enhanced chondrogenesis	Reversed by overexpression of N-cadherin	[155]
BMP-2	GF treatment of micromass cultures of chick limb mesenchymal cells	No effect on condensation; Enhanced of chondrogenesis		[156]
ALK3	Expression of RCAS-CA-ALK3 in chick limb bud	Enhanced of chondrogenesis		[157]
ALK6	Expression of RCAS-CA-ALK6 in chick limb bud	Ectopic condensation; Enhanced chondrogenesis		[157]
ALK6	Expression of RCAS-CA-ALK6 in micromass cultures of chick limb mesenchymal cells	Enhanced condensation; Enhanced chondrogenesis		[157]
Smad7 (Smad antagonist)	*Prx-Smad7* mouse	Inhibited condensation; Inhibited chondrogenesis		[145]

constitutively active receptors improves chondrogenesis, but does not have a consistent effect on condensation (Table 1-1). BMP-2 treatment enhances expression of the cell adhesion molecules connexin43 and N-cadherin, [111, 155], suggesting a role for BMPs in promoting condensation as well. However, blocking BMP signaling using conditional deletion of *ALK3* in *ALK6*^{-/-} mutants does not prevent mesenchymal condensation, but does prevent chondrogenesis [147]. Inhibition of BMP signaling with Noggin in condensed cells or through overexpression of dominant negative *ALK6* in immature chondrocytes prevents chondrogenesis [158, 159]. This means that BMP signaling does not drive chondrogenic lineage commitment or condensation, but is essential for chondrogenesis.

TGF-βs and BMPs both exert their effects in part through induction of Sox9. Implantation of TGF-β1 or BMP-7 soaked beads in the interdigital space in the chick limb bud leads to increased *Sox9* expression [151]. Knocking out *ALK3* in condensed chondroprogenitors abolishes *Sox9* expression [147]. In addition to regulating its transcript levels, TGF-βs and BMPs can increase Sox9 transcriptional activity. In SW1353 immature chondrocytes, phosphorylation of Smad2/3 by TGF-β signaling causes it to form a complex with the transcriptional coactivator p300 and Sox9, leading to enhanced activation of the *Col2a1* promoter [144, 160]. BMP-2 also increases Sox9 transcriptional activity, and overexpression of the inhibitory Smad6 reverses this increase [161]. In the absence of *Sox9*, TGF-βs and BMPs are unable to influence chondrogenesis [141].

β-Catenin and the Canonical Wnt Pathway

The focus of this dissertation is β-catenin, which interacts with many of the aforementioned regulatory elements in regulating chondrogenesis. β-Catenin is a transcriptional regulator that is both part of and itself regulated by canonical Wnt signaling. β-Catenin protein is encoded by the gene *Ctnnb1* and has a transactivation domain in its C-terminus, 12 Armadillo repeats that acts as a binding site for other molecules, and consensus phosphorylation sites in its N-terminus [162]. In the nucleus, β-catenin binds to the N-terminal of T-cell enhancing factor (TCF) and lymphocyte enhancing factor (LEF) transcription factors, switching them from transcriptional repressors to transcriptional activators [163]. β-Catenin can also recruit additional transcriptional co-activators such as cyclic AMP response element-binding protein and Brg-1, among others, to promote activation of target genes [164]. However, β-catenin is typically sequestered in the membrane or cytoplasm before it reaches the nucleus. β-Catenin can bind to N-cadherin via its armadillo domain, and this interaction is stabilized by phosphorylation of cadherin and strengthens cell-cell adhesions [165]. In the cytoplasm, β-catenin is bound in a complex with the scaffolding proteins Axin and adenomatous polyposis coli (APC) and the kinases casein kinase-1α and glycogen synthase kinase (GSK)-3β [162, 163]. In this complex, the kinases phosphorylate β-catenin on serine (S) and threonine (T) residues in its N-terminal, allowing binding of E3 ubiquitin ligase that targets β-catenin for proteasomal degradation [163]. Wnt signaling relieves this constitutive degradation of β-catenin, allowing it to accumulate at membrane or in the nucleus, where it drives transcriptional changes.

The canonical Wnt pathway signals through activation of β-catenin. Wnt proteins are secreted morphogens containing a region of highly conserved cysteine residues. One of the cysteines is palmitoylated to increase Wnt's hydrophobicity, which is required for its activity [163, 164]. Wnt signaling is initiated by its binding to a cysteine rich domain on a Frizzled (Fz) seven-pass transmembrane receptor [164]. Activation of Wnt signaling depends on the presence of the co-receptors LRP5 and/or LRP6. The LRPs are single-pass transmembrane proteins with a proline-proline-proline-serine/threonine-proline (PPPS/TP) motif in their C-termini [164]. When Wnt binds to Fz, the cytoplasmic protein Dishevelled (Dsh), which recognizes Fz's intracellular lysine-threonine-X-X-X-tryptophan (KTXXXW) motif, is phosphorylated [164]. Dsh causes LRPs to aggregate and become phosphorylated, and phosphorylation of the LRP PPPS/TP motif allows for docking of Axin [162-164]. This promotes the release of GSK-3 from the Axin complex, preventing phosphorylation of both Axin and β-catenin [162, 164]. In this way, Axin is made to release β-catenin from the degradation complex, allowing for its accumulation and translocation to the nucleus [164].

In addition to the canonical pathway described above, Wnt ligands can also activate non-canonical pathways including PCP, JNK, cGMP/Ca^{2+}, RAP1, ROR2, PKA, GSK3-MT, aPKC, RYK, and mTOR [166]. Many of these pathways are activated through the same Fz receptor and Dsh protein involved in transduction of the canonical Wnt signal. While all Wnts are theoretically capable of initiating both canonical and non-canonical signaling, the signal output depends on the combination of Wnt, receptors, and other contextual factors [167].

Many of the components of the Wnt signaling machinery are differentially expressed during chondrogenesis, suggesting a role in regulation of chondrogenesis. Various Wnts, including Wnt4, Wnt5a, and Wnt14 are found in mesenchymal cells before condensation, and then become localized to those cells surrounding the condensation [168, 169]. These secreted Wnts likely act on the condensing mesenchymal cells where both Fz-7 and β-catenin are expressed during condensation [168-171]. However, expression of Fz-7 and β-catenin is downregulated as chondrogenesis proceeds, indicating that Wnt signaling may actually be detrimental to this process. The Wnt antagonist Frzb-1 is strongly expressed in the mesenchymal condensation and early chondrogenic cells, and may act to inhibit Wnt signaling at this early stage until the rest of the signaling molecules can be effectively eliminated [172].

When Wnts or their receptors are overexpressed in the limb bud or in micromass culture, the common effect is inhibition of chondrogenesis (Table 1-3). One notable exception is Wnt5a, a non-canonical Wnt, which does not appear to have an effect on chondrogenesis when misexpressed in chick limb bud or micromass culture, and may be required for normal condensation in the mouse [173-175]. Ectopic expression of *Wnt1* in the developing mouse limb disrupts the mesenchymal condensation, and limb buds from this transgenic mouse lack gap junction transcripts in the region of *Wnt1* expression, indicating that Wnt1 may negatively regulate condensation and subsequent chondrogenesis via the downregulation of gap junctions [176]. Other Wnts may also inhibit chondrogenesis by maintaining cell contacts. Overexpression of *Wnt7a* in micromass culture results in the persistence of N-cadherin and NCAM at the membrane, and inhibition of chondrogenesis [153, 173]. The dual implication of canonical Wnts and

Table 1-3: Effects of Wnts in Developmental Chondrogenesis

Molecule	System	Effects on Chondrogenesis	Other Effects	Reference
Wnt1	Expression of RCAS-Wnt1 in micromass cultures of chick limb mesenchymal cells	No effect on condensation; Inhibited chondrogenesis		[177]
Wnt1	Ectopic expression in transgenic mouse limb	Defective condensation and chondrogenesis		[176]
Wnt5a	Expression of RCAS-Wnt5a in micromass cultures of chick limb mesenchymal cells	No effect on condensation; No effect on chondrogenesis		[173]
Wnt5a	Expression of RCAS-Wnt5a in chick limb bud	No effects on condensation or chondrogenesis		[174]
Wnt5a	*Wnt5a$^{-/-}$* mouse	Inhibited condensation; Inhibited chondrogenesis		[175]
Wnt5b	Expression of Ad-Wnt5b in micromass cultures of mouse limb mesenchymal cells	Enhanced condensation; Inhibited chondrogenesis		[178]
Wnt7a	Expression of RCAS-Wnt7a in micromass cultures of chick limb mesenchymal cells	No effect on condensation; Inhibited chondrogenesis		[177]
Wnt7a	Expression of RCAS-Wnt7a in micromass cultures of chick limb mesenchymal cells	Enhanced condensation; Inhibited chondrogenesis	Delayed N-cadherin expression; Persistence of N-cadherin/β-catenin complex at membrane	[173]
Wnt7a	Expression of RCAS-Wnt7a in micromass cultures of chick limb mesenchymal cells	Irregular condensation; Inhibited chondrogenesis	Prolonged expression of NCAM, N-cadherin, β1 integrin; Diffuse FN; Decreased expression of TN-C	[153]
Wnt14	Expression of RCAS-Wnt14 in micromass cultures of chick limb mesenchymal cells	Inhibited chondrogenesis		[179]
Wnt14	Expression of RCAS-Wnt14 in micromass cultures of chick limb mesenchymal cells	Inhibited chondrogenesis		[179]
Wnt14	*Col2a1-Wnt14* mouse	Inhibited chondrogenesis		[168]
Fz-7	Expression of RCAS-Fz7 in micromass cultures of chick limb mesenchymal cells	Inhibited condensation; Inhibited chondrogenesis	Delayed or decreased N-cadherin expression	[170]
LRP5 and LRP6	*LRP6$^{fl/fl}$;Dermo1-Cre;LRP$^{-/-}$* mouse	Ectopic chondrogenesis		[180]
Sfrp-2 (Wnt antagonist)	Implantation of Sfrp-2-expressing cells in mouse limb bud interdigital space	Enhanced chondrogenesis		[175]

N-cadherin in regulating chondrogenesis suggests a role for β-catenin in this process as well since it interacts with both of these.

β-Catenin negatively regulates chondrogenesis via several mechanisms. As with Wnt, misexpression of a constitutively active β-catenin in mesenchymal cells or chondrocyte precursors inhibits chondrogenesis [181-183]. Similarly, treatment of micromass cultures with LiCl, which frees β-catenin from degradative phosphorylation, inhibits chondrogenesis [154]. Conversely, conditional knockout of β-catenin in early chondrocytes results in perichondrial chondrogenesis and ectopic cartilage formation [164, 174, 180]. In micromass cultures, β-catenin is localized in the cell-cell contacts with N-cadherin [167]. Treatments that oppose chondrogenesis such as retinoic acid and IL-1β preserve β-catenin and N-cadherin levels [167]. The relatively low levels of β-catenin in the nucleus during condensation and early chondrogenesis suggests that β-catenin effects are mediated by its role in stabilizing cell adhesions, which negatively regulate chondrogenesis. In the nucleus β-catenin may inhibit chondrogenesis by regulating Sox9. In constitutively active β-catenin mutants, *Sox9* expression is reduced [180]. Further, the Armadillo domain of β-catenin can bind directly to the C-terminal of Sox9 resulting in their mutual degradation [174]. Elevated levels of β-catenin would decrease levels of Sox9 and prevent Sox9-driven chondrogenesis and vice versa. Downregulation of β-catenin is, therefore, required for chondrogenesis to proceed, and β-catenin is required to prevent chondrogenesis in Sox9-expressing mesenchymal cells.

1.5 Chondrocyte Maturation and Endochondral Ossification

After their initial chondrogenic differentiation, chondrocytes continue to mature, and the cartilage anlage is replaced by bone via endochondral ossification. Beginning in the diaphysis, the center of the anlagen, the chondrocytes proliferate, mature, and undergo hypertrophy, lengthening the cartilage element. At the primary ossification center, structures known as growth plates, consisting of chondrocytes arranged in sequential stages of maturation, form along the axis of the future long bone. During the process of endochondral ossification, endothelial cells and osteoblasts from the perichondrium invade and replace the growth plate with bone and concomitant marrow formation. Secondary ossification centers arise at the two epiphyseal ends of the long bone, and these growth plates persist through puberty as sites of ongoing longitudinal growth. Eventually, the entire skeletal structure consists of bone with only the two ends covered with a thin layer of permanent hyaline articular cartilage.

Growth plate architecture is classified in zones according to the different functions of the chondrocytes in each zone. Beginning from furthest away from the center of ossification are zones of resting, proliferative, pre-hypertrophic, hypertrophic, and terminally differentiated calcified chondrocytes [184, 185]. Resting chondrocytes are small rounded cells similar in appearance to articular chondrocytes. In the proliferative zone, the resting chondrocytes start to divide, and the rapidly dividing chondrocytes are packed into dense columns of flattened cells [186]. The pre-hypertrophic chondrocytes form an intermediate zone of cells transitioning from proliferation to hypertrophy. Here, the cells are not mitotic and assume a rounded morphology. These pre-hypertrophic cells still express Col2, but their expression of Indian hedgehog (Ihh) marks them as having

committed to hypertrophic differentiation [187]. In the hypertrophic zone, chondrocytes then enlarge up to ten times their original volume and secrete a matrix consisting mainly of Col10 instead of Col2 [185, 186, 188]. In the zone of terminally differentiated chondrocytes, the fully mature chondrocytes express MMP13, a collagenase capable of digesting any remaining Col2, and ALP to initiate the process of matrix mineralization. Ultimately, these terminally differentiated chondrocytes undergo programmed cell death, leaving behind space for blood vessel infiltration and bone formation [185].

The signals involved in regulating the transitions to proliferating, hypertrophic, and terminally differentiated chondrocytes are tightly regulated by transcription factors, secreted factors, and systemic factors [184]. Important factors that manage each stage of chondrocyte maturation are discussed below in more detail as these signals may also be involved in the development of hypertrophy characteristics during MSC chondrogenesis.

Indian hedgehog

The reserve and proliferative zones are regulated by a negative feedback loop involving Ihh and parathyroid hormone-related peptide (PTHrP). Ihh is expressed by pre-hypertrophic chondrocytes and drives expression of PTHrP in periarticular perichondrial cells and early proliferating chondrocytes [187, 189-191]. The PTHrP receptor (PPR) is highly expressed on chondrocytes at the end of the proliferative zone that are exiting the cell cycle [187]. PTHrP binding to its receptor prevents the differentiation of PPR-expressing cells, thus defining a region of cells that are no longer proliferating, but have not yet committed to a hypertrophic fate: the pre-hypertrophic, Ihh-expressing chondrocytes [190]. As continued proliferation lengthens the proliferative zone, the cells

at the far end of the zone are believed to be pushed beyond diffusion limit of PTHrP. These cells no longer receive the anti-hypertrophy signal from PTHrP and become pre-hypertrophic chondrocytes expressing Ihh. Thus, expression of Ihh by the pre-hypertrophic chondrocytes serves to regulate the proliferative zone via activation of PTHrP expression which prevents more proliferating chondrocytes from becoming pre-hypertrophic.

In addition to its role regulating PTHrP expression, Ihh acts as a positive regulator of proliferation. The proliferative zone in $Ihh^{-/-}$ mice lacks the organized columnar structure of the wild type growth plate [191]. In addition, these Ihh-null mutants demonstrate less bromodeoxyuridine (BrdU) incorporation, an indication of reduced proliferation. Although these mice lack PTHrP, the observed effects on proliferation are Ihh-dependent. The reduction in proliferation is also observed in $Smo^{flox/-};Col2\text{-}Cre$ mice, which have normal Ihh and PTHrP expression, but whose chondrocytes do not respond to Ihh signaling [192]. Conversely, proliferation is increased when Ihh signaling is enhanced [193]. Proliferation is also increased in $Col2\text{-}Ihh$ and $Col2\text{-}caSmo$ mice, in which Ihh or constitutively active Ihh targets are ectopically expressed in chondrocytes [192]. Therefore, Ihh signaling is responsible for inducing and or maintaining proliferation.

Ihh signaling directly targets the perichondrial cells and resting chondrocytes. Ihh is a member of the Hedgehog (Hh) family of proteins that contain a catalytic domain in the C-terminus which modifies the N-terminus signaling domain with lipids to generate the active signaling molecule [194]. Activated Hhs form multimers capable of long range diffusion, which is regulated by heparan sulfate [195]. Like the other Hhs, Ihh signals

through the transmembrane receptors Patched1 (Ptc) and Smoothened (Smo) [196]. Binding of Ihh to Ptc relieves repression of Smo, which in turn activates the Gli family of transcription factors to express Ihh target genes [194, 196]. In the growth plate Ptc, Smo, and Gli3 are expressed with a decreasing gradient from the periarticular chondrocytes to the late proliferating chondrocytes, and in the perichondrium, indicating that these cells are the targets of Ihh [191, 195, 197]. In $Ihh^{-/-}$ and $Smo^{flox/-};Col2$-Cre mice, cyclin-D1 is noticeably downregulated in the proliferating chondrocytes [192]. Positive regulation of proliferation by Ihh may be achieved in part by its control of cell cycle genes in the periarticular and proliferating chondrocytes.

Ihh exerts its effects on proliferation in part via Gli3, which can act as either an activator (Gli-A) or repressor (Gli-R), depending on post-translational modifications [198, 199]. Proliferation is partially restored in the $Ihh^{-/-};Gli3^{-/-}$ double knockout mouse compared to the $Ihh^{-/-}$ mouse, suggesting that in the absence of Ihh, Gli3 represses Ihh target genes [197, 200]. However, there is also evidence that Gli3 acts as an activator of Ihh target genes. Ectopic expression of Ihh in $Col2a1$-expressing chondrocytes results in an increase in proliferation, but this effect is abolished in the absence of $Gli3$ [197]. Thus, in the presence of Ihh, Gli3 acts as a transcriptional activator. In the growth plate, Gli3 is highly expressed in the periarticular chondrocytes with a decreasing gradient through the proliferative zone [197, 201], and the distribution of Gli3 isoforms changes along this gradient. Gli-R is the dominant type in the periarticular cells and decreases toward the prehypertrophic zone, while Gli-A stays relatively constant throughout the proliferative zone [199]. The transition from Gli-A to Gli-R is negatively regulated by Hh signaling, so there is more Gli-R further from the pre-hypertrophic zone, the source of Ihh [199]. By

converting Gli-R to Gli-A, Ihh signaling not only relieves transcriptional repression of proliferation, but activates it as well. This suggests that the diffusion limit of Ihh defines the region at which cells switch from the Gli-R resting chondrocytes to Gli-A proliferating chondrocytes.

FGFRs

Fibroblast-like growth factor receptors (FGFRs) are differentially expressed in skeletal development. FGFR1 and FGFR2 are highly expressed in the mesenchymal condensation and become confined to the perichondrium when the chondrocytes begin to mature [202]. FGFR3 is expressed in the resting and proliferative zones during embryonic development [203]. Activating mutations in FGFR3 causes varying degrees of dwarfism in mammals in which the size of the proliferative zone is noticeably reduced [204-206], and studies suggest that this is because activation of FGFR3 negatively regulates proliferation [204, 207-210]. Conversely, *FGFR3*^{-/-} mice demonstrate skeletal overgrowth, though this phenotype has not been directly correlated with increased proliferation [211]. Beyond the proliferative zone, FGFR1 is found in hypertrophic chondrocytes where it is also negatively regulates proliferation [206]. Differences in the effects of FGFR1 and FGFR3 are likely maturation-stage dependent.

IGF-1 and Growth Hormone

Insulin-like growth factor (IGF)-1 and growth hormone (GH) interact to regulate growth, as well as exerting independent effects on proliferation. While GH regulates postnatal elongation of the long bones in part through IGF-1, IGF-1 has its own effects

before the onset of GH-driven growth. *IGF-1$^{-/-}$* and *IGF-1 receptor (IGF-1R)$^{-/-}$* mutants are born with visible skeletal shortening [212]. After birth, these mice have an enlarged zone of resting chondrocytes, indicating that IGF-1 may be required for these cells to enter the proliferative phase, although the numbers of proliferating chondrocytes are unchanged [213]. Other studies suggest, however, that *IGF-1$^{-/-}$* dwarfism derives from defective chondrocyte hypertrophy [214]. The effects of GH, meanwhile, are better defined. Mice lacking the GH receptor (GHR) have clearly reduced numbers of proliferating chondrocytes [213], while infusion of GH directly into the growth plate increases the number of proliferating cells [215]. There is evidence that IGF-1 is partially responsible for mediating the effects of GH as GH elevates the level of IGF in the growth plate [216] and IGF-1-treated hypophysectomized rats and *GHR$^{-/-}$* mice have an increased proliferative zone compared to their respective controls [217, 218]. These factors also interact with the Ihh-PTHrP feedback loop to regulate chondrocyte proliferation [219, 220].

Runx2

Runt-related transcription factor 2 (Runx2) is a transcription factor also known as core binding factor α1 (Cbfa1) or osteoblast-specific transcription factor 2 (OSF2). It is known primarily for its role in positively regulating osteogenesis, but also plays a role in regulating chondrocyte hypertrophy. During endochondral ossification Runx2 is found in the perichondrium, where it drives the differentiation of these cells into the osteoblasts of the bone collar [221-224]. In the absence of Runx2 there is no bone formation [225]. *Runx2* is also expressed in proliferating, pre-hypertrophic, and hypertrophic chondrocytes

with increasing expression with maturation, suggesting an additional role in these cells [221-224]. *Runx2*^{-/-} mice lack or have severely delayed hypertrophy [222, 223, 226], while restored expression of *Runx2* in chondrocytes within *Runx2*^{-/-} mice restores normal hypertrophy [221]. Expression of a viral *Runx2* construct in limb bud chondrocytes leads to accelerated hypertrophy [224], and misexpression of *Runx2* in chondrocytes results in hypertrophy and mineralization of chondrocytes in the rib cartilage and trachea, which do not normally terminally differentiate [221]. Runx2 is thus required for hypertrophy.

Runx2 induces hypertrophy in immature chondrocytes, suggesting that in the absence of other signals Runx2 is sufficient to foster chondrocyte maturation [227]. Runx2 achieves this in part by driving expression of genes associated with hypertrophy. Runx2 contains a *runt* DNA-binding domain and three transactivation domains: a glutamine/alanine (Q/A) rich domain, one in the N-terminus, and one on the C-terminus side of the DNA-binding domain [228]. Runx2 binds to sequences in the *Ihh* promoter [229], the *Col10* promoter [230, 231], the *MMP13* promoter [232], and the *BSP* promoter [233], and is capable of transcriptional activation of these genes. *Runx2*^{-/-} chondrocytes in which hypertrophy is delayed or prevented do not express these genes [222]. Furthermore, the DNA-binding domain is required for the effects of Runx2 on hypertrophy [221, 224]. This suggests that Runx2 regulates hypertrophy by transcriptional activation of genes associated with maturing chondrocytes.

Sox9

While its role as a chondrogenic induction factor is the best characterized, Sox9 is also required for the proper progression of chondrocyte maturation. *Sox9* is gradually

downregulated as chondrocytes mature [234], and its expression is completely absent in terminal chondrocytes [130]. However, Sox9 remains essential to the maturation process. Heterozygous *Sox9* mutants have serious skeletal defects including a widened zone of hypertrophic chondrocytes [235]. When *Sox9* is expressed under the control of the *Col2a1* promoter in these mutants, the hypertrophic zone is rescued, indicating a regulatory role for Sox9 in these cells [182]. Conditional knockout of *Sox9* in resting and proliferating chondrocytes abolishes the normal progression of chondrogenesis. Instead, mutant resting cells dedifferentiate and undergo apoptosis. Mutant proliferating cells bypass the cell growth and Col10 deposition phases, and transition directly to a terminal state expressing *MMP13* and *BSP* and mineralizing the extracellular matrix [132, 236]. These findings demonstrate that precise spatiotemporal control of Sox9 is required for normal chondrocyte maturation.

Sox9 regulates the induction of *Col10* expression that characterizes hypertrophy. Sox9 is able to bind to and activate the *Col10a1* promoter, and conditional ablation of *Sox9* from proliferating chondrocytes prevents *Col10a1* expression entirely [132, 236]. *Col10a1* expression reaches wild type levels in *Col2a1-Sox9* knock-in mutants, but terminal differentiation is significantly impaired [182]. Therefore, while Sox9 positively regulates *Col10a1* expression, it negatively regulates the other aspects of terminal differentiation.

Sox9 is thought to act opposite Runx2 in maturing chondrocytes. Elevated levels of Sox9 promote degradation of Runx2 in HEK293, while conditional ablation of *Sox9* in chondrocytes results in elevated levels of *Runx2* [236-238]. In chick embryos infected with *Sox9* retrovirus, cartilage nodules form in typical bone domains and chondrocyte

38

hypertrophy is severely delayed or, in some cases, prevented [238]. Infection with *Runx2* retrovirus causes resting cartilage to undergo hypertrophy. In light of their respective effects in regulating chondrogenesis and hypertrophy, it follows that the balance between Sox9 and Runx2 interacts to direct chondrocyte maturation. This transition occurs at the beginning of hypertrophy. Wnt/β-catenin signaling may be involved here as well. Since β-catenin regulates levels of Sox9 [182] and Runx2 [231], increased signaling would favor Runx2 and the hypertrophic phenotype.

PTHrP

PTHrP was introduced above in the context of regulating the proliferative zone, which it achieves by negatively regulating hypertrophy. As described previously, PTHrP is expressed in periarticular chondrocytes and in the perichondrium [189, 190] and diffuses outward to bind its receptor PPR, which is expressed throughout the proliferative zone and most highly in the pre-hypertrophic transition region between the proliferative and hypertrophic chondrocytes [190, 239]. Receptor binding activates a number of intracellular signaling pathways that alter gene expression. In the absence of PTHrP signaling, chondrocytes undergo accelerated hypertrophy. *PTHrP$^{-/-}$* mice have short limbs due to accelerated hypertrophy of the proliferating chondrocytes [240-242] and PPR$^{-/-}$ chondrocytes also experience accelerated hypertrophic differentiation [241]. Conversely, addition of PTHrP to mouse limbs in culture prevents hypertrophic differentiation [241], and activation of PTHrP signaling as in *Col2-PTHrP* and *Col2-caPPR* systems results in delayed chondrocyte hypertrophy [243, 244]. These findings highlight the importance of PTHrP in regulating the transition from proliferation to hypertrophy, but do not define

whether the role of PTHrP is to maintain proliferation of dividing chondrocytes or actively prevent their hypertrophic differentiation.

Observations of abnormal hypertrophy when PTHrP signaling is disrupted suggest that PTHrP does indeed negatively regulate hypertrophy. In PTHrP knockouts, hypertrophy is observed in chondrocytes that do not typically mature. *PTHrP$^{-/-}$* mice exhibit hypertrophic differentiation of rib cartilage chondrocytes [240], and *Ihh$^{-/-}$;PTHrP$^{-/-}$* double knockouts have hypertrophic chondrocytes present in the growth plate near the articular surface [242]. Additionally, when PTHrP signaling is interrupted in proliferating cells, they undergo premature hypertrophy. In *PPR$^{-/-}$* chimeras, mutant cells in the proliferative zone differentiate into hypertrophic chondrocytes [245], and similarly, in *PPR$^{fl/-}$;Osteocalcin-Cre* mice, chondrocytes missing PPR undergo hypertrophy in the proliferative zone [193]. While the zone of proliferating chondrocytes is extended in both PPR mutants, this is due to misexpression of Ihh in the proliferative zone. In *PPR$^{fl/-}$;Ihh$^{fl/-}$;Ost-Cre* mice expansion of the proliferative zone is eliminated because the prematurely hypertrophic cells no longer produce Ihh [193]. Thus, Ihh is responsible for maintaining proliferation, while PTHrP prevents hypertrophy.

PTHrP inhibits hypertrophic differentiation in part by its interaction with Runx2. The delayed hypertrophy observed in *Runx2$^{-/-}$* mice is rescued in *Runx2$^{-/-}$;Col2-Runx2* mice, and PTH treatment abrogates this rescue [226]. PTHrP decreases expression of Runx2 at the levels of both transcription and translation, and this decrease is specific to chondrocytes [226, 246, 247]. Inhibition of Runx2 is sufficient to prevent hypertrophy as described in the previous section. However, PPR activation delays hypertrophy even

when it cannot downregulate Runx2 expression, suggesting that PTHrP regulates hypertrophy by another mechanism as well [226].

Thyroid hormones

Thyroid hormones are known to regulate postnatal skeletal growth. In addition to other symptoms, hypothyroidism slows skeletal growth while hyperthyroidism accelerates growth and growth plate fusion [248]. Thyroidectomy in mice causes growth retardation that is partially rescued with administration of thyroxine (T4) [219]. T4 is a prohormone produced by the thyroid, which is converted to the active triiodothyronine (T3) in its target tissues [249]. There is evidence that the growth plate is a target of thyroid hormones. Both isoforms of T3 receptor (TR), TRα and TRβ, are expressed in resting and proliferative chondrocytes in the growth plate and in osteoblasts, but not in hypertrophic chondrocytes [250]. Further, T4 treatment of thyroidectomized rats have a more organized growth plate than their hypothyroid counterparts [219], indicating that the growth plate is a likely target of T3 action. T3 inhibits proliferation of growth plate chondrocytes [250] and causes them to transition to hypertrophy. Treatment of organ cultured mouse tibias with T3 results in an increased zone of hypertrophic chondrocytes [249]. Increased cell diameter, ALP activity, Col1 expression in growth plate chondrocytes treated with thyroid hormones validates that these cells are undergoing hypertrophy [219, 250, 251]. These effects are observed in micromass culture as well; T3 inhibits proliferation and enhances hypertrophy [252]. Hypothyroid rats have enhanced PTHrP expression throughout their proliferative zone [219], indicating that thyroid hormones may act in part via negative regulation of PTHrP.

41

The TGF-β Superfamily

The TGF-β superfamily has multiple roles in regulating chondrocyte maturation. During the differentiation process, TGF-βs are expressed in the perichondrium and in hypertrophic cartilage [141]. The target cells of these signals are the proliferating and hypertrophic chondrocytes, which express ALK5 and TGF-βRII. Overexpressing or ablating various components of the cascade indicates that TGF-β-Smad signaling inhibits hypertrophy and terminal differentiation (Table 1-4). One mode of action is via repression of Runx2; TGF-β signaling recruits HDACs 4 and 5 to the Runx2-Smad3 complex, where they can repress Runx2 function [253, 254]. TGF-β also increases expression of *PTHrP* [255].

Various BMPs are also expressed in the perichondrium as well as in proliferating and hypertrophic chondrocytes, but the effects on proliferation are unclear. Proliferation is dramatically reduced in the limbs of $BMP2^{-/-}$ mice [256], while BMPs 2, 4, and 6 inhibit proliferation in cultured growth plate chondrocytes [257]. Treatment of mouse limb explants with BMP-2 increases proliferation, while treatment with Noggin inhibits proliferation, even in the presence of Ihh [258]. Expression of a dominant negative ALK6 should have a similar effect to Noggin treatment since it antagonizes BMP signaling, but instead leads to increased proliferation in cultured growth plate chondrocytes [159]. Further, BMP-2 treatment cannot overcome the block in proliferation caused by depleted Ihh signaling [258]. Since the effects of BMP on chondrocyte proliferation depend heavily on context, its signaling must be tied to receptor expression and interaction with other pathways.

Table 1-4: Effects of TGF-β Superfamily in Chondrocyte Maturation

Molecule	System	Effects on Hypertrophy	Other Effects	Reference
TGF-β1	GF treatment of micromass cultures of mouse limb mesenchymal cells	Inhibited hypertrophy		[259]
TGF-β1	GF treatment of mouse metatarsal	Inhibited proliferation; Inhibited hypertrophy	Increased *PTHrP* expression	[255]
TGF-β type II receptor	Expression of DN-TGFBRII in skeletal precursors	Accelerated hypertrophy; Ectopic hypertrophy	Increased *Ihh* expression	[260]
Smad2/3	Expression of RCAS-Smad2/3 in immature chick chondrocytes	Reduced *Col10a1*; Reduced ALP activity		[143]
Smad2/3	Expression of RCAS-DN-Smad3 in immature chick chondrocytes	Increased *Col10a1*; Reduced ALP activity		[143]
Smad3	Immature $Smad3^{-/-}$ mouse chondrocytes	Increased *Col10a1*	Reversed by overexpression of Smad2 or Smad3	[261]
Smad3	$Smad3^{\Delta/\Delta}$ mouse	Accelerated hypertrophy	Ectopic hypertrophy in articular cartilage	[259]
BMP-2	GF treatment of chick or mouse embryonic limb	Enhanced proliferation; No effect on hypertrophy		[258]
BMP-2 and BMP-6	$Bmp2^{+/-};Bmp6^{-/-}$ mouse	No effect on hypertrophy		[262]
ALK3	Expression of RCAS-CA-ALK3 in chick limb bud	Inhibited pre-hypertrophy and hypertrophy		[157]
ALK3	Expression of RCAS-DN-ALK3 in maturing chick chondrocytes	No effect on hypertrophy		[159]
ALK6	Expression of RCAS-DN-ALK6 in maturing chick chondrocytes	Inhibited hypertrophy; Enhanced proliferation		[159]
ALK6	$ALK6^{-/-}$ mouse	Inhibited proliferation		[263]
BMP type II receptor	Expression of RCAS-DN-BMPRII in maturing chick chondrocytes	Strongly inhibited hypertrophy; Enhanced proliferation		[159]
Noggin (BMP antagonist)	GF treatment of chick and mouse embryonic limb	Inhibited proliferation; Accelerated hypertrophy		[258]
Smad7 (Smad antagonist)	*11Enh-Smad7* mouse	Inhibited proliferation		[145]
Smad7 (Smad antagonist)	*11Prom-Smad7* mouse	Inhibited hypertrophy		[145]

BMP receptors are differentially expressed in the growth plate, and are responsible for discrete effects of BMP signaling on both proliferation and hypertrophic differentiation (Table 1-3). ALK6 is distributed throughout the growth plate, ALK2 is localized to resting and proliferating chondrocytes, and ALK3 is found in later proliferating and hypertrophic chondrocytes. The differential expression of these receptors through the growth plate indicates varying roles for BMPs in the maturation process. BMP signaling through ALK6 negatively regulates proliferation [159], while signaling through ALK3 and ALK6 coordinate to regulate hypertrophy. Activation of ALK3 in chick limb bud leads to inhibition of hypertrophy in the developing limb bud [157], while inhibition of ALK6 inhibits hypertrophy [159, 264]. The relative concentrations of ALK3 and ALK6 likely determine the maturation of the chondrocytes.

β-Catenin and the Canonical Wnt Pathway

The differential distribution of Wnts and Wnt receptors in the growth plate belies their significance in regulating chondrocyte maturation. *Wnt5a, Wnt5b, and Wnt11* are expressed in diaphyseal chondrocytes transitioning from prehypertrophy to hypertrophy [169, 265, 266]. *Wnt4* is expressed in hypertrophic chondrocytes and *Wnt5a* is also expressed in the adjacent perichondrium [266]. *Fz-1* is strongly expressed in the perichondrium surrounding the pre-hypertrophic zone, and *Fz-7* is expressed in proliferating chondrocytes [169]. High levels of *Tcf-4* are detected in pre-hypertrophic and hypertrophic chondrocytes, and *Lef-1* is elevated in the perichondrium surrounding the pre-hypertrophic zone [169]. Overexpression of various Wnts in maturing chondrocytes generally leads to accelerated hypertrophy (Table 1-5). The exceptions to

Table 1-5: Effects of Wnts in Chondrocyte Maturation

Molecule	System	Effects on Hypertrophy	Other Effects	Reference
Wnt3a	GF treatment of growth plate chondrocytes	Enhanced hypertrophy		[234]
Wnt4	*Col2a1-Wnt4* mouse	Disorganized growth plate; Accelerated hypertrophy	Decreased proliferation	[267]
Wnt4	Expression of RCAS-Wnt4 in chick limb bud	Accelerated hypertrophy	Increased domain of Ihh; Increased distance between PPR-expressing domains; Increased *Lef-1* expression	[266]
Wnt5a	Expression of RCAS-Wnt5a in chick limb bud	Inhibited hypertrophy	Continuous expression of PPR	[169]
Wnt5a	Expression of RCAS-Wnt5a in chick limb bud	Delayed chondrocyte maturation		[174]
Wnt5a	*Wnt5b$^{-/-}$* mouse	Delayed hypertrophy		[265]
Wnt5b	Expression of Ad-Wnt5b in micromass cultures of mouse limb mesenchymal cells	Inhibited hypertrophy		[178]
Wnt5b	*Col2a1-Wnt5b* mouse	Delayed hypertrophy		[265]
Wnt9a	*Wnt9a$^{-/-}$* mouse	Delayed chondrocyte maturation		[268]
Wnt14	Retroviral transfection of mature growth plate chondrocytes	Enhanced hypertrophy		[181]
Wnt14	*Col2a1-Wnt14* mouse	Accelerated hypertrophy		[168]
Frizzled-1 and Frizzled-7	Expression of RCAS-DN-Fz1 or RCAS-DN-Fz7 in chick limb bud	Inhibited pre-hypertrophy and hypertrophy	Decreased expression of Ihh; Decreased PPR domain	[169]
LRP5 and LRP6	*LRP6$^{fl/fl}$;Dermo1-Cre;LRP$^{-/-}$* mouse	Inhibited hypertrophy		[180]
Frzb-1 (Wnt antagonist)	Expression of RCAS-Frzb1 in chick limb bud	Inhibited hypertrophy		[269]

this pattern are the non-canonical Wnt5a and Wnt5b, which actually inhibit hypertrophy.
That the canonical Wnts all promote hypertrophy suggests that β-catenin is responsible
for this effect.

β-Catenin mutations cause severe growth plate defects. *Ctnnb1$^{ca-fl/+}$;Col2a1-Cre*
mice lack an organized growth plate and have short limbs. When the newly differentiated

chondrocytes begin expressing constitutively active β-catenin they stop maturing, so no organized growth plate is formed to direct chondrocyte maturation [181, 182]. When constitutively active β-catenin is misexpressed in more mature chondrocytes or in the already formed growth plate, the zone of hypertrophic chondrocytes is expanded, and more Col10 and mineral is deposited, indicating that β-catenin promotes hypertrophy and endochondral ossification [169, 236]. More specifically, the more immature chondrocytes closer to the epiphysis undergo dedifferentiation to a mesenchymal cell type, and the more mature chondrocytes in the diaphysis experience accelerated ossification [181]. The rapidly ossifying cells overrun the growth plate resulting in short limbs. In *Ctnnb1*$^{fl/fl}$*;Col2a1-Cre* mice, the limbs are also severely shortened, although this is caused by inhibition of proliferation and delayed hypertrophy rather than premature ossification [168, 182, 270]. When *Ctnnb1* is conditionally knocked out of all skeletal progenitors, osteoblasts fail to form and the perichondrial cells differentiate into chondrocytes instead [168, 271].

Unlike its cadherin-stabilizing role in inhibiting chondrogenesis, in the growth plate β-catenin promotes chondrocyte hypertrophy via transcriptional activation of target genes. Overexpression of constitutively active β-catenin in the growth plate accelerates chondrocyte differentiation, increasing *MMP13* and *VEGF* expression in mature chondrocytes and diminishing expression of *Col10a1* [181]. In monolayer cultures of mature chondrocytes, overexpression of β-catenin results in upregulation of *Runx2*, *Col10a1*, and *ALP* [231]. *Runx2* [231, 234], *ALP* [272], *MMP13* [273], and *VEGF* [274] all contain consensus TCF/LEF binding sites in their promoters while *Col10a1* does not. Therefore, while many hypertrophy-associated genes can be regulated directly by β-

catenin signaling, *Col10* cannot. β-catenin upregulation of *Col10a1* depends on Runx2; when the Runx2 binding site in the *Col10* promoter is mutated, the upregulation of *Col10* is eliminated [231]. This also explains why *Col10* is not always upregulated by β-catenin. In immature chondrocytes lacking Runx2, there is no expectation of increased *Col10* expression. In addition, *Col10* is downregulated in the final stages of terminal differentiation in the presence of both Runx2 and β-catenin, so its regulation necessarily involves other factors as well [181]. Finally, β-catenin treatment also increases *Lef-1*, indicating positive feedback for continued signaling [168, 169].

β-Catenin overlaps with the Ihh/PTHrP signaling axis during chondrocyte hypertrophy through their dual regulation of Runx2. The delayed hypertrophy observed in β-catenin conditional knockouts is turned into accelerated hypertrophy in *Ctnnb1$^{fl/fl}$;Col2a1-Cre;PTHrP$^{-/-}$* double mutants, suggesting that the effects of Wnt signaling can be overwhelmed by PTHrP activity [270]. Similarly, even though constitutively active Ihh signaling increases β-catenin signaling activity, hypertrophy is delayed due to increased PTHrP [275]. Loss of β-catenin signaling under these conditions further delays hypertrophy [276], indicating that PTHrP and β-catenin have independent roles in regulating hypertrophy, even though they share a common target in Runx2.

1.6 Osteoarthritis

Osteoarthritis is termed as such because it is characterized by inflammation ("itis") affecting the joints ("arthros") and underlying bone ("osteo"). Inflammatory markers have been identified in osteoarthritic joints, but the progressive cartilage degeneration of OA can begin in the absence of inflammation. Unlike the smooth surface

of healthy articular cartilage, the surface of OA cartilage is fibrillated or contains lesions or fissures [277]. Early on, the tissue swells, and there is substantial loss of matrix PGs. At this early stage, the chondrocytes become metabolically active in an attempt to repair the damaged extracellular matrix [278]. As the disease progresses the articular cartilage is similarly eroded from the top down, and vascular channels breach the tidemark from below [50]. The chondrocytes proliferate, become hypertrophic, and/or die [279, 280]. In severe OA, the articular surface is completely denuded of cartilage, and fibrocartilage or osteophyte formation is present [49, 277]. The degraded, bony articular surface is unable to move smoothly or bear mechanical loads, leading to pain and loss of joint function.

Since the hallmark of OA is cartilage degeneration, it follows that aggrecanases and collagenases would be involved in the pathology of OA. A Disintegrin and Metalloproteinase with Thrombospondin Motifs (ADAMTS)-4 and ADAMTS-5, or aggrecanase 1 and aggrecanase 2, respectively, and MMP13 are upregulated in OA chondrocytes [281-283]. ADAMTS-4 and 5 cleave aggrecan at glutamine (E) residues E^{373}, E^{1545}, E^{1714}, E^{1819}, and E^{1919}, and fragments of aggrecan cleaved at these sites are detected in OA cartilage and synovial fluid [284, 285]. *ADAMTS-5* knockout mice, but not *ADAMTS-4* knockouts, are more resistant to induced OA, and explants release less PG from the tissue when cultured [284, 286]. In human explants, both *ADAMTS-4* and *ADAMTS-5* siRNA inhibit the release of GAG from cartilage explants [285]. MMP13 is also known as collagenase 3, and its preferred substrate is Col2. In *MMP13* knockout mice the severity of induced OA is reduced [287], whereas *Col2-MMP13* mice develop spontaneous focal lesions and GAG loss compared to wild type [288]. These studies illustrate that ADAMTS-4/5 and MMP13 contribute to the disease progression of OA.

OA shares many features with endochondral ossification. The OA cartilage matrix is degraded, mineralized, and vascularized, and the chondrocytes undergo a process similar to the proliferation-hypertrophy-terminal differentiation-apoptosis sequence observed in endochondral ossification [289]. OA chondrocytes have an increased proliferation capacity [290] and increased expression and secretion of Ihh targets [291], Runx2 [292], Col10 [278, 293], ALP [280], and MMP13 [282, 294, 295]. It is likely that many of the same signals that regulate chondrocyte maturation are also at work in the propagation of OA. Activation of Ihh or the β-catenin pathway in articular chondrocytes causes OA in mice [291, 296, 297], while mice that are unresponsive to TGF-β signaling develop spontaneous OA [259, 260]. Haploinsufficiency of Runx2 protects mice from induced OA [292], and overexpression of Runx2 aggravates it [298]. Ihh, Runx2, and β-catenin signaling are not active in articular cartilage, but are upregulated in OA [291, 292, 296], and TGF-β is downregulated in chondrocytes found in osteophytes [299]. These data suggest that the advancement of OA is aided by deregulation of normal articular chondrocyte signaling.

The initial cause of OA is unknown and probably varies by individual, but collagen and PG fragments released from the matrix when cartilage degeneration begins initiate a feedback loop that sustains the aberrant chondrocyte phenotype. Collagen and PG fragments have been shown to induce MMP and ADAMTS secretion in chondrocytes [300-304]. The chondrocyte response to tissue damage should be to produce more extracellular matrix, which does happen during early OA, but the anabolic response driven by TGF-β is eventually overwhelmed by the increase in catabolic enzymes leading to further degradation. TGF-β signaling is also itself altered due to shifts in TGF-β

receptor expression in OA; an increasing ALK1/ALK5 ratio is observed in experimentally induced OA [142]. The resulting switch from Smad2/3 activation to Smad1/5/8 activation mediates increased *MMP13* expression [142, 254]. In addition, Col2 fragments induce the production of the pro-inflammatory cytokines TNF-α and IL-1β [300, 305, 306]. These cytokines in turn cause chondrocytes to upregulate MMPs and ADAMTS [285, 295, 307-309], generating a positive feedback loop of cartilage degradation and inflammation. The β-catenin signaling pathway is also sensitive to matrix fragments. Upon treatment with papain or collagenase, the number of β-catenin positive cells in articular cartilage is increased [297]. The change in β-catenin localization is reflected in OA; there is virtually no β-catenin present in normal cartilage, but it is widespread in OA tissue [310]. In articular chondrocytes, overexpression of β-catenin leads to increased expression of MMPs and ADAMTS [310]. Since activation of β-catenin signaling in chondrocytes is also associated with hypertrophy, it may play a similar role in the pathogenesis of OA after the initial degradation event.

The subchondral bone is another rich source of signals that may aggravate OA. Healthy articular cartilage is impervious to vascularization, but OA chondrocytes express VEGF with increasing OA severity, which correlates with vascular invasion [50, 311-314]. Breaching of the tidemark by vascular channels brings an influx of signals from the underlying bone into the previously sequestered cartilage. Co-culture with osteoblasts causes chondrocytes to downregulate expression of *Sox9*, *Col2*, and *Aggrecan*, and increase expression of Col10, Runx2, *MMP13*, and ALP as well as matrix mineralization [315-317]. Therefore, vascular invasion may serve to establish another positive feedback

loop via an influx of factors that promote hypertrophic differentiation of chondrocytes leading to further vascular invasion and the advancement of OA.

1.7 Hypothesis and Aims

Regulation of the chondrocyte phenotype depends on the complex interaction of the physical and biological factors described above and more. Many of these regulatory factors are also involved in directing MSC chondrogenesis. Two of the most commonly used parameters to experimentally induce MSC chondrogenesis studies are 3D cultures and medium containing TGF-β. Morphology is an important physical regulator of the chondrocyte phenotype as chondrocytes dedifferentiate in monolayer culture [27]. *In vivo*, the TGF-β superfamily promotes the chondrocyte phenotype, opposes hypertrophy, and its signaling is deregulated in pathological conditions [143, 260, 318]. That these factors regulate articular chondrocytes is used as a guiding principle in MSC chondrogenesis with great success, but the resulting engineered tissues are cannot be used to replace articular cartilage as MSC chondrogenesis also features aspects of maturing and/or diseased chondrocytes. Therefore, it is thus necessary to manipulate other factors in the interest of better controlling the chondrogenic MSC phenotype. Different combinations of growth factors have been proposed to improve MSC chondrogenesis and restore the proper phenotype in diseased articular cartilage [319-321]. The main focus of this work is to identify additional factors that can be used to this end. Our selection of factors was inspired by those that regulate the chondrocyte phenotype *in vivo*.

Hydrostatic pressure is a force unique to articular cartilage. High joint contact forces are resisted by fluid pressure in the highly hydrated cartilage tissue. Compression

and shear forces are present in cartilage during joint loading as well, and reinforce the chondrocyte phenotype in chondrocytes. However, these forces are also present in other tissues, so their role in cells undergoing chondrogenesis will depend heavily on other factors. Physiologic levels of hydrostatic pressure increase synthesis of cartilage matrix components in both chondrocytes and MSCs, but little is known about its effects on hypertrophic differentiation [61]. In a mathematical model of intermittent joint loading, hydrostatic pressures were shown to promote chondrocyte maintenance, while shear and tensile stresses favored terminal differentiation and endochondral ossification [322]. Therefore, hydrostatic pressure may very well prevent differentiation in MSCs as well.

At the convergence of developmental chondrogenesis, endochondral ossification, and OA is the Wnt/β-catenin signaling pathway. After the initial condensation event, β-catenin negatively regulates chondrogenesis and positively regulates hypertrophy. β-Catenin signaling is virtually absent in articular cartilage, but is present at high levels in mesenchymal precursors. MSCs in pellet culture share many features in common with mesenchymal cells from their initial high density to their hypertrophic response to TGF-β withdrawal and T3 supplementation [323]. However, β-catenin signaling has not been characterized in chondrogenic MSCs. If MSCs continue to express β-catenin during chondrogenic culture, they could be predisposed to hypertrophy. Further, TGF-β increases β-catenin signaling in monolayer MSCs, so the CM may actually promote hypertrophy in MSCs [324]. This signaling pathway is a promising target for modulating MSC chondrogenesis.

Many of the factors involved in regulating chondrocytes could be targets for improving MSC chondrogenesis. Of the factors discussed, hydrostatic pressure and β-

catenin are notable regulators of the articular chondrocyte phenotype, because of their specificity; hydrostatic pressure because it is the dominant load modality in cartilage, and β-catenin signaling because of its absence in articular chondrocytes. The hypothesis of this work is that MSC chondrogenesis can be regulated by the same regulatory mechanisms as articular chondrocytes. Specifically, that hydrostatic pressure will promote chondrogenesis and suppress hypertrophy, and β-catenin signaling will inhibit chondrogenesis and promote hypertrophy. To address this hypothesis, we have undertaken the following aims:

Aim 1: Characterize the temporal profile of chondrogenic differentiation in pellet cultures of MSCs (up to 21 days) to identify biological patterns in comparison to those in cartilage development.

    a. Chart the expression of chondrogenic genes and cartilage matrix deposition.

    b. Map the expression of hypertrophy genes and hypertrophic matrix deposition.

    c. Assess the expression of non-chondrogenic genes.

Aim 2: Determine the effects of cyclic hydrostatic pressure on MSC chondrogenesis and intracellular signaling.

    a. Evaluate differences in the development of chondrogenic and hypertrophy characteristics due to hydrostatic pressure.

    b. Determine differences in phenotype regulation by different loading regimes in order to better understand the mechanobiology of chondrogenic MSCs at different stages of differentiation.

c. Identify mechanosensitive transcription factors that mediate the effects of hydrostatic pressure.

Aim 3: Identify changes in β-catenin expression during MSC chondrogenesis.

a. Determine changes in β-catenin transcription.

b. Identify differences in β-catenin activation.

c. Localize the subcellular distribution of β-catenin in the membrane, cytosol, and nuclear compartments.

Aim 4: Assess the functional role of β-catenin-mediated gene transcription in the development of hypertrophy in chondrogenic MSC pellets.

a. Suppress β-catenin signaling, and determine its effects on hypertrophy.

b. Activate β-catenin signaling, and determine its effects on hypertrophy.

The global aim of this work is to identify regulatory elements in MSCs that can be exploited in tissue engineering and regenerative medicine approaches. If hydrostatic pressure and β-catenin are capable of regulating MSC chondrogenesis, these factors could be incorporated into tissue engineering protocols or adapted to modify OA chondrocytes and MSCs in diseased joints.

Chapter 2 Materials and Methods

MSC Isolation

MSCs were isolated from human trabecular bone on the basis of tissue culture plastic adherence. Femoral heads from male and female patients between the ages of 47 and 71 years who had undergone total hip arthroplasty were collected in accordance with Internal Review Board policies at the National Institutes of Health and the University of Pittsburgh. Loose trabecular bone was cored out of the femoral head and placed in a collection dish. The remaining trabecular bone was then flushed from the femoral head with rinsing medium (RM; Dulbecco's Modified Eagle's Medium with 4.5 g/L D-glucose, L-glutamine, and 110 mg/L sodium pyruvate (DMEM; Gibco) and Antibiotic-Antimycotic (AA; Gibco)) using a 16 or 18 gauge hypodermic needle to wash any remaining marrow into the collection dish. The loose trabecular bone was minced to release its marrow into the RM, and the RM-marrow mixture was filtered through a 40 μm sterile mesh filter into conical tubes. The remaining trabecular bone chips were washed with RM and filtered into conical tubes. The tubes were centrifuged for 5 minutes at 300g to produce a cell pellet, the supernatant was aspirated, and the cells were rinsed in RM. The cells were centrifuged and rinsed a second time, and then suspended in expansion medium (EM; α-MEM (Gibco), 10% MSC fetal bovine serum (FBS; Gibco), AA, and 1 ng/mL fibroblast growth factor 2 (FGF2;R&D Systems)). After setting aside cells for colony forming assays to test their clonal capacity and differentiation assays to test their multilineage potential, the remaining cells were divided into two 150 cm^2 tissue culture-treated polystyrene flasks and cultured under the standard culture conditions

described below. After 3-4 days, non-adherent cells were rinsed away with phosphate buffered saline (PBS; Gibco). Adherent cells were defined as passage 1 (P1) MSCs.

MSC Culture and Passaging

MSC cultures were maintained in a humidified incubator at 37°C with 20% O_2 and 5% CO_2. EM or growth medium (GM; DMEM, 10% FBS, AA) was supplied to MSCs at 0.15 mL/cm^2 and replaced every 4-5 days. Upon reaching 80% confluence, MSCs were washed with warm PBS and treated with 30 μL/cm^2 of warm 0.125% trypsin-EDTA (Gibco) for 2 minutes at 37°C followed by mechanical agitation. The trypsin was neutralized with an equal volume of GM, and the resulting cell suspension was centrifuged at 200g for 5 minutes to form a pellet. The supernatant was aspirated and the MSCs were suspended in GM. 3,000 cells/cm^2 MSCs were plated at the next passage (P2, P3, or P4) in GM and returned to standard culture conditions. At this stage, MSCs could also be put into frozen storage or made into pellets.

MSC Storage

For long-term storage, MSCs were cryogenically frozen in liquid nitrogen. 1×10^6 MSCs/mL were suspended in Recovery Cell Culture Freezing Medium (Gibco) and aliquoted into cryogenic vials. The vials were slowly frozen overnight at -80°C in a Mr. Frosty freezing container (Nalgene) and transferred to a CryoPlus storage unit (Thermo Scientific). To recover frozen cells for use, vials were warmed in a 37°C water bath until the suspension was just thawed, about 1 minute. 3,000 cells/cm^2 were plated at the next

passage in 0.15 mL/cm^2 room temperature GM and returned to standard culture conditions.

Chondrogenic Differentiation

Chondrogenic differentiation of MSCs was performed in pellet culture. To form pellets, MSCs were first suspended in chondrogenic differentiation medium (CM; DMEM, AA, ITS+ Premix Universal Culture Supplement (BD Biosciences), 50 µg/mL ascorbic acid (Sigma), 40µg/mL L-proline (Sigma), 0.1 µM water soluble dexamethasone (Sigma), and 10 ng/mL recombitant human TGF-β3 (R&D Systems)) at 8.3×10^5 cells/mL. 300 µL/well of cell suspension was dispensed into a conical bottom 96 well plate, and the plate was centrifuged at 300g for 7 minutes to produce a pellet of 2.5×10^5 cells in each well. MSC pellets were cultured in a humidified incubator at 37°C with 20% O_2 and 5% CO_2 in the 96 well plates. After 16-24 hours, pellets were considered stable. CM was supplied at 300 µL/pellet and replaced every 2-3 days.

Sulfated GAG Quantification

MSC pellets were digested overnight in 100 µL/pellet of 4% papain (Sigma) in papain digestion buffer (PB; 0.1 M sodium acetate, 0.01 M cysteine hydrochloride, 0.05 M EDTA) at 60°C. The sulfated GAG content of the extracellular matrix was determined using the Blyscan Sulfated Glycosaminoglycan Assay (Biocolor Life Science Assays). 1 mL Blyscan Dye Reagent was added to tubes containing up to 20 µL PB sample digest and rocked gently for 1 hour to precipitate GAG-dye complexes. The tubes were centrifuged at maximum speed for 30 minutes to pellet the precipitate. The supernatant

was discarded, and 1 mL Blyscan Dye Dissociation Reagent was added to all tubes and rocked gently for 1 hour to dissolve the dye pellet. The dye was transferred to a clear 96 well plate, and the absorbance of each sample was measured at 656 nm using a Biotek Synergy HT Multi-Mode Microplate Reader. GAG amounts were determined using a standard curve generated from known amounts of chondroitin-6-sulfate (Sigma) and normalized to DNA content. Samples were assayed in duplicate and the results were averaged.

DNA Quantification

DNA was quantified using the Quant-iT PicoGreen dsDNA Assay (Invitrogen). 10 µL pellet digest was dispensed into an opaque white 96 well plate. PicoGreen dsDNA reagent in Tris-EDTA (TE) was added to the wells and mixed by gentle agitation. The plate was incubated in the dark at room temperature for 5 minutes. Fluorescence (excitation: 480 nm, emission: 520 nm) was measured using a Biotek Synergy HT Multi-Mode Microplate Reader. DNA amounts were determined using a standard curve generated from serially diluted Lambda DNA (Invitrogen). Samples were assayed in duplicate and the results were averaged.

RNA Isolation

MSC pellets (1-5 per sample) were dissolved in 1 mL TRIzol reagent (Invitrogen) with a plastic pestle and vortexed for 1 minute. 200 µL chloroform was added, and the samples were vortexed for 15 seconds. After 5 minutes incubation at room temperature, samples were centrifuged at $12,000g$ for 15 minutes at 4°C. The aqueous phase was transferred to

an equal volume of 70% ethanol to precipitate the RNA from solution. For MSCs in monolayer, cells were lysed in 37 µL/cm^2 Buffer RLT (Qiagen), homogenized in QIAshredder columns (Qiagen), and added to an equal volume of 70% ethanol. RNA was purified from the ethanol mixture using the RNeasy Micro Kit (Qiagen). The mixture was added to the silica membrane of an RNeasy MinElute Spin to bind the RNA. The column was serially washed and centrifuged with 350 µL Buffer RW1 (2 times), 500 µL Buffer RPE, and 500 µL 80% ethanol to remove small RNAs and other debris. Between Buffer RW1 washes, the column was treated with 80 µL of DNase I (341 Kunitz units/mL) in Buffer RDD for 15 minutes at room temperature to eliminate genomic DNA. Finally, the RNA was dissolved in 14 µL of water and collected by centrifugation at maximum speed for 1 minute. RNA concentration was determined using a NanoDrop Spectrophotometer (Thermo Scientific).

Reverse Transcription (RT)

RNA totaling between 0.2 and 2 µg in 12 µL was reverse transcribed to cDNA using the Superscript III First-Strand Synthesis System (Invitrogen). The RNA was mixed with 4 µL 25 µM oligo(dT) primers in Annealing Buffer and incubated at 65°C for 5 minutes to hybridize the primers to the RNA. Next, 24 µL First-Strand Reaction Mix containing 1 mM each dNTP and SuperScript III/RNaseOUT Enzyme Mix was added and incubated at 50°C for 50 minutes to reverse transcribe the RNA. The RT reaction was terminated at 85°C for 5 minutes. The cDNA was diluted to 1 ng/µL in RNase-free water with an assumed RNA to cDNA conversion efficiency of 1:1.

Real-Time Reverse Transcription Polymerase Chain Reaction (RT-PCR)

Previously validated primers for the genes of interest were synthesized or purchased (Table 2-1). PCR master mix (MM) was prepared from the primers and SYBR Green PCR Master Mix (Applied Biosystems) and aliquoted into 96 well PCR reaction plates. 5 ng of cDNA was added to wells containing MM and amplified for 40 cycles on a Stratagene Mx3000 QPCR System or an Applied Biosystems StepOne Plus PCR System using the amplification parameters listed in Table 2-2. Fold changes in gene expression relative to day 1 untreated samples were calculated using the Comparative Threshold Cycle ($\Delta\Delta C_T$) method [325] with *glyceraldehyde 3-phosphate dehydrogenase* (*GAPDH*) or *hypoxanthine-guanine phosphoribosyltransferase* (*HPRT*) serving as internal control genes. Each cDNA-primer sample was amplified in triplicate and the ΔC_Ts were averaged. Fold changes were computed relative to a baseline of 0 such that a fold change of 1 corresponded to a 100% increase in gene expression relative to untreated day 1 expression, and a fold change of -1 indicated that expression was 100% greater in untreated day 1 samples.

Paraffin Embedding

Pellets were fixed in 4% paraformaldehyde at 4°C for 2 hours. The pellets were serially dehydrated in ethanol with a drop of alcoholic Eosin Y (SelecTech) and cleared in xylenes (Fisher) 3 times for 20 minutes each. Pellets were incubated in a 1:1 mixture of xylenes and Paraplast X-Tra Tissue Embedding Media (paraffin) for 20 minutes at 58°C and then transferred to 58°C paraffin 3 times for 20 minutes each. Pellets were positioned in a metal mold filled with hot paraffin, and the mold was cooled on a room temperature

Table 2-1: Real-Time RT-PCR Primers

Gene	Forward Primer	Reverse Primer
GAPDH	TGCACCACCAACTGCTTAG	GATGCAGGGATGATGTTC
HPRT	GGTCAGGCAGTATAATCCAAAGA	AGGCTCATAGTGCAAATAAACAGT
Col1a1	TAAAGGGTCACCGTGGCT	CGAACCACATTGGCATCA
Col2a1	CCACACTCAAGTCCCTCAAC	GCTGCTCCACCAGTTCTTC
Col10a1	CCCAACACCAAGACACAGTT	CCTCTATCACCTTTGATGCCT
Ctnnb1	SA Biosciences PPH00643E	
ALP	TGACCTCCTCGGAAGACACTC	TGGTAGTTGTTGTGAGCATAGTCC
Acan	GGGTCAACAGTGCCTATCAG	GGGTCAACAGTGCCTATCAG
Sox9	TGAAGAAGGAGAGCGAGGAG	GTCCAGTCGTAGCCCTTGAG
Runx2	CAACCACAGAACCACAAGTGCG	TGTTTGATGCCATAGTCCCTCC
Oc	AGGAGGGCAGCGAGGTAG	GAAAGCCGATGTGGTCAGC
BSP	TGCCTTGAGCCTGCTTCC	GCAAAATTAAAGCAGTCTTCATTTTG
Ihh	CCTCAGTTGATGCTGCTAAATTC	AACAGTCTCTGGATGTGTCTTG
PTHrP	CGACGACACACGCACTTGAAAC	CGACGCTCCACTGCTGAACC
MMP13	GGACCCTGGAGCACTCATGTTTC	TCGGAGACTGGTAATGGCATCAAG
MMP2	CCCCCAAAACGGACAAAGAG	CACGAGCAAAGGCATCATC

Table 2-2: Real-Time RT-PCR Amplification Parameters

Gene	Melting Temperature	Annealing Temperature	Extension Time at 72°C	Working Concentration
GAPDH	95°C	60°C	0 s	200 nM
HPRT	95°C	55°C	30 s	200 nM
Col1a1	95°C	58°C	30 s	200 nM
Col2a1	95°C	60°C	0 s	150 nM
Col10a1	95°C	60°C	0 s	100 nM
Ctnnb1	95°C	60°C	0 s	500 nM
ALP	95°C	60°C	0 s	150 nM
Acan	95°C	56°C	15 s	50 Nm
Sox9	97°C	60°C	0 s	50 nM
Runx2	95°C	56°C	0 s	50 nM
Oc	95°C	60°C	0 s	200 nM
BSP	95°C	60°C	0 s	100 nM
Ihh	95°C	60°C	0 s	150 nM
PTHrP	95°C	60°C	0 s	150 nM
MMP13	95°C	60°C	0 s	150 nM
MMP2	95°C	58°C	0 s	150 nM

surface to set the positions of the pellets. An embedding cassette was placed over the mold and frozen at -20°C for 10 minutes until the cassette was easily separated from the mold. Paraffin blocks were sectioned to 5 μM thickness and mounted on glass slides.

Safranin O Staining

Paraffin sections were deparaffinized in Histoclear (National Diagnostics) and rehydrated through an ethanol series to tap water. Slides were stained with Hematoxylin (SelecTech) for 5 minutes and destained in acid-alcohol (0.25% HCl in 70% ethanol) with washes in running tap water in between. Next, slides were counter-stained with 0.001% Fast Green (Electron Microscopy Sciences) for 5 minutes, rinsed with 1% acetic acid for 15 seconds, and stained with 0.1% Safranin O solution (Sigma) for 10 minutes. After staining, slides were dehydrated in ethanol and cleared with Histoclear. Cover slips were mounted over stained sections using Permount (Fisher) and sealed with clear nail polish.

Collagen Immunohistochemistry

Paraffin sections were deparaffinized in Histoclear and rehydrated through an ethanol series to tap water. Antigen retrieval was achieved via treatment with 2 mg/mL hyaluronidase (Millipore) for 15 minutes at 37°C followed by treatment with 1 mg/mL pronase (Roche Diagnostics) for 30 minutes at 37°C. Endogenous peroxidase activity was blocked with 3% H_2O_2 for 5 minutes. Sections were washed 3 times in PBS, blocked in 2% horse serum for 1 hour, and incubated with primary antibody (see Table 2-3 for antibody specifics) for 2 hours at room temperature. Sections were then washed 3 times with PBS and incubated with a biotinylated secondary antibody. The signal was

amplified with the VECTASTAIN Elite ABC Kit (Vector Laboratories) and visualized

with the VIP Peroxidase Substrate Kit (Vector Laboratories). After staining, slides were

dehydrated in ethanol and cleared with Histoclear. Cover slips were mounted over stained

sections using Permount and sealed with clear nail polish.

Table 2-3: Collagen Immunohistochemistry Antibodies

Antigen	Product Number	Working Concentration
Collagen, Type II	Developmental Studies Hybridoma Bank II-II6B3	2.5 μg/mL
Collagen, Type X	Courtesy of Jurgen Mollenhauer, NMI	5 μg/mL or whole hybridoma supernantant
Mouse IgG	Vector Laboratories BA-2000	7.5 μg/mL

Hydrostatic Loading

Cyclic hydrostatic pressure was applied to chondrogenic MSC pellets using a custom-

built apparatus (Figure 2-1). Pellets were transferred to 25 mL glass vials filled with CM

and capped with flexible Teflon-coated silicone septa to allow for pressure to be

transferred to the fluid inside the vial. Glass vials were placed in 2.5 mm thick polyester

pouches (Kapak) filled with distilled water, which were then heat-sealed to create an

entirely fluid phase environment. The pouch was then placed in the loading chamber,

which was also filled completely with water and sealed air-tight. Attached to the loading

chamber was a pressure input port and a pressure transducer to monitor the level of

pressure inside the chamber. A LabVIEW program was designed to regulate a computer-

controlled valve connected to a pressurized air supply, generating a sinusoidal wave of air

pressure. The air pressure was converted to hydrostatic pressure by a pneumatic-to-

hydraulic pressure booster connected to the pressure input port on the loading chamber.

Pellets were loaded for 3 or 4 hours per day at 0.8 Hz with a peak pressure of 10 MPa.

The loading chamber was maintained at 37°C in a water bath. After loading, pellets and CM were transferred from the vials to 100 mm suspension culture dishes to resume chondrogenic culture. Pressure-free controls were likewise prepared in vials and immersed in a 37°C water bath for the duration of loading.

Alcian Blue Staining
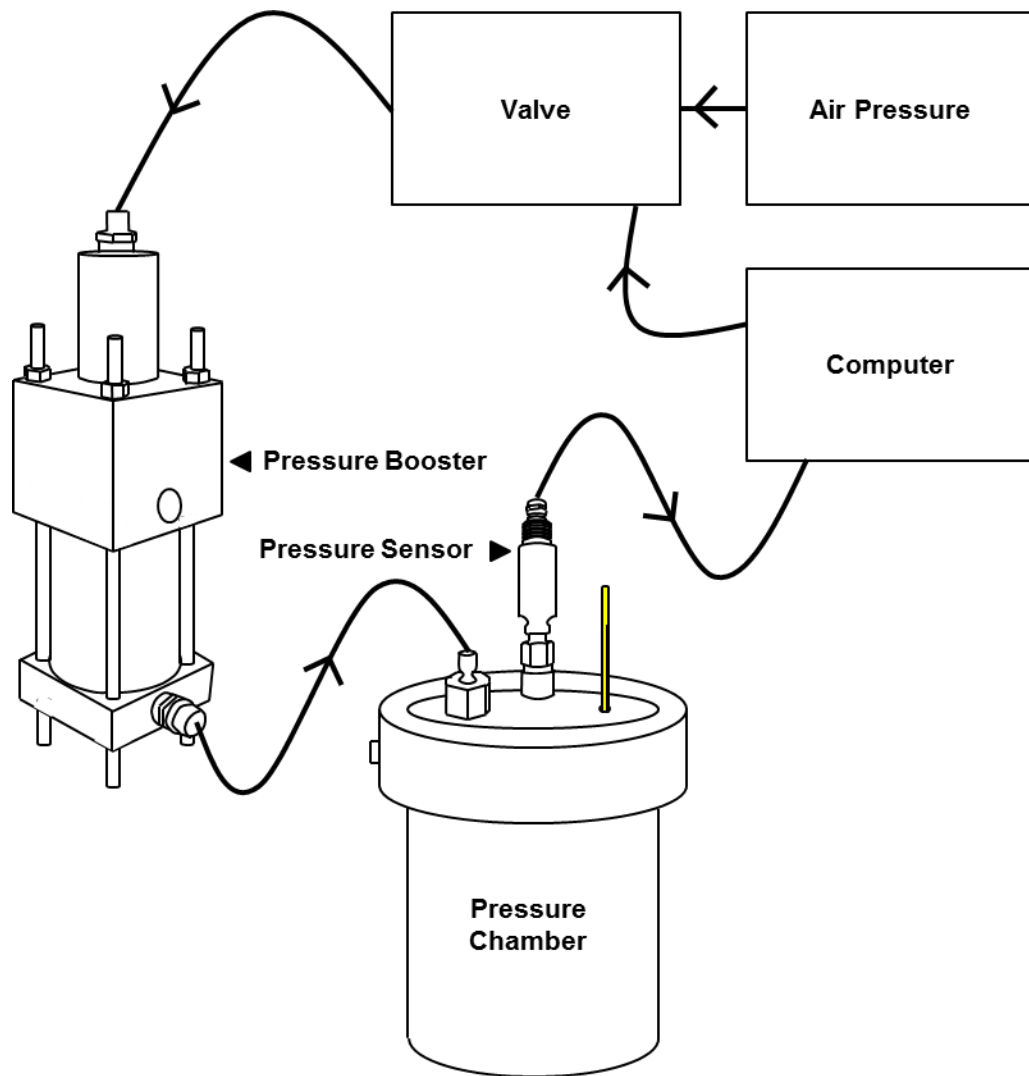
Figure 2-1: Schematic of Hydrostatic Loading Apparatus. Air pressure delivery was regulated by a computer controlled proportional air valve. Air pressure was converted to hydrostatic pressure and amplified by a pneumatic-to-hydraulic pressure booster (49:1). Hydrostatic pressure was then transferred to the fluid-filled pressure chamber containing MSC pellets. A pressure sensor attached to the chamber provided feedback to the computer controlling the pressure delivery valve in order to generate the desired

Paraffom sections were deparaffinized in Histoclear and rehydrated through an ethanol series to distilled water. Slides were immersed in 3% acetic acid for 3 minutes and then stained with Alcian blue for 10 minutes. Slides were then destained in acid-alcohol for 3 minutes. Next, slides were dehydrated in ethanol and cleared with Histoclear. Cover slips were mounted over stained sections with Permount (Fisher) and sealed with nail polish.

Reporter Plasmid Transfection

MSCs were transfected with luciferase reporter plasmids (Table 2-4) by electroporation using an Amaxa Nucleofector II Device (Lonza). 7.5×10^6 MSCs/mL were suspended in Human MSC Nucleofector Solution (Lonza) with 37.5 μg/mL Firefly reporter plasmid or pcDNA3 control and 150 ng/mL Renilla control plasmid. The nucleofection sample was transferred to an Amaxa cuvette and electroporated using the U-23 setting on the Amaxa Nucleofector II. Immediately after electroporation, cells were flushed from the cuvette bottom with warm transfection recovery medium (TRM; DMEM, 20% FBS, Anti-Anti). Transfected MSCs were plated at 4.5×10^6 cells/cm^2 in TRM and cultured for 24 hours before being switched back to GM. After another day MSCs were used for experiments.

Table 2-4: Luciferase Reporter Plasmids

Plasmid	Vector	Size
pAP1-Luc *Cis*-Reporter	Stratagene 219074	5.7 kb
pNFAT-Luc *Cis*-Reporter	Stratagene 219088	5.8 kb
NFκB-Luc *Cis*-Reporter	Stratagene 219078	5.7 kb
TOPFlash TCF Reporter	Millipore 21-170	5.5 kb
pRL *Renilla* Luciferase Control	Promega E2241	4.1 kb
pcDNA3[+]	Invitrogen V79020	5.4 kb

Luciferase Reporter Assay

MSC pellets were manually disrupted in 100 µL/pellet of Passive Lysis Buffer (PLB; Promega) using a plastic pestle until the extracellular matrix was no longer visible. The cells were allowed to lyse at room temperature for 10 minutes and then frozen at -80°C. Luciferase activity was determined using the Dual-Luciferase Reporter Assay (Promega). PLB lysate was centrifuged at 12,000g for 10 minutes at 4°C. 20 µL supernatant was mixed with 100 µL Luciferase Assay Reagent, and the firefly luminescence was measured immediately on a Promega GloMax 20/20 Luminometer. Next, 100 µL Stop & Glo Reagent was mixed into the sample, and the Renilla luminescence was measured immediately on the luminometer. The firefly luminescence was normalized to the Renilla luminescence. Samples were assayed in duplicate or triplicate, and the results were averaged. The luminescence of a blank tube was subtracted from all values.

Cellular Protein Collection

MSC pellets were washed in cold PBS to remove serum proteins and lysed in 100 µL/pellet cold Lysis Buffer (LB; 0.5% Triton-X, 10 mM Tris, 150 mM NaCl, 1 mM EDTA, 6 M urea, Protease Inhibitor Cocktail (Millipore), Halt Phosphatase Inhibitor Cocktail (Pierce)). The pellets were manually disrupted using a plastic pestle on ice until the extracellular matrix was no longer visible and lysed on ice for 10 minutes. Lysate was centrifuged at 12,000g for 15 minutes at 4°C to remove any remaining precipitate.

Western Blotting

Protein samples were subjected to reducing SDS-PAGE. Cell lysate in LB was heated with 30% Laemmli Sample Buffer (Bio-Rad) and 5% β-mercaptoethanol at 95°C for 5 minutes to denature the proteins and then run in an acrylamide gel in Tris/Glycine/SDS buffer (Bio-Rad) at 200 V for 1 hour. Gels were equilibrated in 10% methanol in SDS-free Towbin buffer (Santa Cruz Biotechnology) for 30 minutes, and transferred to a polyvinylidene fluoride (PVDF) membrane (Millipore) at 100 V for 1 hour. Membranes were blocked in 3% milk (Bio-Rad) in 0.25% Tween-20 (Sigma) in Tris-Buffered Saline (TBS-T) for 1 hour and incubated with primary antibody in 1% milk in TBS-T for 90 minutes at room temperature or overnight at 4°C (see Table 2-5 for antibody specifics). After 3 washes with TBS-T, PVDF membranes were incubated with a horseradish peroxidase (HRP)-conjugated secondary antibody (Pierce) in 1% milk in TBS-T for 1 hour at room temperature. After 7 washes with TBS-T, SuperSignal Working Solution (Pierce) was added to the membrane and incubated for 5 minutes at room temperature.

Table 2-5: Western Blot Antibodies

Antigen	Product Number	Working Concentration	Band Size
Active β-Catenin	Millipore 05-665	2 μg/mL	92 kDa
Phospho-Erk1/2	Cell Signaling 9101	1:1000	42, 44 kDa
Erk1/2	Millipore 05-1152	250 ng/mL	42, 44 kDa
GAPDH	Millipore MAB374	1 μg/mL	38 kDa
β-Tubulin	Abcam ab7792	1 μg/mL	50 kDa
Caveolin	BD Biosciences 610059	1:5000	22 kDa
HDAC2	Abcam ab51832	1 μg/mL	60 kDa
Total β-Catenin	Abcam ab32572	1:1000	92 kDa
MMP13	Abcam ab39012	1 μg/mL	60 kDa
MMP1	Abcam ab28196	1 μg/mL	54 kDa
MMP2	Abcam ab38919	1 μg/mL	72 kDa

Bands were visualized using the Fotodyne FOTO/Analyst Luminary/FX System. Molecular weights of bands were estimated based on a fluorescent protein ladder (Bio-Rad). All Western blots were repeated twice and representative images are presented.

Active β-Catenin Enzyme-Linked Immunosorbent Assay (ELISA)

The Multi-Kinase ELISA Array System (Symansis) was used to detect active β-catenin (dephosphorylated at serines 33 and 37, and at threonine 41). The lysate was diluted 1:5 with Sample Dilution Buffer and added to a microwell plate coated with antibody against active-β-catenin for 2 hours at room temperature. Wells were washed 3 times with Wash Buffer (WB), and Biotin-Conjugated Detection Antibody was added for 2 hours at room temperature. After 3 washes with WB, HRP-conjugated streptavidin was added to each well for 30 minutes at room temperature, and then the wells were washed 3 more times with WB. Tetramethylbenzidine Substrate Solution was added to the wells and incubated in the dark for 20 minutes or until the first well on the plate turned dark blue. Stop Solution was added to each well and the plate was gently agitated until all wells turned yellow. The absorbance at 450 nm was measured using a Biotek Synergy HT Multi-Mode Microplate Reader. Samples were assayed in duplicate and the results were averaged.

Subcellular Fractionation

MSCs were separated into cytoplasmic, membrane, and nuclear fractions using the Thermo Scientific Subcellular Protein Fractionation Kit. All incubation and centrifugation steps were performed at 4°C unless otherwise specified. Pellets were washed in ice cold PBS and ground up in 25-40 μL/pellet ice cold Cytoplasmic

Extraction Buffer in a Duall Tissue Grinder (Kontes) on ice. The lysate was incubated for 10 minutes with gentle mixing and centrifuged at $500g$ for 5 minutes. The supernatant containing the cytoplasmic fraction (CF) was transferred to a new tube. Ice cold Membrane Extraction Buffer was added to the pellet, vortexed at maximum speed for 5 seconds, incubated for 10 minutes with gentle mixing, and centrifuged at $3000g$ for 5 minutes. The supernatant containing the membrane fraction (MF) was transferred to a new tube. Ice cold Nuclear Extraction Buffer was added to the pellet, vortexed at maximum speed for 15 seconds, incubated for 30 minutes with gentle mixing, and centrifuged at $5000g$ for 5 minutes. The supernatant containing the soluble nuclear fraction was transferred to a new tube. Room temperature Nuclear Extraction Buffer containing 5 mM $CaCl_2$ and ≥ 3 units/μL Micrococcal Nuclease was added to the pellet, vortexed at maximum speed for 15 seconds, incubated for 15 minutes at room temperature, and vortexed again at maximum speed for 15 seconds. After centrifugation at $16,000g$ for 5 minutes, the supernatant containing the chromatin-bound nuclear fraction was transferred to the tube containing the soluble nuclear fraction to yield the whole nuclear fraction (NF). The fractions were used for Western blotting as described above.

Lentiviral Luciferase Reporter Transduction

MSCs were plated at a density of 10,000 cells/cm^2 in GM and allowed to adhere overnight. Adherent cells were washed with PBS and given 0.1 mL/cm^2 viral transduction medium (VM) at room temperature. VM was prepared by adding 2×10^5 transducing units (TU)/mL of Cignal Lenti TCF/LEF Reporter (SABiosciences) or Cignal Lenti

Negative Control Reporter (SABiosciences), 1×10^5 TU/mL Cignal Lenti Renilla Control Reporter (SABiosciences), 1μL/mL polybrene transduction reagent (Millipore) to serum-free GM. MSCs were incubated with VM at 32°C with 20% O_2 and 5% CO_2 for 16-18 hours. The VM was then replaced with fresh GM, and the cells were returned to 37°C. After 2-3 days, transduced MSCs were suspended and used for experiments. Luciferase activity was determined as described above.

β-Catenin Small Molecule Inhibitor and Enhancer Treatments

During chondrogenesis of MSC pellets, CM was supplemented with concentrations of 0.1, 1, or 10 μM XAV939 (Sigma) to inhibit β-catenin signaling, or 5, 10, or 20 μM of SB216763 (Sigma) or 500 nM CHIR99021 (StemRD) to enhance β-catenin signaling beginning on day 1. All concentrations of XAV939, SB216763, and CHIR99021 were prepared at 1000x in DMSO. Controls were treated with 0.1% DMSO. Other culture conditions remained the same including CM changes of 300 μL/pellet every 2-3 days.

β-Catenin siRNA Transfection

MSCs were suspended at 5×10^4 cells/mL in OptiMEM (Gibco) with 10% FBS. siPORT Lipid Transfection Agent (Ambion) was diluted 1:20 in OptiMEM and incubated for 10 minutes at room temperature. siRNA targeting three different sections of the *Ctnnb1* sequence (Ambion) were diluted to 1.5, 3.0, or 15 μM in OptiMEM. Lipid transfection medium (LM) was made by mixing the siRNA and siPORT solutions and incubating for 10 minutes at room temperature. Control LM contained scrambled siRNA in place of *Ctnnb1* siRNA. 20 μL/cm² of LM was added to the tissue culture plate, and 0.2 mL/cm²

of cell suspension was layered over it. When reporter-infected cells were used, LM was added to adherent cells and topped with OptiMEM with 10% FBS. Cells were cultured under standard culture conditions for 24 hours before replacing the LM with GM.

β-Catenin Immunocytochemistry

Monolayer MSCs seeded at 10^4 cells/cm^2 on glass coverslips in 24-well tissue culture-treated polystyrene dishes were washed in PBS and fixed with 4% paraformaldehyde for 15 minutes. After washing again with PBS, cell membranes were permeabilized with 0.1% Triton-X in PBS for 5 minutes and washed again. Cells on coverslips were blocked in 1% BSA for 1 hour and incubated with anti-β-catenin antibody (Abcam) 1:250 in 1% BSA for 1 hour. Next, MSCs were washed in PBS for 20 minutes and incubated with anti-rabbit secondary antibody conjugated to Alexa Fluor 647 fluorescent dye (Invitrogen) 1:1000 in 1% BSA for 1 hour. The cells were washed in PBS for 15 minutes and the nuclei were labeled with DAPI (Invitrogen) 1:2000 in PBS for 2 minutes. After another washing, the coverslips were mounted on glass slides with VECTASHIELD (Vector Laboratories) and sealed with clear nail polish.

Conditioned Medium Collection

Pellets were cultured in phenol-free CM made from DMEM with 4.5 g/L D-glucose, L-glutamine, and 25 mM HEPES (Gibco) buffer supplemented with the standard amounts of AA, ITS+ Premix, ascorbic acid, L-proline, dexamethasone, and TGF-β3. After 3 days, conditioned CM was collected from each well and centrifuged at 2500g for 5 minutes at 4°C to remove debris.

MMP Activity Assay

Conditioned medium samples were incubated with 1 mM 520 MMP FRET Substrate XI (Anaspec; diluted 1:100 in phenol-free CM) for 1 hour in a black bottom 96 well plate. The fluorescence (excitation: 480 nm, emission: 520 nm) was recorded every 5 minutes on a Biotek Synergy HT Multi-Mode Microplate Reader. MMP activity was calculated by subtracting the fluorescence of the control medium from that of the conditioned medium samples and plotting the fluorescence of each sample over time. The slope of each sample corresponds to MMP activity. Samples were assayed in duplicate and the slopes were averaged.

Alkaline Phosphatase Activity Assay

Conditioned medium samples were incubated with 2 mg/mL phosphatase substrate (Sigma) in 750 mM alkaline buffer solution (Sigma) in a clear 96 well plate. The absorbance at 405 nm was recorded was recorded every 5 minutes for 90 minutes on a Biotek Synergy HT Multi-Mode Microplate Reader. ALP activity levels were determined in the linear region of the absorbance over time graph using a standard curve generated from known concentrations of p-nitrophenol (Sigma). Samples were assayed in duplicate and the results were averaged.

Statistics

Unless otherwise stated, each sample was analyzed over 3 experimental replicates per patient. For each patient, significant differences between conditions were determined by two-tailed Student's unpaired t-test for two condition mean comparisons. Results across

at least 5 patients were evaluated by two-tailed Student's paired t-test for two condition mean comparisons. P-values (p) of less than 0.05 were considered significant. In some cases results from a single representative patient are presented.

Chapter 3

Characterization of MSC Chondrogenesis

3.1 Introduction

MSCs are converted into cartilage-producing chondrocytes through the process of chondrogenesis. As detailed in Chapter 1, factors known to support MSC chondrogenesis are a 3D culture configuration [28, 29], a chemically defined medium containing a TGF-β-family growth factor [40], and physiological levels of mechanical stimulation [41]. In pellet culture, TGF-β family members have been shown to induce expression of genes associated with chondrogenesis as well as stimulate the production of an extracellular matrix containing GAG and Col2. Chondrogenesis is typically assessed after three weeks of chondrogenic culture. However, the temporal acquisition of these characteristics is unclear due to variability in the time points at which they are analyzed in different studies (see Table 3-1).

In addition to markers of chondrogenic differentiation, even the first studies of MSC chondrogenesis reported phenotypic characteristics typical of chondrocyte hypertrophy [2, 28-30]. Reports of such traits have become more common as chondrogenic MSCs are evaluated for regenerative cartilage therapies. Again, the temporal development of hypertrophy is not well characterized due to variability in the selection of experimental end points (see Table 3-2). Nonetheless, markers of hypertrophic differentiation are invariably observed in chondrogenic MSC pellets. Furthermore, many of these studies have noted the similarities between chondrogenic

MSC pellets and chondrocytes progressing through the process of endochondral ossification, which undergo hypertrophy in an organized fashion [184].

Table 3-1. Temporal development of chondrogenic markers in MSC pellets.

Cell Source	GAG Deposition	*Acan* Expression	Col2 Deposition	*Col2a1* Expression	Reference
Rabbit	D21	--	D21	D7	[28]
Human	--	--	D10	--	[2]
Human	D7	D1	D7	D3	[29]
Human	D14	--	--	D7	[30]
Bovine	D7	D20	D7	D20	[31]
Human	D16	--	D16	--	[326]
Human	--	D14	D14	D14	[46]
Human	D28		D28	D14	[323]
Human	D42	--	D42	--	[327]
Human	D14	--	D14	--	[38]
Human	--	--	D42	D21	[45]
Human	--	--	D12	D24	[328]
Human	D21	--	D10	--	[329]

Table 3-2. Temporal development of hypertrophic markers in MSC pellets.

Cell Source	Col10 Deposition	*Col10a1* Expression	ALP activity	Other	Reference
Rabbit	D21	D7	D7	--	[28]
Human	--	--	?	--	[2]
Human	D7	D3	--	--	[29]
Human	--	D7	--	--	[30]
Human	--	D8	--	--	[326]
Human	D7	D7	--	Increased *MMP13* on D14	[46]
Human	D28	D7	D28	Decreased *PTHrP*, *RARα* on D7, Decreased *FGFR1*, *VEGF* on D14, Increased *MMP13* on D21, Increased *Ihh* on D28	[323]
Human	D42	--	D14	--	[327]
Human	--	D21	D42	Increased *MMP13* on D7	[45]
Human	D21	--	D10	--	[329]

Since the primary aim of this work was to evaluate regulation of MSC chondrogenesis by cyclic hydrostatic pressure and β-catenin modulation, we first endeavored to identify the ideal time point at which to assess chondrogenic differentiation. The main requirement for an appropriate time point is definitive detection of chondrogenesis. In our characterization of MSC chondrogenesis we used GAG and

Col2 deposition, and *Sox9*, *Col2a1*, and *Acan* expression as indicators of chondrogenesis, and tracked them over the course of 21 days. In addition, we profiled the expression of hypertrophy genes during MSC chondrogenesis in order to compare the development of hypertrophic characteristics with the sequential process of endochondral ossification.

3.2 Results

Chondrogenesis

In order to determine the temporal progression of chondrogenesis in MSCs, cell pellets were cultured in CM, and their extracellular matrix content and gene expression was profiled over 21 days. GAG content was quantified using the Blyscan assay. Changes in expression of *Sox9*, *Col2a1*, and *Acan* were measured by RT-PCR. Finally, the composition of the extracellular matrix was qualitatively assessed by histological and immunohistochemical staining for GAG and Col2. The differentiation profile was also used to determine the earliest point at which chondrogenesis could be definitively identified for use in future studies.

GAG deposition within pellets was normalized to DNA content. MSCs from 5 different donors were used: 51 year old female (51F), 52 year old male (52M), 53 year old male (53M), 56 year old male (56M), and 60 year old male (60M). GAG content increased significantly over the three week culture period in pellets from all five patients tested (Figure 3-1). In general, there was a lag of about one week before GAG deposition began to increase rapidly, between days 9 and 11. In three of the patients (52M, 53M, and 60M), GAG levels plateaued at around 15 μg GAG/μg DNA, and this occurred around

76

A
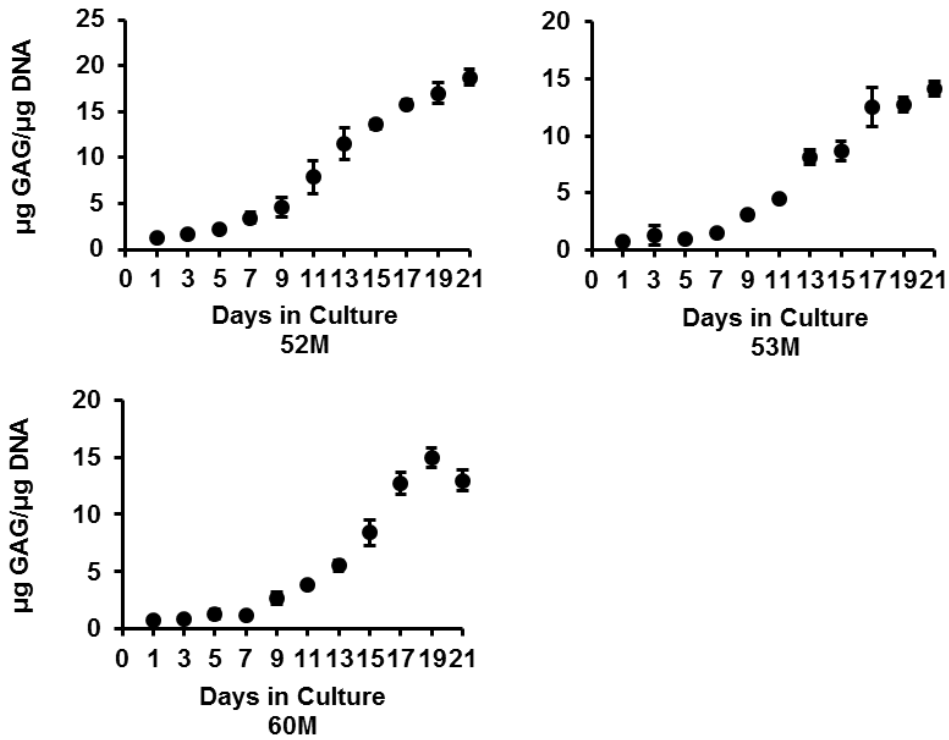
B
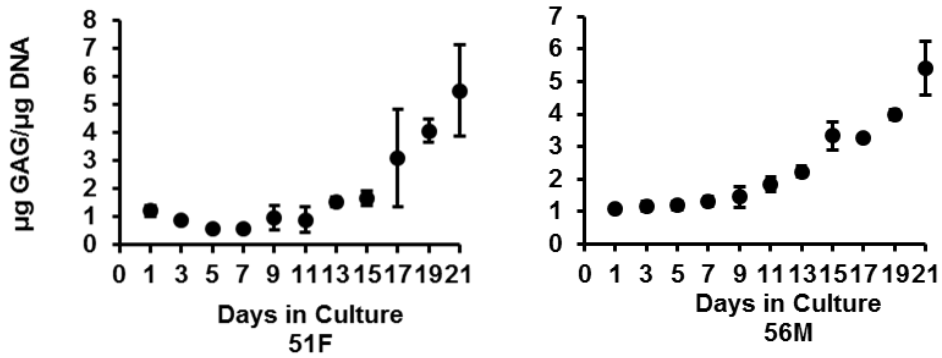
Figure 3-1. The magnitude of GAG production during chondrogenesis distinguishes between strongly and weakly chondrogenic MSCs. Sulfated GAG content of chondrogenic pellets from 5 donors was measured every other day and normalized to DNA content for each patient. GAG accumulation increased during chondrogenesis, and on day 21 could be classified as either (A) high ($\geq$12 μg/μg DNA) in strongly chondrogenic MSCs or (B) low ($\leq$6 μg/μg DNA) in weakly chondrogenic MSCs.

day 17 (Figure 3-1 A). In the other two patients (51F and 56M), the rate of GAG production appeared to increase exponentially after the initial lag phase, although these MSCs only reached about 6 μg GAG/μg DNA after 21 days, but did not appear to level off (Figure 3-1 B). Based on their GAG content at day 21, MSCs from the former 3 patients could be described as strongly chondrogenic, while cells from the latter 2 patients were only weakly chondrogenic or at least delayed in their chondrogenesis. Because the pellets were not assessed beyond 21 days, it remains unknown if GAG levels from the latter 2 patients would continue to increase exponentially, plateau around 15 μg GAG/μg DNA as in the other 3 patients, or plateau at a lower level.

Interestingly, the strongly and weakly chondrogenic MSCs exhibited two distinct patterns of cell viability. In the strongly chondrogenic pellets, cell numbers fluctuated slightly up or down early in culture and were increased by 10-25% at the end of 3 weeks. In the weakly chondrogenic pellets, cell numbers decreased initially by up to 28%, and at the end of the culture period had only recovered to 90-95% of their original value. Therefore, not only is differentiation less robust in the weakly chondrogenic pellets, but they experience greater cell death as well, which may alter the differentiation capacity of the remaining cells. The quality of chondrogenesis was not correlated with age. MSCs from 51 and 56 year old donors were weakly chondrogenic compared to strongly chondrogenic MSCs from 52, 53, and 60 year old donors. Gender-based differences could not be determined since only one of the donors was female. Because this study was conceived to characterize chondrogenesis, cells from strongly chondrogenic patients were the focus of subsequent analyses.

Strongly chondrogenic MSCs from three donors—52M, 53M, and 60M—were evaluated for expression of *Sox9*, *Col2a1*, and *Acan* during chondrogenesis. At each time point, the mRNA from five pellets was amplified. Therefore, each data point represents the gene expression for five combined pellets. Gene expression was calculated relative to day 1 and normalized to expression of *GAPDH*. At the end of the culture period, all three genes were upregulated in cells from all donors. In fact, the genes were consistently increased starting at day 11 through day 21 (Figure 3-2).

Until day 11, *Sox9* did not have a consistent profile across patients. In MSCs from donors 52M and 60M, *Sox9* decreased during the initial culture period and then increased from day 11 onward (Figure 3-2 A). In 53M cells, *Sox9* started increasing from the very first day, dips at day 11, and then continued to increase thereafter. From day 11 onward, all three donors exhibited an identical profile with increasing expression of *Sox9* that peaked between days 17 and 19 and then decreased slightly to close out the culture period. However, the magnitude of the fold changes over this time differed between patients. Fold changes of 0.11, 0.48, and 1.38 on day 11, corresponding to 11%, 48%, and 138% increases in *Sox9* levels, respectively, were further increased to 0.85, 2.27, and 1.31 on day 21.

The shape of the gene expression profile of *Col2a1* was virtually the same for MSCs from all strongly chondrogenic donors. Expression increased at relatively steady rate at the beginning of chondrogenesis before taking off between days 7 and 11 (Figure 3-2 B). *Col2a1* continued to increase until the end chondrogenic culture, and expression appeared to flatten out at the very end. The magnitude of *Col2a1* expression contrasted starkly with that of *Sox9*, with fold changes reaching the tens of thousands by day 21. The
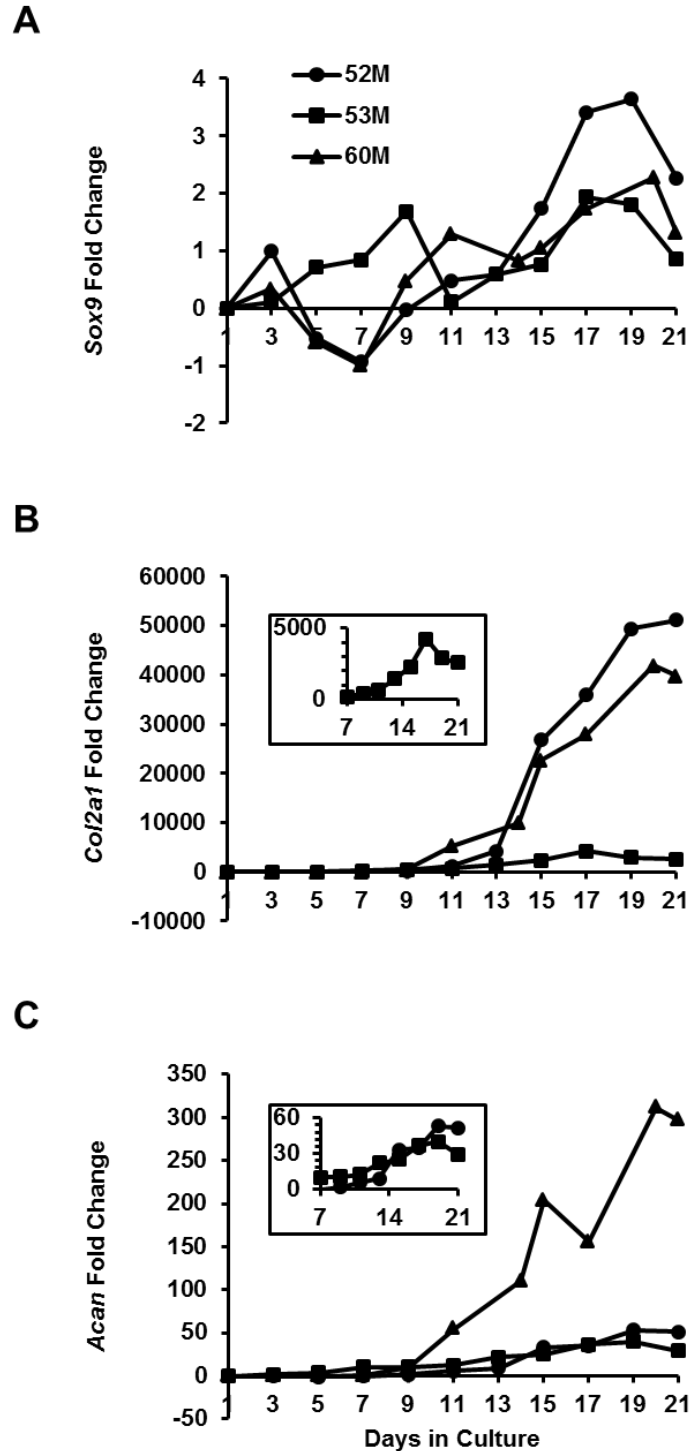
Figure 3-2. Culture day 11 is a common time point in the expression profiles of cartilage-specific genes during MSC chondrogenesis. Expression of *Sox9*, *Col2a1*, and *Aggrecan* was measured during MSC chondrogenesis of pellets from 3 strongly chondrogenic patients. From day 11 onward, all genes were upregulated compared to day 1, although the magnitudes of their fold changes differed. (A) The expression profile of *Sox9* followed a consistent trajectory only after day 11. (B) *Col2a1* and (C) *Aggrecan* expression increased over time and were subject to strong upregulation by day 11. Insets show expression profiles of donors with lower magnitude fold changes.

fold change magnitude of *Col2a1* expression also varied by donor. At the point when *Col2a1* began to increase sharply in all MSCs, around day 11, *Col2a1* levels had already increased by more than 5,000-fold (60M), 1,000-fold (53M), and 600-fold (52M) in MSCs from the various donors. By day 21, *Col2a1* those fold changes increased even further to more than 40,000-fold, 2,500-fold, and 50,000-fold, respectively. Thus, the magnitude of the fold change increase at day 11 does not necessarily correspond to its magnitude at day 21.

The expression profile of *Acan* closely mirrored that of *Col2a1*. Expression started off flat, began rapidly increasing between days 7 and 11 through the end chondrogenic culture, where it possibly leveled off (Figure 3-2 C). As with *Col2a1*, on day 11, the point at which all MSCs had begun to rapidly increase production of *Acan*, transcript levels had already increased by at least 5-fold compared to day 1. On day 21, *Acan* was upregulated more than 50-fold in all cells. The fold changes retained the same order of magnitude across patients until day 9, but by day 11, the fold change increase in *Acan* in cells from the 60M was more than five times greater than the fold change exhibited by the other MSCs. This difference persisted for the remainder of the culture period. On day 21, 60M MSCs exhibited a nearly 300-fold increase in *Acan* expression compared to 50-fold and 30-fold increases in 52M and 53M MSCs, respectively. The pattern of *Aggrecan* expression mirrored that of GAG accumulation in profile.

One of the meaningful observations that can be derived from the gene expression profiles is that day 11 is a common point at which all cartilage associated genes are upregulated, and after which all genes follow a common expression pattern, despite differences in their fold change magnitudes. Therefore, this time point was chosen as an

earlier point at which to evaluate chondrogenesis in subsequent studies instead of the traditional three week culture period.

GAG deposition was detected in paraffin-embedded pellet sections with Safranin O dye (Figure 3-3 A). As expected, there was no Saf O in day 1 pellets, as MSCs had not yet had sufficient time to produce a substantial extracellular matrix. On day 21, all pellets stained strongly for Saf O, demonstrating successful chondrogenesis. The Saf O staining was stronger toward one side of the pellets, and there was a thick band of Fast Green counterstain at the edge of the other side of the pellet. In addition there was a thin ring of counterstain along the entire edge of the pellet and sporadic sites of faint counterstaining throughout, indicative of heterogeneity within the pellet. In regions of strong Saf O staining the nuclei were localized to lacunae surrounded by extracellular matrix, which contrasted with the tissue morphology in weakly staining regions, but paralleled the tissue morphology of articular cartilage (Figure 3-3 B). In day 11 sections Saf O staining was apparent in all pellets to varying degrees. In 52M pellets Saf O staining was visible throughout the pellet except at the outer edge and in the center. The Saf O staining appeared to be stronger on one side of the pellet than the other. In 53M pellets light Saf O staining was visible through most of the pellet. As with 52M, counterstaining appeared in a ring around the outer edge of the pellet, but also extended inward on one side. 60M pellets on the other hand had only very sparse, light Saf O staining on day 11, visible in several irregular patches in the pellet. The lack of histologically identifiable chondrogenesis in 60M pellets, which were previously classified as strongly chondrogenic, indicated that the qualitative selection criterion of GAG production/cell was insufficient to identify which MSCs were actually chondrogenic at day 11. Though
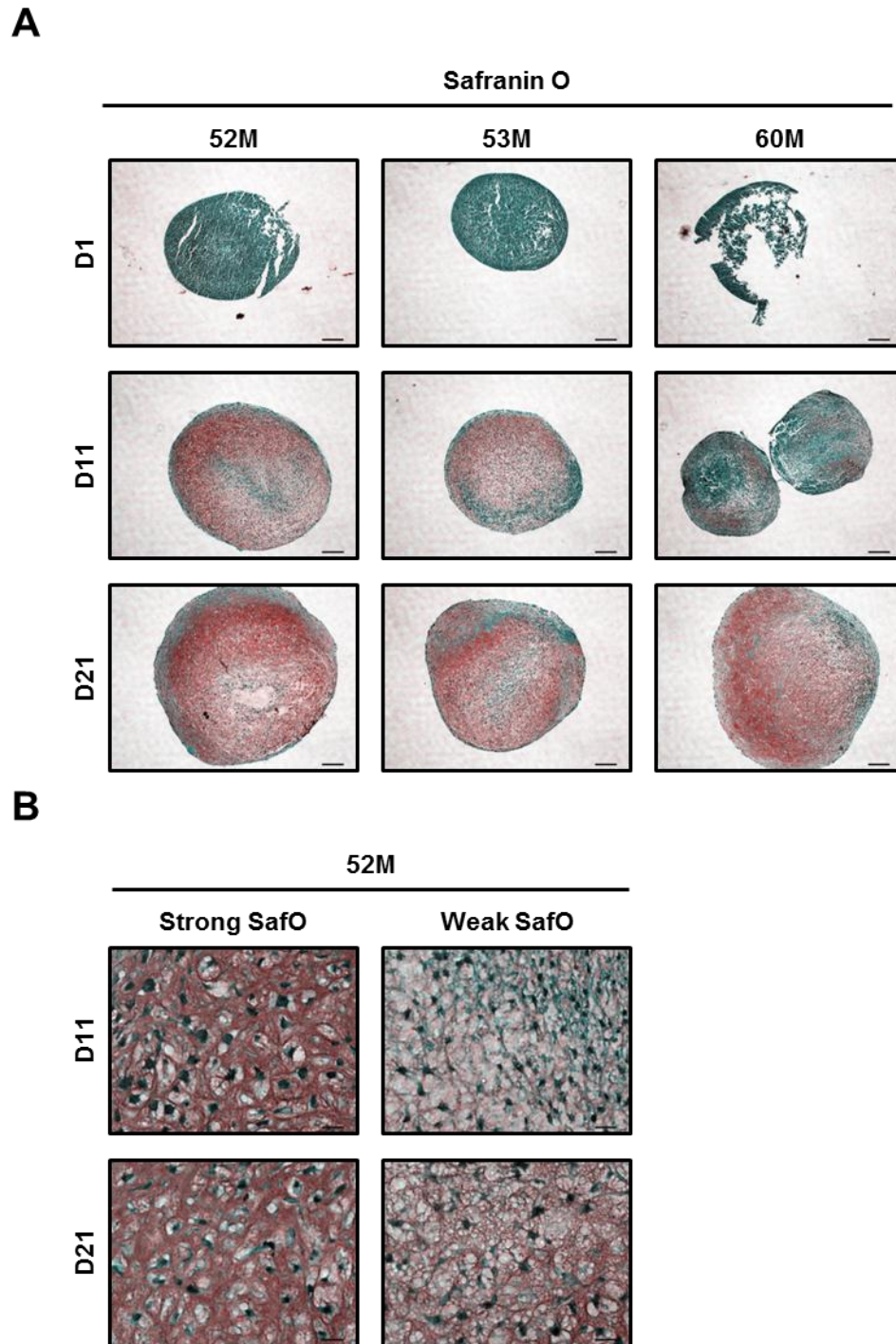
Figure 3-3. Timing of GAG deposition varies even among strongly chondrogenic MSC pellets. (A) Images of Safranin O staining of chondrogenic MSC pellets captured at 4x magnification revealed GAG accumulation (red) over the course of 21 days. At day 11, GAG deposition was delayed in 60M pellets. Scale bars: 100 μm. (B) 40x magnification images revealed nuclei in individual lacunae in regions of strong SafO staining, while no distinct lacunae were evident in regions of weak SafO staining. The density of nuclei decreased between days 11 and 21 in all regions. Scale bars: 20 μm.

its pellets were strongly chondrogenic at day 21, 60M exhibited a delayed chondrogenesis profile earlier in culture, suggesting that the arbitrary designations of strongly and weakly chondrogenic do not adequately capture the full spectrum of the different chondrogenic phenotypes observed between donors.

Col2 deposition was detected in strongly chondrogenic MSC pellets via immunohistochemistry using an antibody against a Col2-specific epitope. No Col2 staining was apparent on day 1, but staining was visible in all pellets on day 21 (Figure 3-4A). In general, Col2 staining was visible in the same regions as strong Saf O staining, but absent in regions with weak or no Saf O staining, indicating functional chondrogenesis in these regions. In 52M and 53M pellets, the donors that exhibited extensive Saf O staining by day 11, the pellets stained very strongly for Col2. In 60M pellets, which demonstrated delayed chondrogenesis at day 11, Col2 staining was much patchier on day 21. These staining patterns suggest that regions demonstrating GAG deposition at day 11 correspond with those that stain positive for Col2 at day 21 even though little to no Col2 staining is evident on day 11. It is noteworthy that *Col2a1* expression on day 21 was on the order of 40-50 thousand fold in 52M and 60M versus 5 thousand fold in 53M, and these fold change differences emerged at day 21. Thus, Col2 deposition in chondrogenic MSC pellets on day 21 seemed to correspond better with Saf O deposition on day 11 than with gene expression between days 11-21.

Hypertrophy

In order to determine the temporal acquisition of hypertrophic characteristics in MSCs, cell pellets were cultured in CM, and their extracellular matrix content and gene

A

Col2 Immunohistochemistry

	52M	53M	60M
D11			Undetected
D21			

B

Col10 Immunohistochemistry

	52M	53M	60M
D21			Undetected
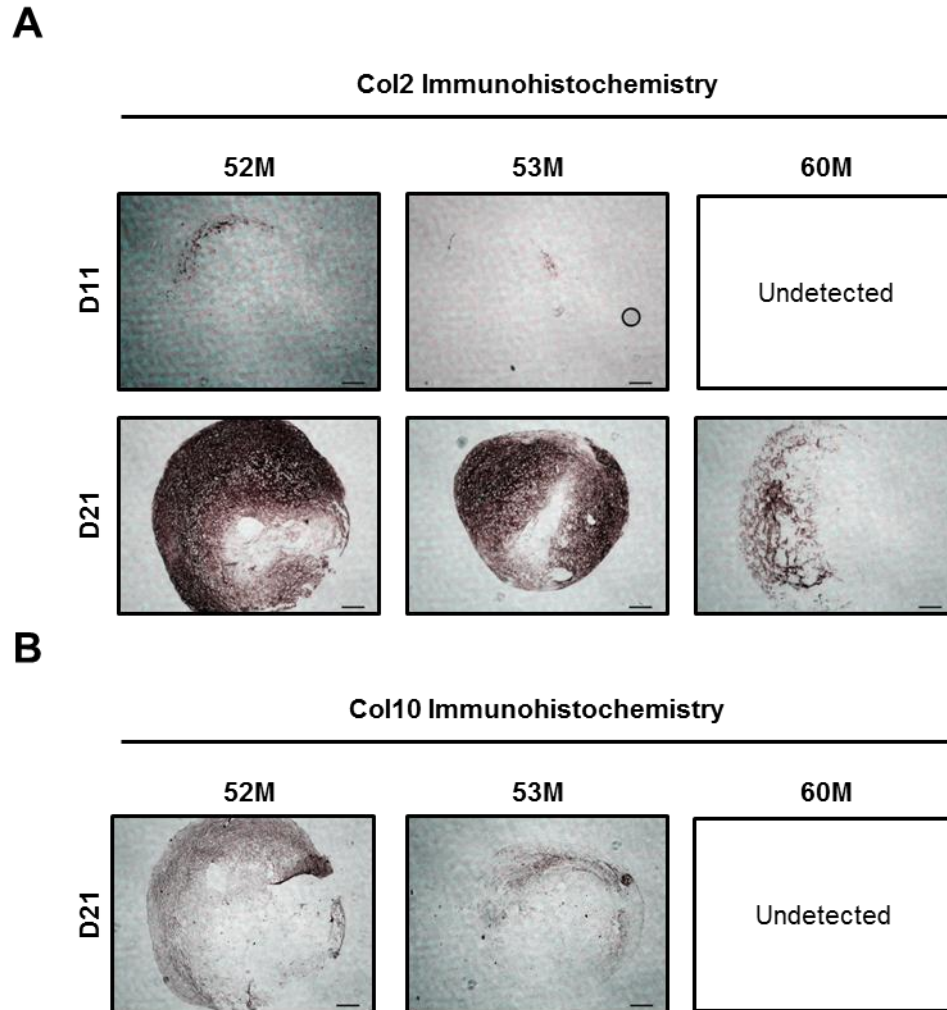
Figure 3-4. Col2 is detected in regions of strong GAG staining, and is followed by Col10 deposition in overlapping regions. Col deposition was detected by immunohistochemistry at 4x magnification. (A) While little to no Col2 staining was detected at day 11, staining was very strong on day 21 sections. On day 21, Col2 staining was localized to regions that previously stained for SafO and intensity was correlated to the intensity of SafO staining on day 11. (B) Col10 staining at day 21 was weaker than that of Col2. Scale bars: 100 μm

expression was profiled over 21 days. Col10 deposition was qualitatively assessed by immunohistochemical staining of histological sections. Changes in expression of *Runx2*, *PTHrP*, *ALP*, *Col10a1*, *MMP13*, and *BSP* were measured by RT-PCR.

Col10 deposition was detected in strongly chondrogenic MSC pellets via immunohistochemistry using an antibody against a Col10-specific epitope. Col10

staining was only weakly detected in one day 11 pellet from one donor, but was more consistently detected on day 21. On day 21, Col10 staining was much lighter than Col2 in 52M and 53M pellets, but localized to the same areas (Figure 3-4 B). In 60M, which exhibited delayed Saf O and Col2 deposition, no Col10 staining was observed. Based on the single time point where staining was apparent, it appeared that Col10 deposition followed that of Col2.

As with markers of chondrogenesis, many of the genes characteristic of terminal chondrocytes exhibited common patterns over the course of chondrogenesis. *Runx2* expression decreased steadily during the 21 day culture period (Figure 3-5 A). Since Runx2 regulates hypertrophy and osteogenesis, and its balance with Sox9 predicts the phenotype of skeletal precursors, it is expected that its expression would be regulated during chondrogenesis. An equilibrium with more Sox9 and less Runx2 should favor a chondrocyte phenotype. However, even though this pro-hypertrophy transcription factor is downregulated during chondrogenesis, many other markers of hypertrophy are oppositely regulated. *PTHrP* expression also decreased steadily over 21 days (Figure 3-5 B). PTHrP is expressed by articular chondrocytes [330] and serves as an anti-hypertrophy signal in the growth plate [190, 240-242]. Therefore, a decrease in PTHrP expression in chondrogenic MSCs indicates either a transition to hypertrophy or that undifferentiated MSCs express high levels of PTHrP. Unlike growth plate chondrocytes, chondrogenic MSCs never actually experienced any significant upregulation of PTHrP, suggesting that their functional chondrogenesis does not fully replicate the articular chondrocyte phenotype. In addition, genes indicative of hypertrophy and terminal differentiation were upregulated in parallel with chondrogenic genes. Pellets from all donors exhibited

increased expression of *ALP* beginning at day 5 that persisted during the full culture period (Figure 3-5 C). Expression of *Col10a1* began with a relative lag phase of slowly increasing *Col10a1* expression for the first 9 days, followed by strong upregulation beginning at day 9 and continuing through day 21 (Figure 3-5 D). *MMP13* exhibited a
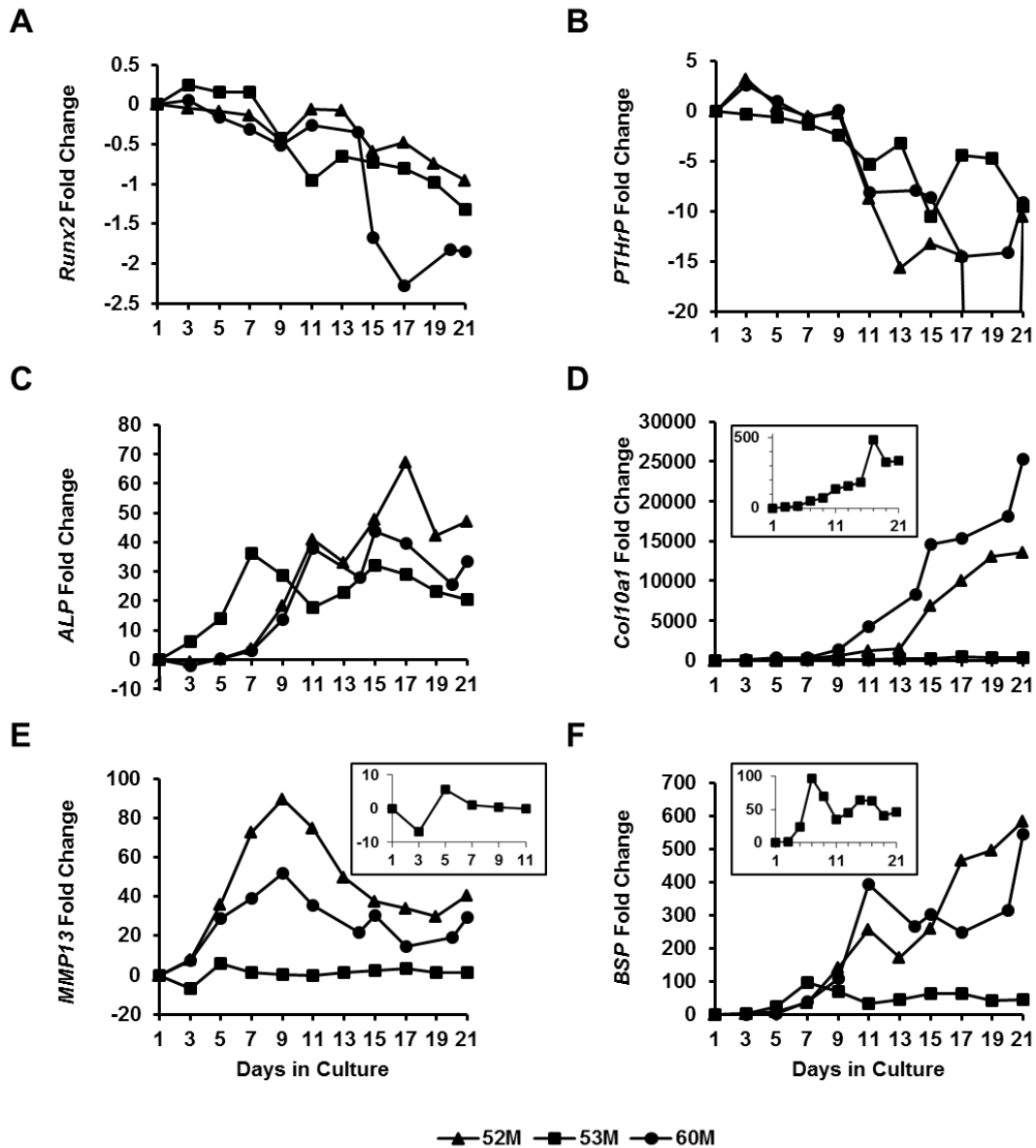
Figure 3-5. Genes which are markers of chondrocyte hypertrophy and terminal differentiation are expressed in parallel with *Sox9*, *Col2*, and *Acan* in chondrogenic MSCs. Expression of (A) *Runx2*, (B) *PTHrP*, (C) *ALP*, (D) *Col10a1*, (E) *MMP13*, and (F) *BSP* were mapped over the course of chondrogenesis. Regulation of these genes began as early as day 3 of chondrogenesis. Insets show the expression profiles of 53M pellets when the fold change magnitudes were much lower than the others.

spike in expression early during chondrogenesis (days 5-9), which then declined to a stable value, although in two donors the steady expression levels were still well above their initial expression of *MMP13* (Figure 3-5 E). Even though expression of *Col10a1* and *MMP13* followed similar patterns among all three donors, the fold changes observed in 53M pellets were much lower compared to the other two donors. Finally, *BSP*, the gene encoding bone sialoprotein, which is found in the hypertrophic cartilage matrix, increased steadily beginning at day 5 in 52M and 60M pellets, while its expression in 53M pellets increased and was then stabilized at a much lower fold change magnitude (Figure 3-5 F).

Thus, chondrogenic MSCs do not proceed through a sequential maturation process as in the growth plate, but express many of the same genes in parallel with markers of chondrogenesis. The co-expression of these genes suggests a phenotype more similar to that of OA chondrocytes with deregulated gene expression. The parallel expression patterns also means that these markers of imperfect chondrogenesis can be detected before chondrogenesis is complete, even before the day 11 time point suggested for early detection of successful chondrogenesis.

Dedifferentiation and Transdifferentiation

In order to verify that expression of non-chondrogenic genes was not due to dedifferentiation or transdifferentiation into osteoblastic cells, expression of *Col1* and *Oc* were profiled. *Col1* is expressed by undifferentiated mesenchymal cells [94] as well as osteoblasts [331]. In chondrogenic MSCs, *Col1a1* was slightly upregulated over time (Figure 3-6 A). The increase in *Col1a1* expression on day 21 ranged between 2-8 fold,
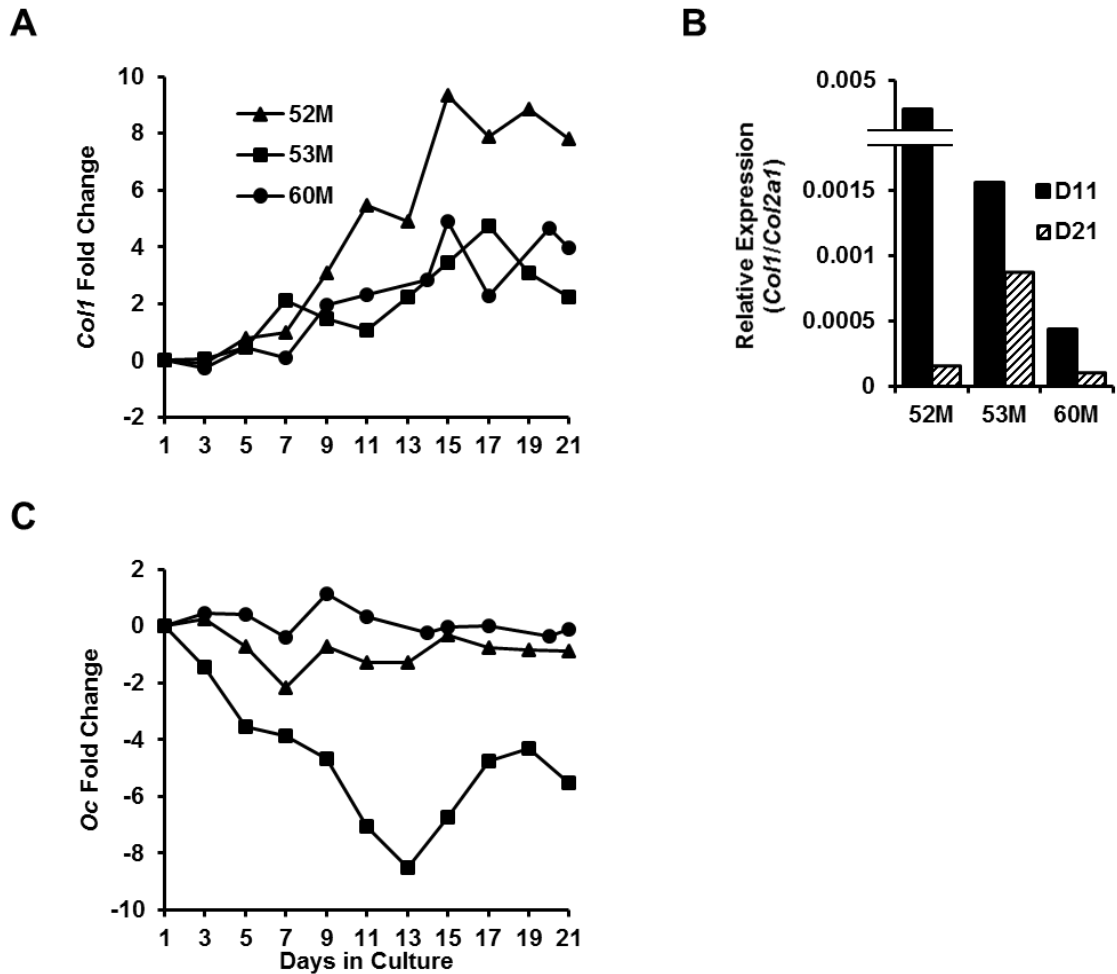
Figure 3-6. Chondrogenic MSCs do not dedifferentiate or transdifferentiate. (A) Expression of *Col1* was mapped over the course of chondrogenesis and demonstrated a slight increase. (B) However, when compared to expression of *Col2a1* on days 11 and 21, *Col1* was decreased over time. (C) Expression of *Oc* was held steady or downregulated over time in MSCs from all strongly chondrogenic donors.

and was dwarfed by fold changes of 2,500-50,000 for *Col2a1* on day 21, suggesting that changes in *Col1a1* expression are not significant relative to those of *Col2a1*. Further, the increase in *Col1a1* relative to *Col2a1* decreased between days 11 and 21 (Figure 3-6 B), indicating that the cells switched from an undifferentiated state to a chondrocyte-like phenotype. *Oc* encodes osteocalcin, a non-collagenous protein produced by osteoblasts [331]. Oc expression did not change in pellets from 2 donors and decreased 6 fold on

average in pellets from another donor (Figure 3-6 C). This indicates that chondrogenic

MSC pellets did not differentiate into osteoblastic cells.

Chapter 4

Regulation of MSC Chondrogenesis by Cyclic Hydrostatic Pressure

4.1 Introduction

Mechanical forces including hydrostatic pressure regulate the chondrocyte phenotype from early in development. Immobilization of chick embryos results in the development of inferior articular cartilage and other limb deformities [332, 333]. During development, human embryos experience up to 1.7 kPa of amniotic pressure *in utero* [334]. *In ovo* development is also subject to a basal level of hydrostatic pressure. While the levels of hydrostatic pressure in embryonic cartilage have not been measured, mathematical models of skeletal development correlate hydrostatic pressure with regions of cartilage maintenance and suppression of chondrocyte maturation and endochondral ossification[335]. In post-natal articular joints, physiological magnitudes of hydrostatic pressure (5-15 MPa), have been shown to enhance the anabolic phenotype of adult chondrocytes and chondrogenic MSCs *in vitro*, and some examples of this phenomenon can be found in Table 1-1.

The variety of forces experienced by chondrocytes in articular cartilage, which were detailed earlier, include compression, tension, shear fluid flow, and hydrostatic pressure. In this work, we chose to focus on hydrostatic pressure for several reasons. First, high hydrostatic pressures are unique to cartilage. No other highly hydrated tissue is subjected to the intermittent loading patterns found in cartilage that generate its characteristic hydrostatic pressure. Joint contact pressures range between 0 and 20 MPa [59]. Pressures are generated cyclically with a frequency of 0.1 to 10 Hz for up to 16

hours per day with intermittent periods of rest [59]. Second, in an experimental setting, hydrostatic pressure can be isolated from other forces. Compressive loading necessarily gives rise to hydrostatic pressure and fluid flow *in vitro* as in native cartilage. Our CHP bioreactor applied hydrostatic forces to the MSC pellets, but not compressive or shear forces. Thus, our results represent the discrete effects of CHP.

Several studies have already demonstrated that CHP is beneficial to MSC chondrogenesis, and are summarized in Table 4-1. The central finding is that CHP increases markers of chondrogenesis in MSCs that can be observed between days 7 and 21. In C3H10T1/2 murine embryonic fibroblasts, pro-chondrogenic effects were seen as early as day 3. Notably, effects of CHP-treatment are not seen over longer culture periods, indicating that non-loaded MSCs eventually reach the same degree of differentiation as their loaded counterparts [336]. In addition, some effects are only observed at low levels of TGF-β, indicating that TGF-β is a more potent stimulus than CHP [337]. In this work, we added 10 ng/mL TGF-β3 to the chondrogenic culture medium because we were interested how the effects of CHP on MSC chondrogenesis synergize with TGF-β.

There are still gaps in understanding how CHP regulates chondrogenesis. First, while hypertrophic characteristics are commonly described in studies of TGF-β-driven MSC chondrogenesis, there are comparatively few reports on the effects of CHP on MSC hypertrophy. One study using porcine MSCs demonstrated decreased *Col10a1* expression with CHP after 14 days [337]. Another showed reduced ALP activity with CHP after 21 days [338]. Second, most of the studies do not consider variability between donors, instead focusing on the effects of CHP on pooled cells or cells from a single donor. As

Table 4-1: Effects of CHP on MSC Chondrogenesis

Cells	Culture System	Growth Factors	CHP	Results	Reference
Human BM MSCs	2×10^5 cells/pellet	TGF-β1	4 h; 1 Hz; 5 MPa	Increased GAG and collagen 7 and 21 days after CHP	[339]
Human BM MSCs	2.5×10^5 cells/pellet	-	4 h; 1 Hz; 10 MPa	Increased *Sox9*, *Col2a1*, *Acan*, Increased GAG at days 7 and 14	[340]
Human BM MSCs	2.5×10^5 cells/pellet	TGF-β3	4 h; 1 Hz; 0.1 MPa	Increased *Sox9*, *Acan* at 14 days	[341]
Human BM MSCs	2.5×10^5 cells/pellet	TGF-β3	4 h; 1 Hz; 1 MPa	Increased *Sox9*, *Acan*, Increased GAG at 14 days	[341]
Human BM MSCs	2.5×10^5 cells/pellet	TGF-β3	4 h; 1 Hz; 10 MPa	Increased *Sox9*, *Col2a1*, *Acan*, Increased GAG at days 7 (GAG) and 14	[341]
Human BM MSCs	9×10^6 cell/mL in 4% agarose	-	4 h; 1 Hz; 7.5 MPa	Increased *Sox9* at 14 days	[342]
Human BM MSCs	1×10^6 cell per 12.5 mm × 5 mm collagen I	TGF-β1 + β-GP	4 h; 1 Hz; 1 MPa	Increased *Sox9*, *Col2a1*, *Acan*, *Col1*, Increased GAG at 10 days	[343]
Porcine BM MSCs	15×10^6 cells/mL in 2% agarose	TGF-β3	1 h; 1 Hz; 10 MPa	No differences at 42 days	[336]
Porcine BM MSCs	15×10^6 cells/mL in 2% agarose	TGF-β3	4 h; 1 Hz; 10 MPa	No change in GAG, Decreased ALP activity at 21 days	[338]
Porcine BM MSCs	15×10^6 cells/mL in fibrin	TGF-β3	4 h; 1 Hz; 10 MPa	Increased GAG, Decreased ALP activity at 21 days	[338]
Porcine synovial MSCs	2.5×10^5 cells/pellet	TGF-β3	4 h; 1 Hz; 10 MPa	Increased *Sox9* with low TGF, Increased *Col2a1* and *Acan* with high and low TGF, Decreased *Col10a1* and *Ihh* with high and low TGF, No differences in GAG or Col2 accumulation, Increased GAG with low TGF at 14 days	[337]
Rabbit synovial MSCs	4×10^6 cells/mL in 1.2% alginate	-	1 h; 0.5 Hz; 5 MPa	Increased *Sox9*, *Col2a1*, *Acan*, No change in *Col1*, Increased GAG after 4 days	[344]
C3H/10T1/2 mouse embryo fibroblasts	7.5×10^4 cells/pellet	BMP-2	1 h; 10 m on/10 m off; 1 Hz; 5 MPa	No change in GAG or collagen at 3 days	[345]
C3H/10T1/2 mouse embryo fibroblasts	7.5×10^4 cells/pellet	BMP-2	3 h; 10 m on/10 m off; 1 Hz; 5 MPa	Increased GAG and collagen at 3 days	[345]

demonstrated in the previous chapter, MSCs from different donors exhibit considerable variability in their responses to TGF-β stimulation. Differential responses to mechanical stimulation would be expected as well. Therefore, our study examined the effects of CHP on MSCs from multiple donors. Finally, very little is known about how CHP potentiates changes in MSCs. Because hydrostatic pressure imparts stress to the MSCs without any accompanying strain, it likely does not initiate signaling through direct conformational changes. It has been shown that hydrostatic pressure leads to changes in ion concentrations [61] and activates c-Jun N-terminal kinases as part of a mitogen-activated protein kinase (MAPK) signaling cascade [344]. Changes in intracellular signaling are responsible for phenotypic modulation and demand further investigation.

Based on previous results we hypothesized that CHP would enhance MSC chondrogenesis. We investigated how chondrogenic MSCs respond to CHP at 0.8 Hz with a peak of 10 MPa for 3 or 4 hours daily (depending on equipment availability) to mimic physiological conditions. Based on mathematical models of joint loading that show that hydrostatic pressure corresponds with regions of non-hypertrophic cartilage formation [335], we further hypothesized that CHP would inhibit the acquisition of a hypertrophic phenotype in chondrogenic MSCs. The results of our studies also led us to examine variations in the effects of CHP due to different temporal loading patterns. Finally, we hypothesized that the signaling pathways involved in regulating chondrogenesis and hypertrophy, particularly the Wnt/β-catenin pathway, would be modulated by CHP. In this work, we examined the response of 4 different pathways to mechanical loading.

4.2 Results

Cyclic Hydrostatic Pressure Enhances Chondrogenesis on Day 11

In order to evaluate the effects of CHP on MSC chondrogenesis, MSC pellets cultured in CM under CHP loading conditions were compared to control pellets grown under static conditions. Beginning on day 1 of culture, CHP pellets were exposed to 0.8 Hz of hydrostatic pressure with a peak pressure of 10 MPa for 3 or 4 hours daily, representative of physiological pressures that arise during joint loading. Control pellets were immersed in an unpressurized water bath for the duration of the daily loading regime. Chondrogenesis was assessed on days 11 and 21, after 10 or 20 days of loading, respectively.

GAG content was measured in MSC pellets from 5 different donors: 46M, 53F, 58M, 71F, and 75M. Unlike subsequent studies on the role of β-catenin in chondrogenesis, these MSCs were used without prior evaluation of their chondrogenic capacity because these studies predated the characterization studies described in Chapter 3. On day 11, GAG content was increased in CHP versus control pellets from all donors, though this result was not significant for every individual donor (Figure 4-1 A). However, on day 21, no trend was observed in any particular direction.

The quantitative analysis of GAG production correlated with trends observed for Alcian blue staining of GAGs within the pellets. Sections of pellets from 7 different donors were evaluated: 46M, 47M, 53F, 57M, 58M, 71F, and 75M. On day 11, Alcian blue staining was even throughout pellets from both groups, but appeared more intense in sections of CHP pellets than in control pellets for all but donor 57M (Figure 4-1 B). On
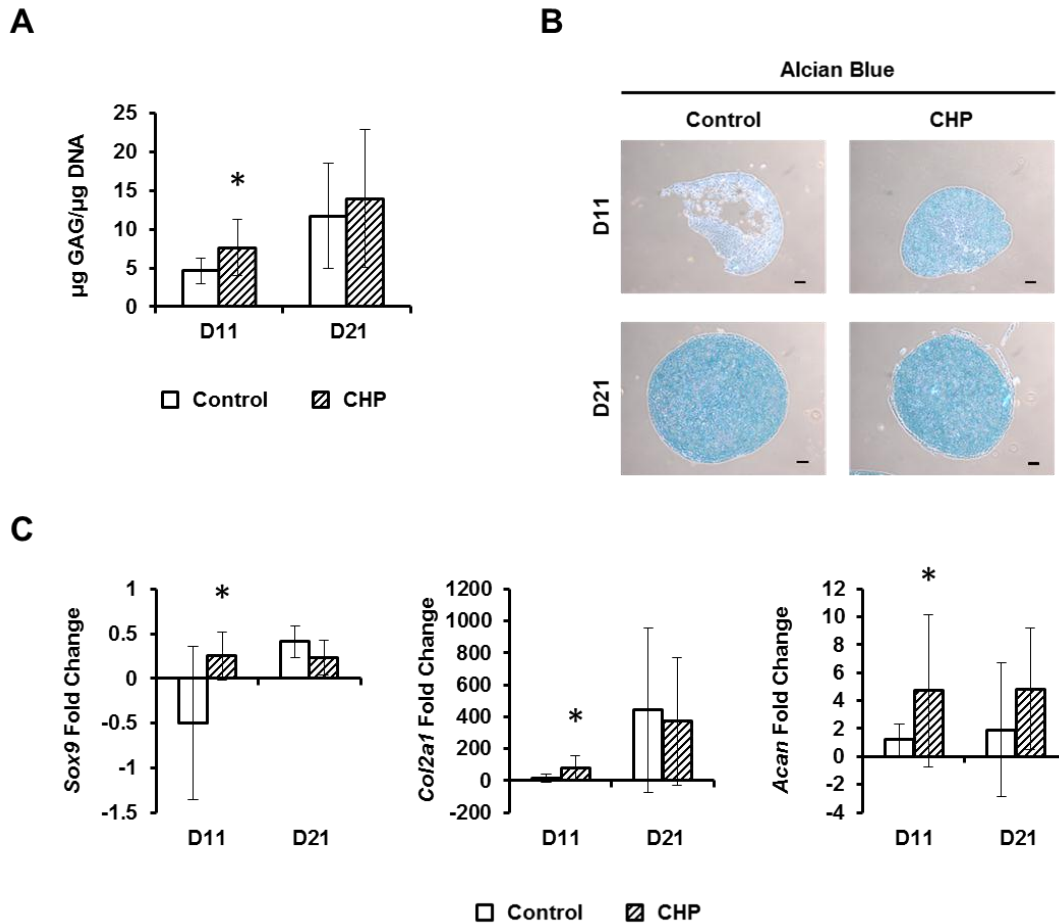
Figure 4-1. Cyclic hydrostatic pressure (CHP) enhances chondrogenesis of MSC pellets on day 11, but not day 21. MSC pellets were exposed to 4 hours of CHP daily. (A) Loaded pellets contained more GAG than control pellets on day 11. Graph depicts average GAG for pellets from 5 donors. * indicates trend among all pellets tested (n=5). (B) Alcian blue staining of MSC pellets corroborates quantitative GAG results. (C) Expression of chondrogenic genes in strongly chondrogenic pellets was enhanced in those that were loaded compared to controls on day 11. No CHP effects were observed on day 21 or for weakly chondrogenic pellets at any time point. Graph depicts average expression levels for pellets from 3 strongly chondrogenic donors. * indicates trend among strongly chondrogenic pellets (n=3).

day 21, staining was darker than on day 11. The staining distribution was relatively even within all pellets, except for donor 57M in which the Alcian blue was more intense around the edges of the pellet than in the center. The staining intensity appeared similar in CHP and Control pellets from 5 donors. In the remaining 3 donors, Alcian blue was darker in CHP pellets compared to controls.

Post-hoc classification of strongly and weakly chondrogenic pellets revealed that GAG synthesis was increased by CHP on day 21 in strongly chondrogenic MSCs. Of the donors for which sGAG levels were quantified, only MSCs from 53F would be considered strongly chondrogenic based on the GAG content of its pellets. Pellets from two others, 58M and 75M, had intermediate levels of GAG. It was these three donors in which the Alcian blue staining was increased in the CHP group on day 21. Thus, when analysis was confined to the strongly chondrogenic donors, CHP did result in increased GAG accumulation at the conclusion of 21 days.

Expression of chondrogenic genes was evaluated in strongly chondrogenic MSCs on days 11 and 21 (Figure 4-1 C). At each time point, the average relative gene expression for five pellets was calculated and normalized to *HPRT*. For all CHP experiments gene expression was normalized to *HPRT* rather than *GAPDH* because *GAPDH* expression has previously been shown to be sensitive to mechanical perturbations by J. Taboas (unpublished data). *Sox9*, *Col2a1*, and *Acan* expression was increased in strongly chondrogenic MSCs subjected to CHP on day 11 compared to controls, but not on day 21. When the weakly chondrogenic donors were included in the analysis, no trends were observed on either day 11 or 21.

Cyclic Hydrostatic Pressure Suppresses Aspects of Hypertrophy on Day 21

Expression of hypertrophic genes was evaluated on days 11 and 21 in chondrogenic MSCs cultured under CHP and static loading conditions (Figure 4-2). Fold changes in the expression of *Ihh*, *Runx2*, *Col10a1*, *BSP*, and *Col1a1* was measured in 6 different donors: 47M, 52M, 53F, 57M, 71F, and 75M. None of the genes were affected
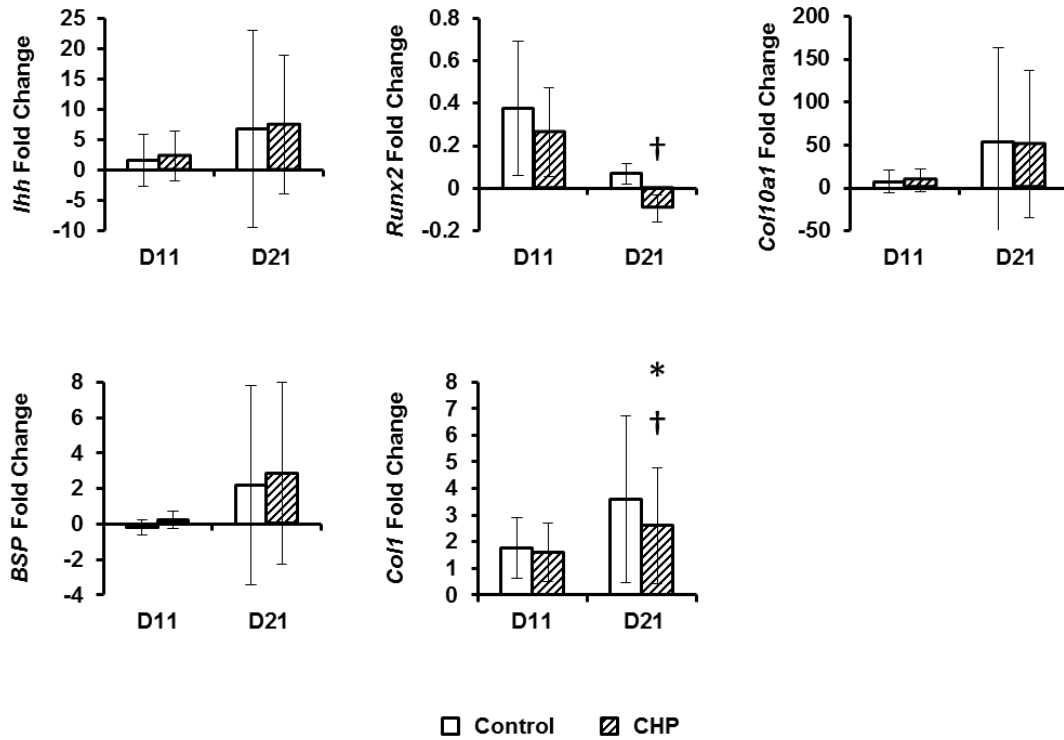
Figure 4-2. CHP suppresses expression of *Col1a1* and *Runx2* on day 21. The relative expression of hypertrophy genes on days 11 and 21 in MSCs cultured with or without CHP was normalized to *HPRT*. Graph depicts average gene expression levels for pellets from 6 donors. *p<0.05 compared to control (n=6). † indicates trend among all pellets tested (n=6).

by CHP on day 11. On day 21, expression of *Ihh*, *Col10a1*, and *BSP* were similarly unchanged in response to loading. Decreases in *Runx2* and *Col1a1* expression due to CHP were detected on day 21. *Runx2* expression was decreased in loaded MSCs from 5 of 6 donors. In the remaining donor, 71F, *Runx2* expression was increased by a negligible 3%. *Col1a1* expression was significantly decreased in loaded MSCs from all 6 donors. Unlike chondrogenic genes which were sensitive to CHP at day 11, but not day 21, these hypertrophy genes were responsive to mechanical stimulation at day 21, but not day 11, suggesting a temporal component in CHP mechanobiology. Also, while expression of *Sox9*, *Col2a1*, and *Acan* was increased by CHP on day 11, *Col1* and *Runx2* were

decreased by CHP on day 21, suggesting differential regulation of the chondrocyte phenotype by CHP by favoring an articular phenotype and inhibiting a hypertrophy one.

Effects of CHP on Chondrogenesis Occur Early in the Chondrogenic Culture Period

That the beneficial effects of CHP on chondrogenesis were observed primarily at day 11 and not day 21 gave rise to several questions. Is CHP beneficial only for less differentiated MSCs, such that a pro-chondrogenic effect is observed only at an earlier point during chondrogenesis? If so, exposing control MSCs to CHP beginning on day 11 would not have a pro-chondrogenic effect because the differentiated MSCs would not be expected to respond to mechanical stimulation. Or is the duration of CHP effects short-lived, such that any differences are abolished beyond 11 days. If so, exposing control MSCs to CHP beginning on day 11 might indeed have a pro-chondrogenic effect even on the pre-differentiated MSCs. Are few effects observed at day 21 because CHP is detrimental to the chondrocyte phenotype in differentiated MSCs? Is loading during the first 11 days sufficient for inducing an enhanced chondrogenic phenotype, such that

	D1-D10	D11-D20
☐ Rest-Rest	No load	No load
▨ Rest-CHP	No load	0.8 Hz; 10 MPa; 3-4 h/day
■ CHP-Rest	0.8 Hz; 10 MPa; 3-4 h/day	No load
▨ CHP-CHP	0.8 Hz; 10 MPa; 3-4 h/day	0.8 Hz; 10 MPa; 3-4 h/day

Figure 4-3. CHP Loading Regimens. Depiction of the loading patterns applied to different groups of pellets.

removal of CHP beginning on day 11 will actually favor continued chondrogenesis compared to steady loading? To answer some of these questions, MSCs were cultured for 21 days in CM and exposed to 4 regimens of CHP (Figure 4-3). One group received CHP daily for 21 days and will be referred to as CHP-CHP. Another group, known as CHP-Rest, was loaded daily on days 1-10 and treated like control pellets on days 11-20. The third group, Rest-CHP, were treated like controls on days 1-10 and then exposed to daily CHP on days 11-20. Control pellets were not loaded and will be referred to here as Rest-Rest. The parameters of CHP remained the same at 0.8 Hz with a peak pressure of 10 MPa for 4 hours.

The GAG content was measured in MSC pellets from the 1 strongly chondrogenic and 2 moderately chondrogenic donors—53F, 58M, and 75M—and several trends were observed on day 21 due to different loading schemes (Figure 4-4 A). In all pellets, GAG was decreased in the Rest-CHP group compared to the CHP-CHP group. This suggests that loading during the early stages of differentiation is the source of the increased GAG synthesis since pellets loaded only during the latter half of the full culture period did not produce as much GAG as those exposed to CHP for the duration of chondrogenic culture. In pellets from 2 out of 3 donors GAG was increased in CHP-Rest pellets compared to Rest-Rest pellets and decreased in the Rest-CHP group compared to the Rest-Rest pellets. While this is too small a sample size from which to draw a definitive conclusion, it again suggests that CHP is beneficial during the first half of the culture period. Furthermore, the lower GAG content of the Rest-CHP group compared to the Rest-Rest group suggests a detrimental effect of CHP when applied later in chondrogenic culture. None of these

differences were reflected in Alcian blue staining, which appeared equal in pellet sections

from all groups (Figure 4-4 B).
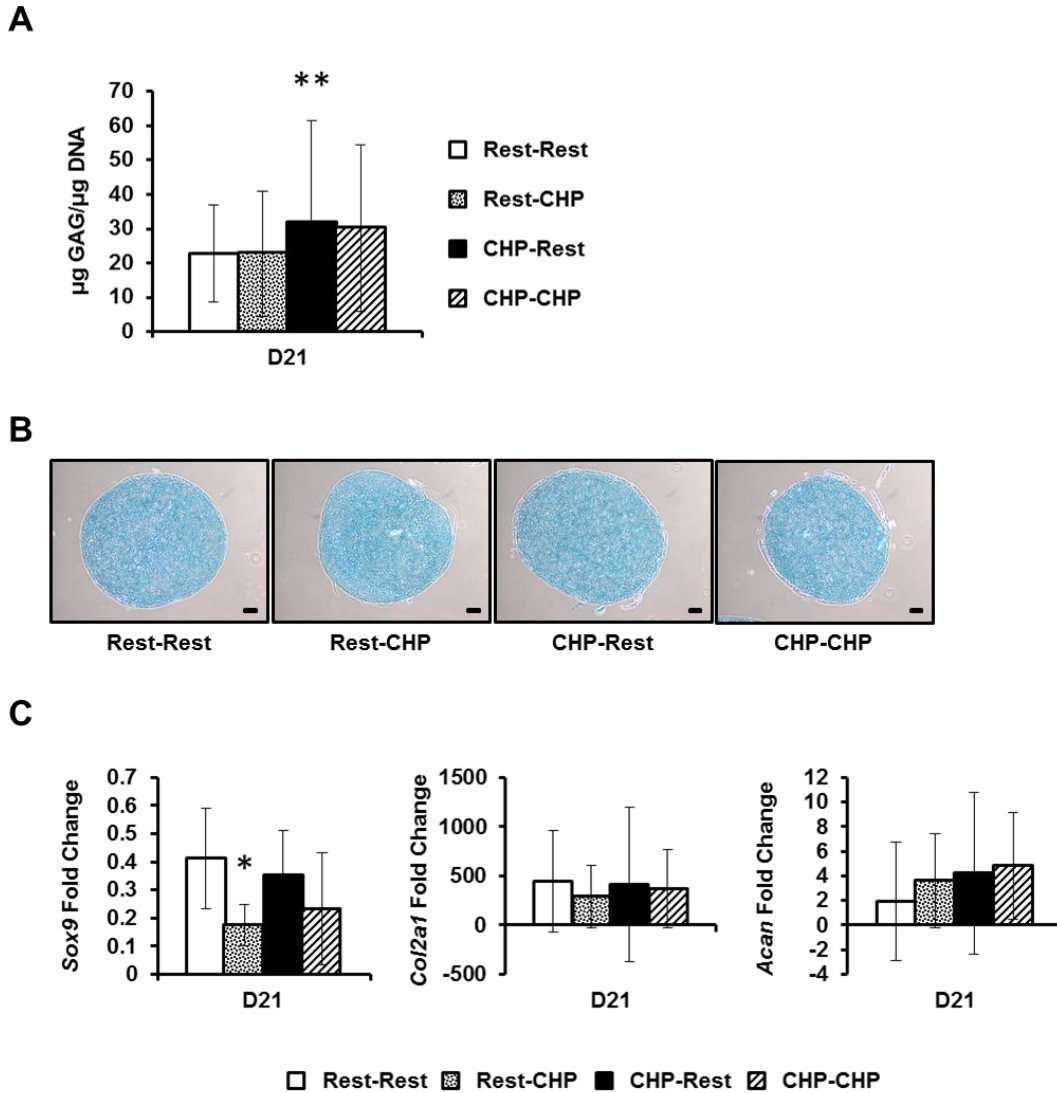
Figure 4-4. Early application of CHP enhances GAG deposition, and late application of CHP inhibits *Sox9* expression. (A) CHP-Rest pellets contained more GAG than CHP-CHP pellets on day 21. Graph depicts average GAG for pellets 3 strongly chondrogenic donors. * indicates trend among strongly chondrogenic pellets compared to CHP-CHP (n=3). (B) Alcian blue staining of MSC pellets revealed no differences between groups. (C) Expression of Sox9 was decreased in Rest-CHP pellets compared to Rest-Rest pellets on day 21, but other chondrogenic genes were unchanged. Graph depicts average expression levels for pellets from 3 strongly chondrogenic donors. * indicates trend among strongly chondrogenic pellets compared to Rest-Rest (n=3).

Fewer differences in the expression of chondrogenic genes by strongly chondrogenic MSCs were seen between the loading groups. Actually, the only trend observed was decreased *Sox9* in the Rest-CHP group compared to the Rest-Rest group (Figure 4-4 C). Together with the GAG data, this reduction might suggest an anti-chondrogenic effect of CHP during the second half of chondrogenic culture.

Effects of CHP on Hypertrophy Occur Later in the Chodnrogenic Culture Period

Expression of hypertrophy genes was evaluated on day 21 in chondrogenic MSCs exposed to the Rest-Rest, Rest-CHP, CHP-Rest, and CHP-CHP regimens of loading
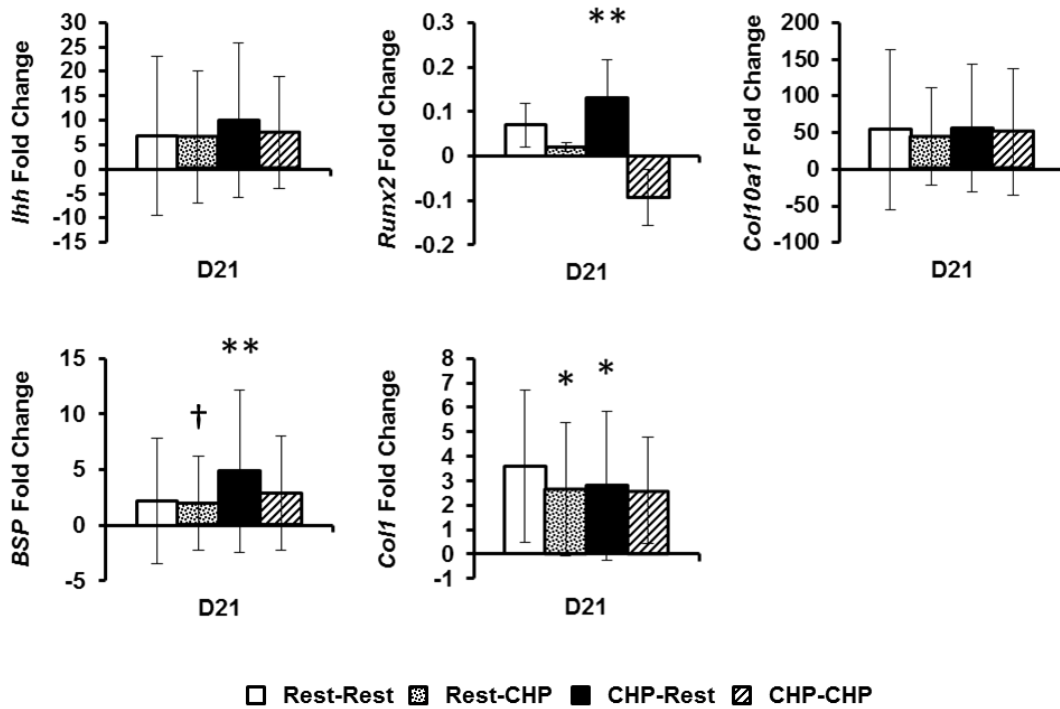
Figure 4-5. Late application of CHP suppresses Runx2 and BSP. The relative expression of hypertrophy genes on day 21 in MSCs cultured with varying patterns CHP was normalized to *HPRT*. Graphs depict average gene expression levels for pellets from 6-8 donors. * $p<0.05$ compared to Rest-Rest (n=6). ** indicates trend for 5 of 6 (Runx2) or 6 of 8 (BSP) pellets tested compared to CHP-CHP. † indicates trend for all strongly chondrogenic pellets compared to Rest-Rest (n=3 donors).

described earlier (Figure 4-5). Relative expression of *Ihh*, *Col10a1*, and *BSP* was measured in 8 different donors: 46M, 47M, 52M, 53F, 57M, 58M, 71F, and 75M. *Runx2* and *Col1a1* were not measured in 46M and 58M for a total of 6 donors. *Runx2* was decreased in CHP-CHP pellets from 5 of 6 donors compared to the CHP-Rest group. *BSP* was decreased in CHP-CHP pellets from 6 of 8 donors compared to the CHP-Rest group. This suggests that some aspects of terminal differentiation are negatively regulated by CHP during the latter half of the chondrogenic culture period. When only strongly chondrogenic MSCs were considered, *BSP* expression was down in all Rest-CHP pellets compared to Rest-Rest pellets, which implies negative regulation of *BSP* by CHP when applied starting on day 11. *Col1* was decreased in MSCs from 5 of 6 donors from both the Rest-CHP and CHP-Rest groups compared to the Rest-Rest group, indicating that when applied at any point during chondrogenesis, CHP inhibits dedifferentiation.

Cyclic Hydrostatic Pressure Suppresses ERK1/2 and β-catenin Signaling

In order to determine how CHP modulates the signaling pathways involved in regulation of chondrogenesis and hypertrophy, a luciferase reporter system was employed. MSCs were transfected with luciferase reporter plasmids containing binding sites for the following transcription factors: AP-1, NFAT, NF-κB, and TCF/LEF. AP-1 is a target of mitogen-activated protein kinase (MAPK) signaling [346], NFAT is a target of calcinuerin signaling [347], NF-κB is a target of inflammatory TNF and IL-1 receptor signaling [348], and TCF/LEF is a target of canonical Wnt/β-catenin signaling. Therefore, expression of luciferase would be indicative of the activity of these respective pathways. MSCs from 4 random donors were used for these reporter experiments: 37F,

38F, 47M, and 65F. After transfection, MSC pellets were exposed to 0.8 Hz CHP with a peak pressure of 10MPa for 4 hours. Luciferase activity was measured in pellets 24 hours after loading.

Of the four pathways examined, CHP decreased Wnt/β-catenin and MAPK signaling in all donors as shown by the decrease in the respective reporter activities of the TCF/LEF and AP-1 plasmids (Figure 4-6 A). A trend of CHP-dependent reduction in NFAT signaling was also observed, although replicates from individual patients tended to vary considerably. Mean NF-κB signaling increased under CHP compared to controls, but the direction of change was inconsistent between patients. While the magnitude of pressure-induced changes varied across MSCs pellets derived from different patients, the luciferase data indicate that CHP consistently decreased Wnt/β-catenin and MAPK signaling.

In order to verify the reporter results, the activation of β-catenin and ERK1/2, a MAPK pathway mediator, in response to CHP were assessed via Western blot. MSC pellets from the same donors were exposed to 0.8 Hz CHP with a peak pressure of 10MPa for 10 minutes or 4 hours. Luciferase activity was measured in pellets either 5 minutes or 8 hours after loading. Western blots for active β-catenin and phosphorylated ERK1/2 (pERK1/2) indicated differences only in pellets loaded for 4 hours and harvested after 5 minutes. Both active β-catenin and pERK1/2 were decreased in response to this duration of CHP in pellets all donors (Figure 4-6 B-C). The decrease in active signaling molecules confirms the luciferase reporter data and together with it suggests that CHP inhibits Wnt/β-catenin and MAPK signaling in MSC pellets.
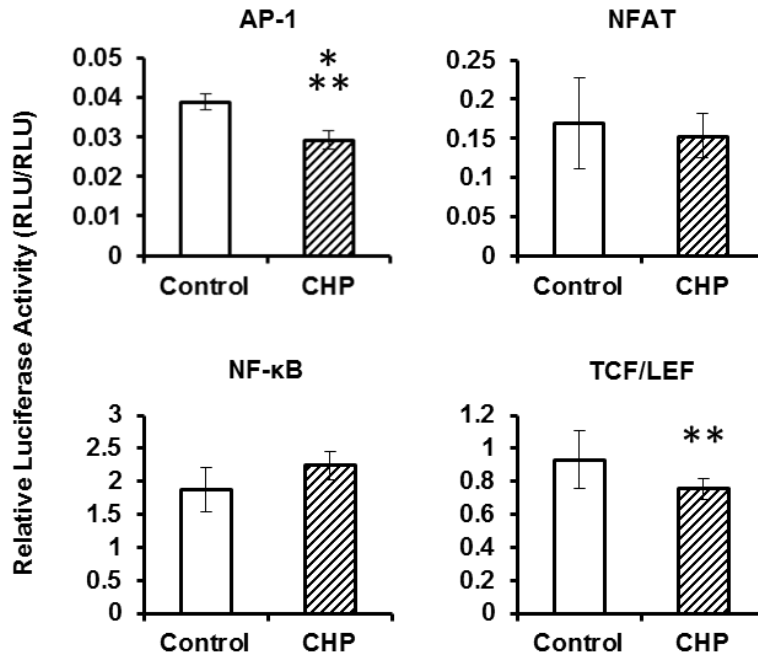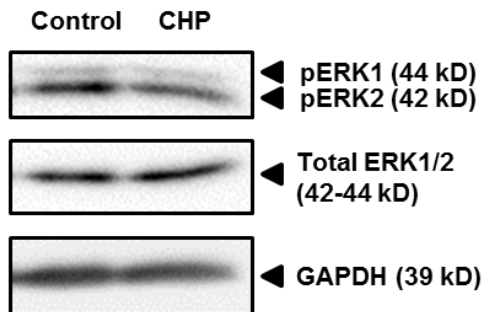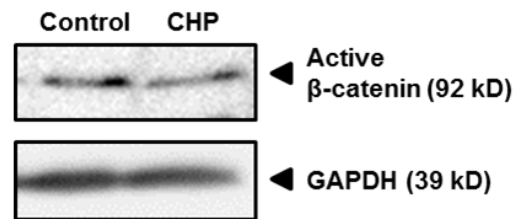
Figure 4-6. CHP represses the canonical Wnt/β-catenin and MAPK signaling pathways. (A) Normalized reporter activities of MSC pellets exposed to CHP or control conditions. Each graph depicts data from one representative donor. *p<0.05 for donor shown (n=3). ** indicates trend among all donors (n=3). (B) Western blots for pERK1/2 revealed reduced levels with 4 hours of CHP while ERK1/2 levels remained steady under the same loading conditions. Blot from one representative patient. (C) Western blots for active β-catenin also revealed reduced levels with 4 hours of CHP. Blot from one representative patient.

These data imply that CHP regulation of chondrogenic differentiation might occur in part through the suppression of canonical Wnt/β-catenin and ERK1/2 signaling. β-catenin is plays a central role in regulating the chondrocyte phenotype at every stage of differentiation, so its ability to regulate the chondrogenic MSC phenotype that encompasses aspects of so many other chondrocytes was selected at the focus of future studies. The rest of this work focuses on the role of β-catenin in MSC chondrogenesis and hypertrophy.

Chapter 5

Regulation of β-Catenin During MSC Chondrogenesis

5.1 Introduction

The dual roles of β-catenin in developmental chondrogenesis are well characterized. In the developing limb β-catenin is highly expressed in prechondrogenic mesenchymal cells and is decreased in a pattern opposite the expression of Col2 as they differentiate into chondrocytes [169, 171]. At this stage, β-catenin is localized at the membrane in association with N-cadherin, and its role is to stabilize cell-cell adhesions in the condensation. Prolonged expression of β-catenin prevents both the loss of N-cadherin and the progression of chondrogenesis [169, 171]. As the chondrocytes continue the process of maturation, β-catenin is once again observed in prehypertrophic and hypertrophic chondrocytes in the growth plate, where it serves as a transcriptional regulator [269]. Notably, in these chondrocytes β-catenin assumes more nuclear localization, indicating that in these cells it functions as a signaling molecule. Expression of constitutively active β-catenin in the growth plate accelerates chondrocyte maturation [169]. Thus, β-catenin promotes condensation and negatively regulates chondrogenesis by stabilizing cell to cell adhesions, positively regulates endochondral ossification via increased transcriptional activity, and is restricted in articular chondrocytes.

If MSCs behaved exactly like articular chondrocytes, β-catenin would be reduced with advancing chondrogenesis, and if MSCs behaved like perfect hypertrophic chondrocytes, β-catenin signaling would become activated during chondrogenesis. However, we have previously demonstrated that MSCs express characteristics of both

kinds of chondrocytes. Therefore, how β-catenin changes during MSC chondrogenesis is less predictable. Further, the artificial packing in MSC pellets may stimulate the formation of cell-cell adhesions containing β-catenin. Several studies have suggested that some level of β-catenin is present in chondrogenic MSCs, but only one recent study has shown that umbilical cord-derived MSCs downregulate total β-catenin over time during chondrogenesis [349]. Its regulation in bone marrow-derived MSCs like the ones used in this work is unknown.

β-Catenin can be regulated at several levels. Like all proteins, β-catenin can be regulated at the transcriptional and translational levels. Levels of β-catenin protein are also regulated by post-translational phosphorylation. In the cytoplasm, phosphorylated β-catenin is targeted for proteasomal degradation [163]. Dephosphorylated "active" β-catenin can be found at the membrane or in the nucleus, where it serves adhesive and transcription factor roles, respectively [163, 165]. Thus, the function of β-catenin depends on its subcellular localization. Finally, activation of β-catenin target genes in the nucleus depends on other transcriptional co-activators [164]. In the following experiments we examined changes in β-catenin in MSC chondrogenesis at multiple levels: transcription, translation/post-translation, subcellular localization, and transcriptional transactivity. The goal of this experiment was to understand the mechanisms of β-catenin regulation during MSC chondrogenesis and use this information to inform our subsequent β-catenin pathway modification studies.

5.2 Results

Ctnnb1 Expression is Increased during MSC Chondrogenesis

In order to determine if β-catenin is regulated at the level of transcription during MSC chondrogenesis, relative expression of *Ctnnb1*, the gene encoding β-catenin, was measured in 11 day old pellets via real-time RT-PCR using with *GAPDH* serving as an internal reference gene. PCR analysis showed a significant 92% increase in β-catenin mRNA expression on day 11 compared to day 1 (Figure 5-1). This result indicates that even under the influence of chondrogenic induction factors, MSC pellets produce β-catenin transcripts at even greater levels than in undifferentiated MSCs. This contrasts with the observation during developmental chondrogenesis that expression of β-catenin mRNA is higher in condensing mesenchymal cells, pre-hypertrophic chondrocytes, and hypertrophic chondrocytes, but is reduced in *Col2a1*-expressing chondrocytes [169, 350, 351]. However, expression of β-catenin likely drives condensation of undifferentiated
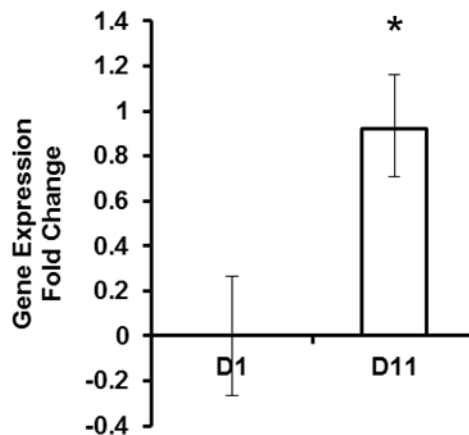
Figure 5-1. Expression of *Ctnnb1* increases during MSC chondrogenesis. MSC pellets were differentiated in CM for 11 days. Pellets were harvested at days 1 (D1) and 11 (D11) and RNA samples were analyzed by real-time RT-PCR for *CTNNB1* expression (n=3, *p<0.05). Each sample consisted of RNA from 5 pellets.

mesenchymal cells, whereas the artificial packing of MSC pellets may drive the increased expression of β-catenin observed here due to cellular proximity despite the induction of chondrogenesis by TGF-β3.

β-Catenin Protein Levels and/or Post-Translational Modifications Change during MSC Chondrogenesis

In order to determine the effects of MSC chondrogenesis on the regulation of β-catenin protein, the level of active β-catenin in chondrogenic MSC pellets was measured on days 1 and 11 by ELISA. The antibody used to probe β-catenin recognizes the domain containing amino acid residues 33-41, which, when phosphorylated, renders β-catenin inactive. Therefore, only active β-catenin is bound by the antibody and is measurable by ELISA. The ELISA measurements were normalized to DNA content, to yield a measure of the active β-catenin per cell. The amount of active β-catenin per cell increased by more than 80% over the 11 days of chondrogenesis (Figure 5-2). This could reflect one of
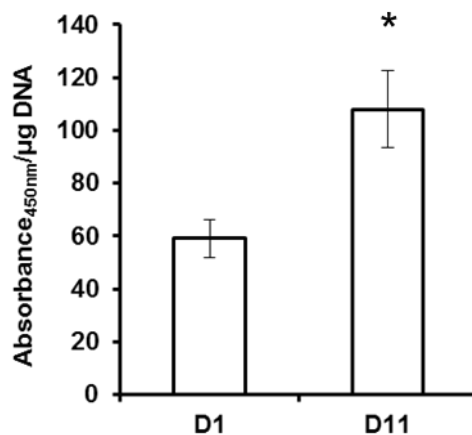
Figure 5-2. Activation status of β-catenin during MSC chondrogenesis. MSC pellets were differentiated in CM for 11 days. Pellets were lysed in 100 μL LB/pellet at days 1 (D1) and 11 (D11) and levels of active β-catenin in the lysate were detected by ELISA and normalized to DNA content (n=3, *p<0.05). Total lysate was 100-200 μL, or 1-2 pellets per sample.

several scenarios. One possibility is that β-catenin is being regulated at the level of translation; on day 11 the MSCs are producing more β-catenin compared to day 1, while the proportion of β-catenin being phosphorylated remains the same. Another possibility is that the post-translational modification of β-catenin is altered during MSC chondrogenesis such that levels of β-catenin protein remain the same, but more of it remains in the de-phosphorylated active state. A combination of translational or post-translational effects could also be responsible for the increase in active β-catenin during MSC chondrogenesis. Ultimately, whether β-catenin is regulated at the translational or post-translational level during MSC chondrogenesis, the result is more active β-catenin protein as differentiation progresses.

β-Catenin Levels Increase at the Membrane and Decrease in the Nucleus During MSC Chodnrogenesis

Active β-catenin is found primarily in the plasma membrane and in the nucleus. In order to better understand the increase in active β-catenin during chondrogenesis, the distribution of β-catenin in the different subcellular fractions was assessed by Western blot in 1 and 11 day old chondrogenic MSCs. To verify complete separation of the cellular compartments, β-tubulin was used as a marker of the cytoplasmic fraction, oligomerized caveolin as a marker of the membrane fraction [352], and HDAC2 as a marker of the nuclear fraction [353]. The Western blots demonstrate that each of these proteins is found in the expected fraction, with virtually no cross contamination between fractions (Figure 5-3). The decrease in the intensity of the bands between 1 day pellets

and 11 day pellets suggests either that lysis of whole pellets is more efficient on day 1 or that the pellets contain more living cells at the earlier time point.

Side by side comparison of the cytoplasmic, membrane, and nuclear compartments on days 1 and 11 of chondrogenesis indicates that most of the cellular β-catenin was located in the membrane at both time points (Figure 5-4 A). While β-catenin was strongly detected in the nuclear fraction as well, almost none was detected in the cytoplasmic fraction. This suggests that phosphorylated β-catenin is degraded quickly, leaving the de-phosphorylated active β-catenin as the main type that is detected. This is consistent with what is known about β-catenin protein regulation [163].

Comparison of β-catenin on days 1 and 11 in each of the fractions revealed differential localization over the course of MSC chondrogenesis. In the cytoplasmic fraction, β-catenin was undetectable at day 11 and appeared only weakly on day 1. Even
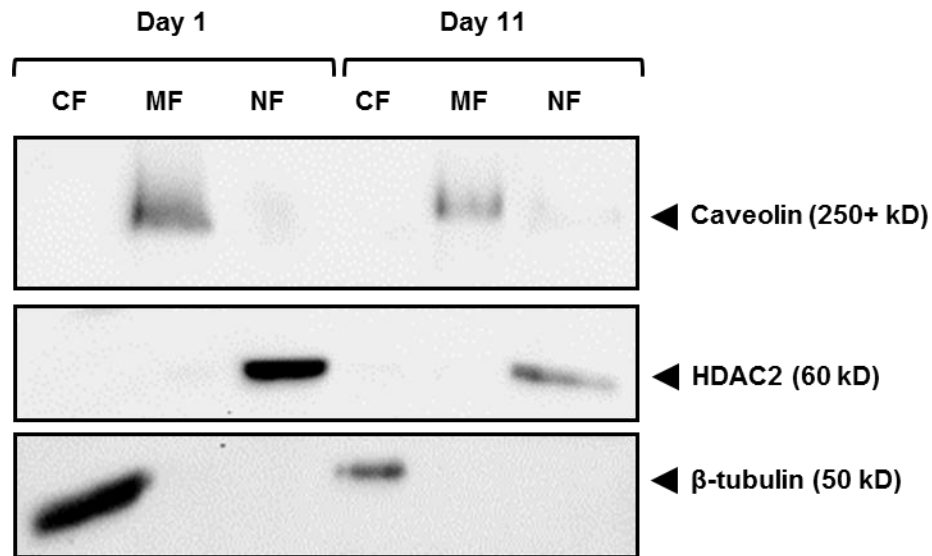
Figure 5-3. Validation of subcellular fractionation of MSC pellets. Chondrogenic MSC pellets from days 1 and 11 days were fractionated using the Pierce Subcellular Protein Fractionation Kit for Cultured Cells. 20 μL of each fraction was analyzed by Western blotting using antibodies against proteins specific to each fraction. β-tubulin was used as a marker of the cytoplasmic fraction (CF), oligomerized caveolin was used as a marker of the membrane fraction (MF), and HDAC2 was used as a marker of the nuclear fraction (NF).
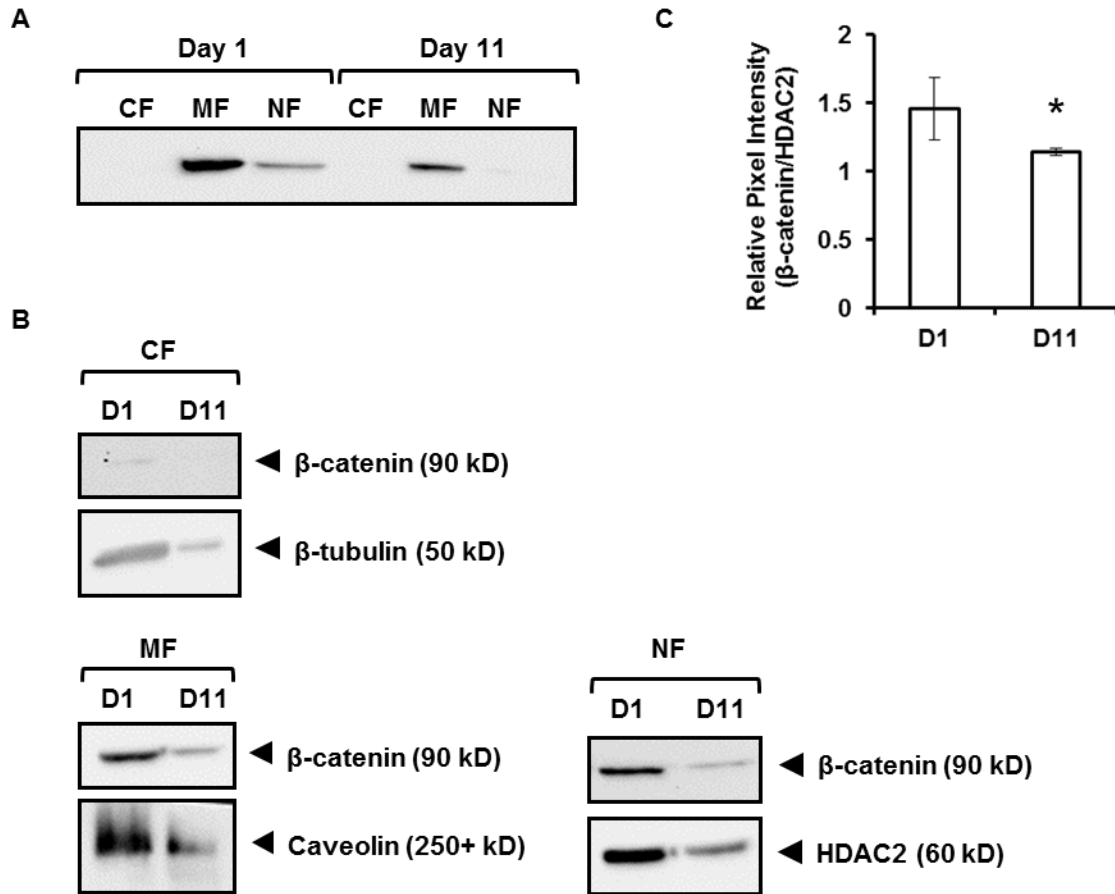
Figure 5-4. Subcellular localization of β-catenin during MSC chondrogenesis. The presence of β-catenin in the different cellular compartments was visualized by Western blot. (A) Side by side comparison of the cytoplasmic (CF), membrane (MF), and nuclear (NF) compartments on days 1 and 11 of chondrogenesis. (B) Comparison of the levels of β-catenin in each fraction on days 1 (D1) and 11 (D11). (C) The relative intensity of the nuclear β-catenin band to the HDAC2 band was calculated using NIH ImageJ software (n=3, *$p<0.05$).

though the β-tubulin band also decreased in intensity between days 1 and 11, it is impossible to make a comparison, since the β-catenin band could not be measured on day 11. In the membrane fraction, the intensity of the caveolin band seemed to decrease between days 1 and 11 by a greater degree than the β-catenin band, suggesting an increase in β-catenin in the membrane fraction. This could indicate an increase in cellular adhesions stabilized by β-catenin since high numbers of cell to cell contacts should form due to the high density of pellet culture. By day 11, individual cells might not yet be

completely isolated in lacunae and thus retain their adhesions containing β-catenin. Since β-catenin is not phosphorylated when part of an adhesive complex, the increase in β-catenin in the membrane fraction likely accounts at least in part for the increase observed in active β-catenin protein. Nuclear β-catenin, on the other hand, seemed as though it is decreased on day 11 compared to day 1. The ratio of intensity of the nuclear β-catenin band to the intensity of the HDAC2 band on day 11 is lower than on day 1 (Figure 5-4 C). This would suggest a decrease in β-catenin-mediated transcription of its target genes despite the increase in *Ctnnb1* transcription and decrease in β-catenin phosphorylation reported above.

Comparison of the levels of β-catenin on days 1 and 11 in each fraction is made difficult by the lack of an appropriate marker with which to normalize the protein levels in each compartment. Caveolin is an imperfect marker because its expression varies with chondrocyte maturation status [354]. It is unknown how caveolae formation changes during MSC chondrogenesis in ways that might affect comparison of proteins in the membrane fraction. Similarly, regulation of HDAC2 in MSC chondrogenesis has not been described, so these results must be interpreted with caution. In order to definitively determine activation of β-catenin signaling, a reporter assay was used.

β-Catenin Signaling is Elevated during MSC Chondrogenesis

While the levels of active β-catenin were increased during MSC chondrogenesis, its subcellular localization seemed to suggest that β-catenin is accumulating in the membrane while being reduced in the nucleus on day 11 compared to day 1. A decrease in the nucleus should indicate a reduction in β-catenin signaling, although other signaling

factors could combine to further increase or decrease its transcriptional activity. In order to determine specifically how the transcriptional activity of β-catenin is altered during MSC chondrogenesis, a β-catenin-driven reporter system was used. While other β-catenin quantities were assessed on days 1 and 11, luciferase expression was not measured until day 2 in order to allow sufficient time for expression of the transgene. Luciferase expression was significantly higher on day 11 than on day 2, indicating that β-catenin signaling is more active on day 11 than earlier in chondrogenesis. Therefore, either there is actually more β-catenin in the nucleus, which could not be observed because HDAC2 is upregulated during MSC chondrogenesis, or β-catenin transcriptional co-factors become more abundant during MSC chondrogenesis leading to increased signaling activity. An increase in β-catenin signaling activity contrasts with the decrease reported in developmental chondrogenesis and may provide an explanation for the mixed phenotype observed during MSC chondrogenesis. In order to evaluate the influence of β-
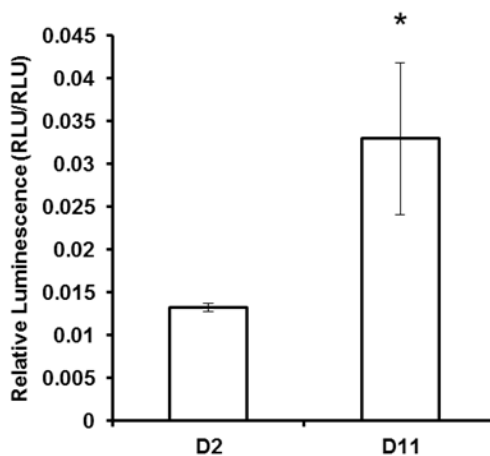
Figure 5-5. β-Catenin-regulated transcriptional activity increases during MSC chondrogenesis. The level of β-catenin responsive transcriptional activity was assessed using promoter-reporter construct containing TCF/LEF firefly luciferase, with a Renilla luciferase reporter as control. MSCs were transfected with the lentiviral reporter genes before pellet formation, and then differentiated in CM for 11 days. Pellets were lysed in 100 μL PLB/pellet at days 2 (D2) and 11 (D11) and luciferase activity was determined using the Promega DualGlo Assay (n=3, *p<0.05). Total lysate was 100-200 μL, or 1-2 pellets per sample.

catenin on the chondrogenic MSC phenotype, we modulated β-catenin signaling during

MSC chondrogenesis and the results are reported in the next chapter.

Chapter 6

β-catenin Signaling Regulates MSC Chondrogenesis

6.1 Introduction

In the previous chapter, we demonstrated that β-catenin-driven transcription is increased during the course of MSC chondrogenesis. This contrasts with its downregulation during developmental chondrogenesis, and suggests that canonical Wnt/β-catenin signaling may play a role in modulating the phenotype of chondrogenic MSCs. In this chapter, we endeavored to discover the ways in which β-catenin signaling regulates chondrogenesis in MSCs.

β-Catenin differentially regulates the phenotype of chondrocytes at various stages of chondrocyte differentiation. Constitutive activation of LEF-1 in nascent chondrocytes severely compromises chondrogenesis in transgenic mice [181]. *In vitro*, constitutively active β-catenin causes immature chondrocytes to dedifferentiate, which may explain the defective chondrogenesis observed *in vivo* [181, 268]. Conversely, conditional inactivation of β-catenin in condensing mesenchymal cells enhances chondrogenesis, resulting in ectopic cartilage formation [168]. In maturing chick chondrocytes, constitutive activation of β-catenin signaling accelerates the development of a hypertrophic phenotype, while inhibition of β-catenin signaling increases markers of chondrogenesis and decreases markers of hypertrophy [169, 181, 269, 355, 356]. In articular chondrocytes, constitutive activation of β-catenin causes them to assume a hypertrophic phenotype [296]. *In vitro*, when articular chondrocytes are dedifferentiated in serial monolayer culture, β-catenin becomes more abundant and translocates to the

nucleus [171]. Thus, β-catenin negatively regulates chondrogenesis in immature chondrocytes and positively regulates hypertrophy in more mature chondrocytes.

The differentiation state of chondrogenic MSCs varies in culture, so how they will respond to β-catenin modulation is not clear. One study on fracture healing in *Col2a1-ICAT* mice may provide some insight. In these mice, inhibitor of β-catenin/TCF (ICAT) is expressed in *Col2a1*-expressing cells, leading to reduction in callus formation and delayed callus ossification following fracture [357]. Since MSCs are involved in callus formation, this suggests that inhibition of β-catenin may inhibit their differentiation into chondrocytes as well as subsequent endochondral ossification. While the latter result is consistent with effects in maturing chondrocytes, the former is unexpected. Two recent studies have examined the role of β-catenin in *in vitro* MSC chondrogenesis. Im et al. showed that Wnt inhibitors enhance MSC chondrogenesis [358, 359]. Zheng et al. showed that stimulation of β-catenin during the first week of chondrogenesis enhanced hypertrophy of MSC pellets after 5 weeks, but continued stimulation of β-catenin decreased hypertrophy [360]. These studies in MSCs were used to guide the design of our experiments investigating the role of β-catenin in MSC chondrogenesis.

There are myriad ways to modulate β-catenin signaling. We chose to use small molecules targeting different components of the canonical Wnt/β-catenin pathway because of the ease of their incorporation into the existing culture system requiring only the addition of an extra component to the CM. The aforementioned studies in MSCs used Dickkopf (Dkk)-1 and secreted Frizzled-related protein (sFRP)-1 to inhibit Wnt signaling and LiCl to stimulate it. Since we wanted to specifically target nuclear β-catenin signaling, we wanted to use the most specific small molecules available. To review,

cytoplasmic β-catenin is bound in a complex with Axin, APC, and GSK-3β. GSK-3β phosphorylates β-catenin, leading to its proteasomal degradation. Wnt binds to and activates the Fz and LRP5/6 receptors, activating Dsh and promoting disassembly of the β-catenin destruction complex. Newly free β-catenin can then translocate to the nucleus, complex with TCF/LEF, and activate transcription of its target genes.

In order to study the effects of β-catenin inhibition we wanted a molecule that directly targeted β-catenin-mediated transcription because inhibition of other parts of the canonical Wnt pathway might allow cross-communicating pathways to continue to regulate β-catenin as well as inhibition non-canonical signaling. Dkk-1 and sFRP-1, which inhibit Wnt receptor activation, and LiCl, which non-specifically inhibits GSK-3β were deemed inappropriate choices. We initially identified PKF115-584, a small molecule that disrupts the association of β-catenin with TCF/LEF [361], but it was not commercially available so we turned our attention to XAV939. XAV939 has been identified as a small molecule inhibitor of β-catenin itself [362]. XAV939 inhibits the catalytic activity of TNKS1/2, a pair of tankyrases that interact with the N-terminal of Axin via their ankyrin domain. TNKS1/2 modify their substrates with ADP-ribose units in a process known as PARSylation. XAV939 binds the catalytic domain of TNKS1/2 with high affinity (K_d=0.1 μM), inhibiting PARSylation. Since PARSylation of Axin leads to its degradation, XAV939 increases the abundance of Axin, and promotes activity of the β-catenin destruction complex. Correspondingly, it has been shown that XAV939 inhibits β-catenin signaling, decreases β-catenin abundance, and increases β-catenin phosphorylation. Meanwhile, XAV939 had no effects on CRE, NF-κB, or TGF-β reporters [362], demonstrating the specificity of XAV939 in inhibiting canonical Wnt

signaling by promoting the degradation of β-catenin. However, other byproducts of Axin activation remain unknown.

In order to study the effects of elevated β-catenin signaling we used a GSK-3β inhibitor that resulted in accumulation of active β-catenin protein. Lithium salts are known inhibitors of GSK-3β, and increase β-catenin signaling, but lithium also inhibits other cellular enzymes and high concentrations are needed [363]. We chose the small molecule CHIR99021, whose specificity for GSK-3β inhibition (IC_{50}=6.7 nM) was shown to be up to 10^4 times greater than for other kinases [363]. In 3T3-L1 cells, CHIR99021 increased the amount of β-catenin within the cells without altering its occurrence in the membrane [364]. In H4IIE cells, CHIR99021 induced dose-dependent activation of β-catenin signaling [365]. Together these results demonstrate that CHIR99021 stimulates canonical Wnt signaling by preventing the degradation of β-catenin through selective inhibition of GSK-3β.

Based on its effects in chondrocytes, we hypothesized that β-catenin inhibition would promote MSC chondrogenesis and inhibit hypertrophy, and that β-catenin activation would promote MSC hypertrophy and inhibit chondrogenesis. In the next section we describe the effects of β-catenin modulation on MSC chondrogenesis using the small molecules XAV939 and CHIR99021.

6.2 Results

XAV939 Decreases β-catenin Signaling and Protein Levels

The inhibitory effect of XAV939 on β-catenin signaling was validated in MSCs via luciferase reporter, ICC, and ELISA. First, MSCs from a single donor were transfected with a lentiviral β-catenin-driven luciferase reporter plasmid and a constitutively active Renilla luciferase plasmid. Pellets of infected MSCs were treated with different concentrations of XAV939 in CM in order to determine the concentration that produces the largest reduction in β-catenin signaling. MSC pellets exhibited a reduction in relative luciferase activity at all concentrations of XAV939 on day 2 and day 11 (Figure 6-1 A). This inhibition was significant at XAV939 doses of 1 μM and 10 μM on day 2, with the greatest response observed at 1 μM. While the reduction in luciferase activity was not significant at day 11, the dose-response behavior was identical to that observed on day 2. Based on the outcome of the initial dose-repose experiment, relative luciferase activity was assessed in MSC pellets from three different donors treated with 1 μM XAV939. A significant reduction in luciferase activity was verified on day 2 in all donors. The decrease in luciferase reporter activity indicates a reduction in β-catenin signaling with XAV939 treatment.

In monolayer MSCs, treatment with 1 μM XAV939 for 24 hours resulted in decreased β-catenin signal upon immunocytochemical tagging. While background noise made it difficult to identify the localization of β-catenin, there is distinctly less overall signal in the XAV939-treated MSCs versus control cells (Figure 6-1 B). This indicates a reduction in the amount of total β-catenin in treated MSCs. In pellets, the amount of

A

B

β-catenin Immunocytochemistry

Control　　　　　　1 μM XAV939

C

D11
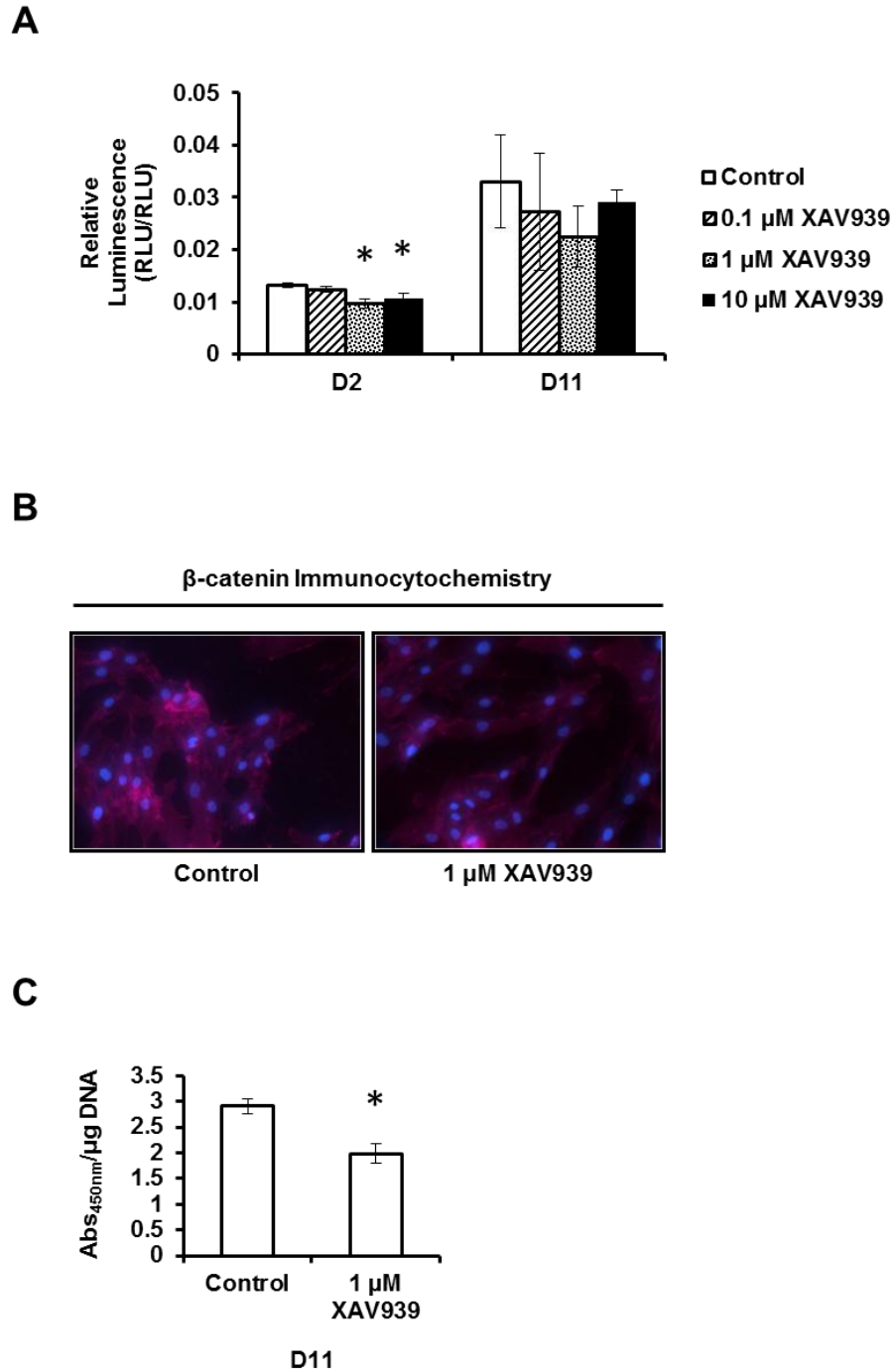
Figure 6-1. Validation of the effects of XAV939 on β-catenin signaling. (A) MSC pellets from one donor were cultured in CM for 11 days with various concentrations of XAV939. Changes in transcriptional activity between days 2 and 11 were assessed using a TCF/LEF luciferase reporter system (n=3, *p<0.05). The greatest inhibition of reporter activity was observed at 1 μM XAV939 at both time points. (B) In monolayer MSCs from 4 donors, β-catenin was tagged with the fluorophore AlexaFluor647, depicted here in fuchsia. After only 24 hours of treatment with XAV939, less of the fluorescent marker was detected. (C) As measured by ELISA, the level of active β-catenin in chondrogenic pellets was decreased in pellets from one donor treated with 1 μM XAV939 for 11 days of chondrogenic culture (n=3, *p<0.05).
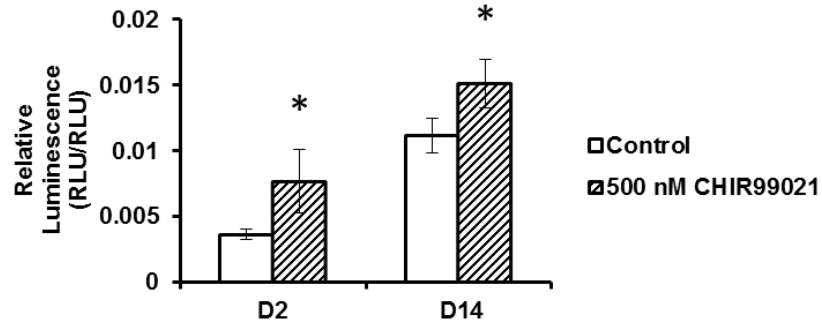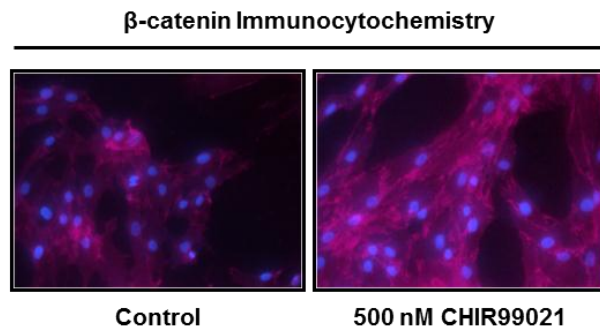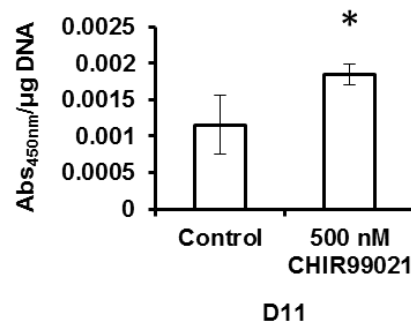
Figure 6-2. Validation of the effects of CHIR99021 on β-catenin signaling. (A) Changes in luciferase activity in MSC pellets from a single donor cultured in CM for with 500 nM CHIR99021 were assessed on days 2 and 11 using a TCF/LEF luciferase reporter system (n=3, *p<0.05). Significant enhancement of reporter activity was observed at both time points. (B) In monolayer MSCs from 4 donors, after only 24 hours of treatment with CHIR99021, more of fluorescently labeled β-catenin (fuchsia) was detected by ICC. (C) MSC pellets from one donor supplemented with 500 nM CHIR99021 during chondrogenesis exhibited increased levels of active β-catenin on day 11 as measure by ELISA (n=3, *p<0.05).

active β-catenin was evaluated by ELISA and normalized to the DNA content. After 11 days of chondrogenic culture, pellets that were supplemented with 1 μM XAV939 contained less active β-catenin (Figure 6-1 C). The reporter, immunocytochemistry, and ELISA results all support the conclusion that XAV939 inhibits β-catenin signaling in MSCs.

CHIR99021 Increases β-catenin Signaling and Protein Levels

To validate the stimulatory effect of CHIR99021 on β-catenin signaling in MSCs, both MSC pellets and monolayer cultures were analyzed. The manufacturer's recommendation of 500 nM was used for all experimental treatment groups. Pellets supplemented with 500 nM CHIR99021 during chondrogenesis exhibited significantly increased expression of a β-catenin-driven luciferase reporter gene on both days 2 and 14 of culture (Figure 6-2 A). Similar stimulation of relative luciferase activity was observed in pellets from three different donors, indicating enhanced β-catenin signaling with CHIR99021 treatment.

The increase in reporter gene expression correlated with changes observed in β-catenin expression both in monolayer MSCs and in pellets. In monolayer, treatment of MSCs with CHIR99021 for only 24 hours led to increased immunocytochemical labeling of β-catenin, which indicates an increase in total β-catenin within the MSCs (Figure 6-2 B). In pellets, a significant increase in active β-catenin was observed after 11 days of chondrogenesis (Figure 6-2 C). As a GSK-3 inhibitor, CHIR99021 inhibits phosphorylation and targeted ubiquitination of β-catenin, which leads to accumulation of the active form of the molecule as observed here. Together with the reporter and

immunocytochemistry results, this data validates CHIR99021 as a stimulator of β-catenin signaling.

GAG Accumulation in Chondrogenic MSCs is Negatively Regulated by β-catenin

The effect of β-catenin inhibition and stimulation on sGAG deposition in chondrogenic MSC pellets was assessed on day 11. MSCs from 6 different donors were treated with XAV939 to inhibit β-catenin signaling: 52 year old male (52M), 53 year old male (53M), 55 year old male (55M), and 59 year old male (59M), which were strongly chondrogenic, 60 year old male (60M), which exhibited delayed chondrogenesis, and 63 year old male (63M), which was weakly chondrogenic. For stimulation of β-catenin signaling, the same donors were used with the exception of 60M, for a total of 5 donors.

On day 11, treatment with XAV939 enhanced the amount of GAG per cell in all pellets (Figure 6-3 A). The increased GAG deposition was significant in pellets from 3 of 4 of the strongly chondrogenic donors and in pellets from 60M, but not in weakly chondrogenic pellets. Conversely, treatment with CHIR99021 resulted in decreased GAG deposition on day 11 of chondrogenesis in pellets from all donors, although this result was only significant in one donor. These quantitative data suggest that β-catenin negatively regulates GAG accumulation.

In order to qualitatively assess sGAG accumulation within the pellets, paraffin-embedded sections of 11 day old pellets were stained with Saf O. Strongly chondrogenic pellets cultured with XAV939 exhibited more intense Saf O staining than control pellets (Figure 6-3 B). Whereas some control pellets had regions that did not stain positive, which were typically found in the center of the pellet, there was usually an even

distribution of Saf O throughout the XAV939-treated pellets. Pellets cultured with CHIR99021, on the other hand, had only very weak Saf O staining, if any. Regions without staining were more prevalent in CHIR99021-treated pellets compared to controls. Pellets from delayed and weakly chondrogenic donors had little staining in the control

A
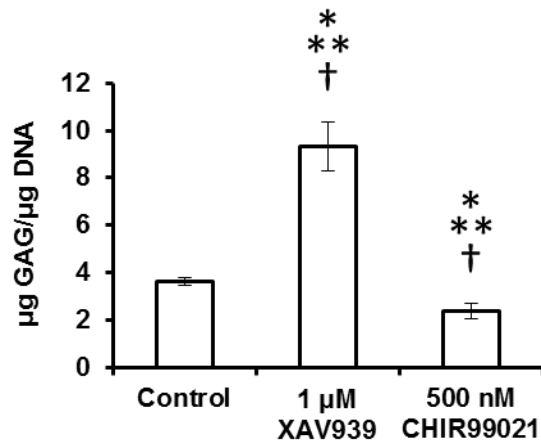
B
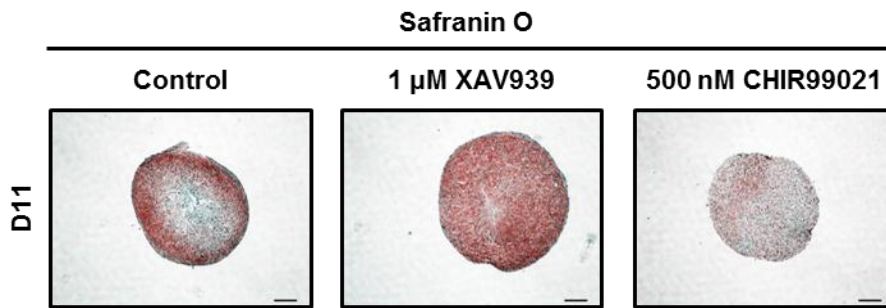
Figure 6-3. Modulation of β-catenin signaling affects GAG deposition during MSC chondrogenesis. MSC pellets were cultured in CM for 11 days with 1 μM XAV939, 500 nM CHIR99021, or 0.1% DMSO (Control). (A) Sulfated GAG content of digested pellets on day 11 was increased with XAV939 treatment and decreased with CHIR99021 treatment. Data shown from one patient is representative of 5-6 patients tested. *$p<0.05$ indicates significance for donor shown (n=3). ** indicates trend among strongly chondrogenic pellets (n=4). † indicates trend among all pellets (n=5-6). (B) Safranin O/Fast Green staining of paraffin-embedded sections revealed increased staining with XAV939 treatment and decreased staining with CHIR99021 treatment in pellets from strongly chondrogenic donors. Images shown from one representative donor.

pellets, which made it impossible to compare GAG deposition with the other treatment groups. Increased staining in the XAV939 treatment group and decreased staining in the CHIR99021 treatment group corroborated the quantitative GAG results that β-catenin inhibition promotes GAG synthesis, while stimulation of β-catenin signaling negatively regulates GAG accumulation in chondrogenic MSCs.

Chondrogenic Gene Expression is Negatively Regulated by β-catenin

Transcriptional regulation of genes associated with chondrogenesis was assessed in chondrogenic pellets treated with XAV939 and CHIR99021 via RT-PCR. Expression levels were normalized to *GAPDH* expression. On day 11, expression of *Sox9*, *Col2a1*, and *Acan* was increased in all strongly chondrogenic pellets cultured with XAV939 (Figure 6-4 A-C). Expression of *Col2a1* and *Acan* was decreased on day 11 when pellets were cultured with CHIR99021 in all pellets (Figure 6-4 D-F). Expression of *Sox9* was also decreased in CHIR99021-treated pellets from all but a single donor. These results indicate that inhibition of β-catenin enhances expression of chondrogenic genes, while stimulation of β-catenin suppresses their expression.

Variability in the magnitude of response to β-catenin was observed between donors. The increases in chondrogenic gene expression with XAV939 treatment were statistically significant in many of the pellets tested. In pellets of strongly chondrogenic MSCs, the increase in *Sox9* was significant in 50% of the donors, but never in delayed or weakly chondrogenic pellets. The increase in *Col2a1* was significant in 100% of strongly chondrogenic MSC pellets and in pellets of weakly chondrogenic donor cells. However, in 60M pellets, which exhibited delayed chondrogenesis, *Col2a1* was significantly

127
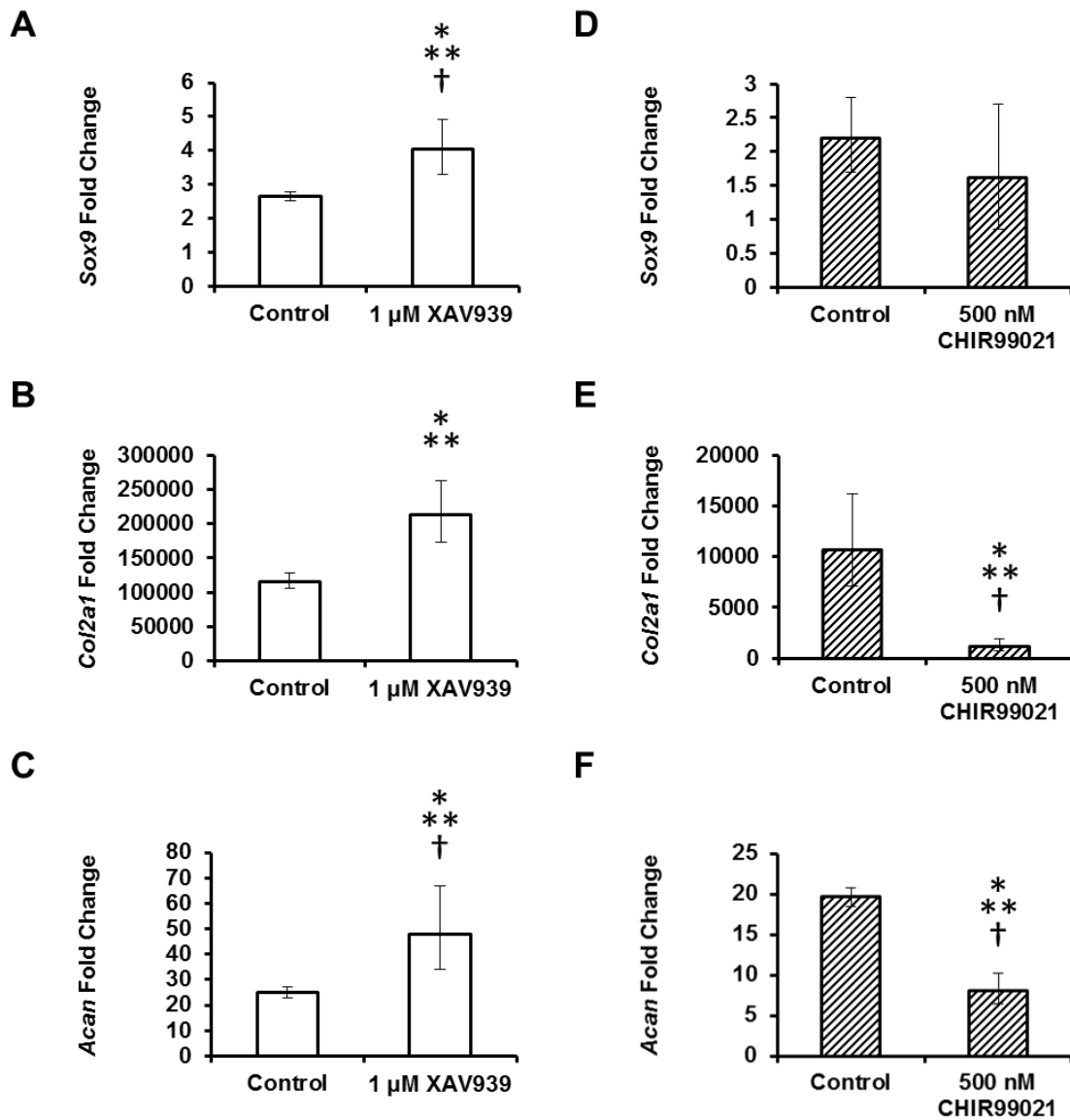
Figure 6-4. Inhibition of β-catenin signaling increases expression of chondrogenic genes, while stimulation of β-catenin signaling decreases expression of chondrogenic genes. MSC pellets were cultured in CM supplemented with 1 μM XAV939, 500 nM CHIR99021, or 0.1% DMSO (Control). Expression of chondrogenic genes on day 11 was normalized to GAPDH and are depicted as fold changes relative to day 1 expression. Treatment with XAV939 resulted in upregulation of (A) *Sox9*, (B) *Col2a1*, and (C) *Acan*, while treatment with CHIR99021 led to downregulation of (D) *Sox9*, (E) *Col2a1*, and (F) *Acan*. Each graph depicts data from one representative donor. *p<0.05 for donor shown (n=3). ** indicates trend among strongly chondrogenic pellets (n=4). † indicates trend among all pellets (n=5-6).

decreased in the XAV939 treatment group compared to the control group. *Acan* was significantly upregulated in all strongly chondrogenic pellets treated with XAV939, but the increase in *Acan* expression was not significant in pellets from either delayed or weakly chondrogenic pellets.

In CHIR99021-treated pellets the alterations in *Sox9* were not significant, but the decreases in *Col2a1* and *Acan* were statistically significant in strongly chondrogenic pellets. *Sox9* was decreased in 75% of the strongly chondrogenic pellets supplemented with CHIR99021 and in weakly chondrogenic pellets, but none of these decreases were significant. In pellets from one donor, *Sox9* expression was increased by 20% compared to controls, but this was not significant. In addition to the strongly chondrogenic pellets, *Col2a1* expression was significantly decreased in weakly chondrogenic pellets cultured with CHIR99021 as well. The decrease in *Acan* expression, however, was not significant in CHIR99021-treated pellets from weakly chondrogenic donors. Despite differences between donors, RT-PCR data support the conclusion that β-catenin negatively regulates chondrogenic gene expression in MSCs.

Hypertrophic Gene Expression is Differentially Regulated by β-catenin

Transcriptional regulation by XAV939 and CHIR99021 was assessed for genes associated with chondrocyte hypertrophy. Unlike the chondrogenic genes which demonstrated clear patterns of regulation upon β-catenin signaling modification, the regulation of hypetrophic gene expression was less straightforward. On day 11, XAV939 treatment tended to decrease *Runx2*, *ALP*, *MMP13*, and *BSP*, but had little discernible effect on Col10a1 or *PTHrP* expression (Figure 6-5). Treatment with CHIR99021 tended
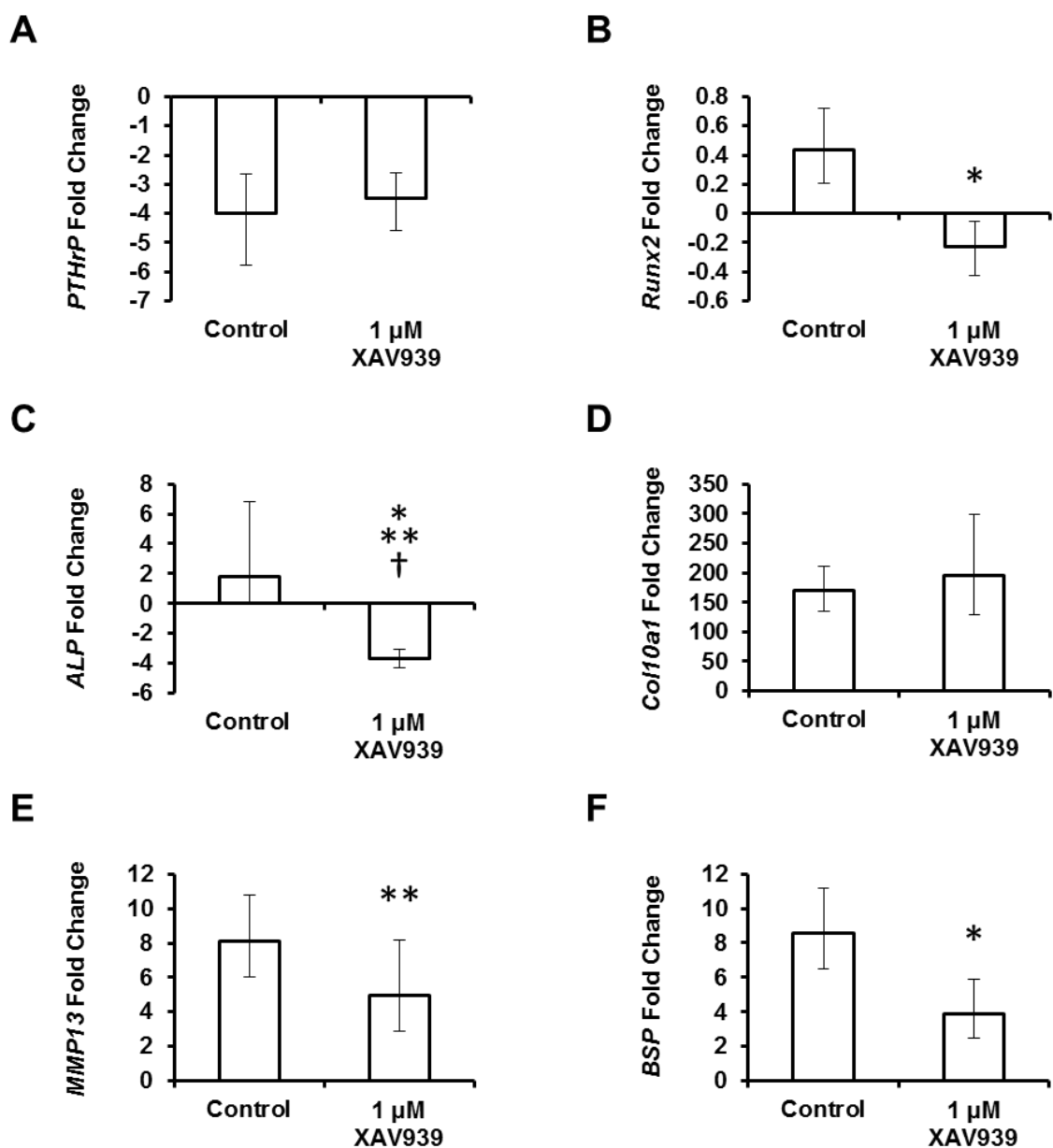
Figure 6-5. Inhibition of β-catenin signaling decreases expression of some hypertrophic genes. MSC pellets were cultured in CM supplemented with 1 μM XAV939 or 0.1% DMSO (Control). Expression of hypertrophic genes on day 11 was normalized to GAPDH and are depicted as fold changes relative to day 1 expression. Treatment with XAV939 resulted in downregulation of (C) *ALP* and (E) *MMP13* and indeterminate effects on (A) *PTHrP*, (B) *Runx2*, (D) *Col10a1*, and (F) *BSP*. Each graph depicts data from one representative donor. *p<0.05 for donor shown (n=3). ** indicates trend among all strongly chondrogenic pellets (n=4). † indicates trend among all strongly and weakly chondrogenic pellets (n=6).
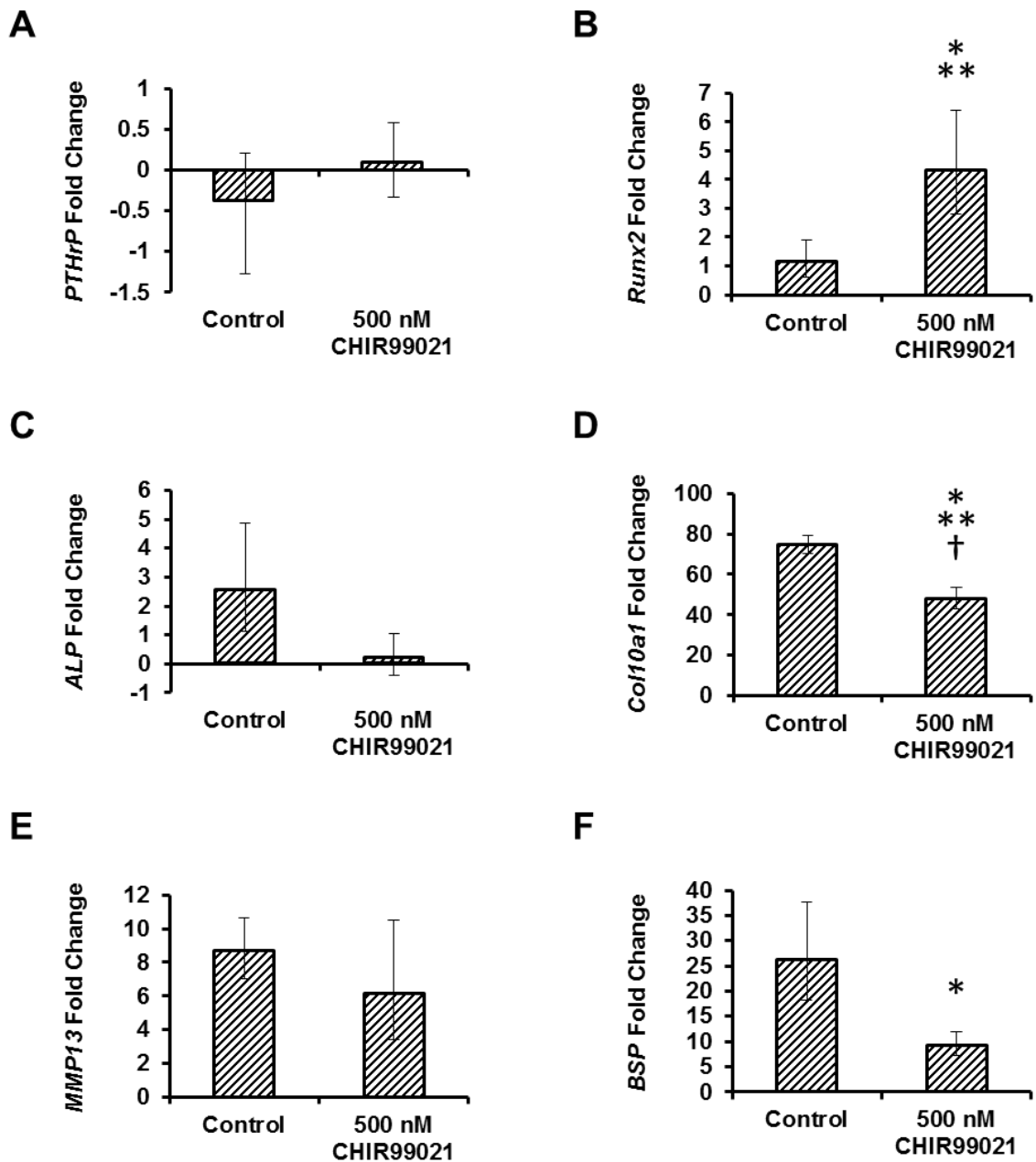
Figure 6-6. Stimulation of β-catenin signaling decreases expression of most hypertrophic genes, but not *Runx2*. MSC pellets were cultured in CM supplemented with 500 nM CHIR99021 or 0.1% DMSO (Control). Expression of hypertrophic genes on day 11 was normalized to GAPDH and are depicted as fold changes relative to day 1 expression. Treatment with CHIR99021 resulted in upregulation of (B) *Runx2* and downregulation of (D) *Col10a1*. There were no consistent effects on (A) *PTHrP*, (C) *ALP*, (E) *MMP13*, and (F) *BSP*. Each graph depicts data from one representative donor. *p<0.05 for donor shown (n=3). ** indicates trend among all strongly chondrogenic pellets (n=3). † indicates trend among all strongly and weakly chondrogenic pellets (n=5).

to increase *Runx2* and PTHrP, and decrease *ALP*, *Col10a1*, *MMP13*, and *BSP* (Figure 6-6). Inhibition and stimulation of β-catenin signaling did not have opposing effects on hypertrophy gene expression as they did on markers of chondrogenesis.

Inhibition of β-catenin signaling with XAV939 had a mostly suppressive effect on genes associated with hypertrophy with the following differences observed between donors. *Runx2* was downregulated in pellets from 75% of strongly chondrogenic donors, significantly in one, and significantly downregulated in 60M pellets that exhibited delayed chondrogenesis. *ALP* was downregulated in all pellets, including those from delayed or weakly chondrogenic donors, and this was significant in all but 2 donors. *MMP13* expression was also reduced in all strongly chondrogenic pellets, but not significantly. *MMP13* was upregulated in pellets from delayed and weakly chondrogenic donors. *BSP* was downregulated in pellets from 3 of 4 strongly chondrogenic donors, significantly in 2. It was also significantly reduced in 60M pellets. Conversely, *Col10a1* expression was increased in pellets from 3 of 4 strongly chondrogenic donors cultured with XAV939, although never significantly. In pellets from delayed and weakly chondrogenic donors, *Col10a1* was downregulated, but not significantly. There was no obvious effect on *PTHrP* expression, which was up in half of the strongly chondrogenic pellets and down in the other half (Figure 6-5A). None of the alterations in *PTHrP* expression were significant, except in pellets experiencing delayed chondrogenesis in which *PTHrP* was significantly upregulated. These data indicate that inhibition of β-catenin signaling has a suppressive effect on most indicators of chondrocyte hypertrophy while still enhancing expression of Col10a1.

Stimulation of β-catenin signaling in chondrogenic MSC pellets with CHIR99021 tended to increase expression of genes encoding signaling molecules and decrease expression of genes encoding functional hypertrophic proteins, again with some observed donor variability. *PTHrP* expression was increased in pellets from 2 of 3 strongly chondrogenic donors, though not significantly. *Runx2* was also upregulated in all strongly chondrogenic MSCs, and significantly in 50% of them. In weakly chondrogenic pellets, *Runx2* was downregulated, but not significantly. Meanwhile, *ALP* was downregulated in pellets from 75% of the strongly chondrogenic donors. In weakly chondrogenic MSCs, *ALP* expression was increased, but this increase was not significant. CHIR99021 treatment downregulated *MMP13* in pellets from 2 of 3 strongly chondrogenic donors, but not significantly. MSC pellets from the other strongly chondrogenic donor had significantly increased *MMP13* expression. *Col10a1* was significantly downregulated in nearly all strongly and weakly chondrogenic MSCs. *BSP* was significantly downregulated in pellets from 2 of 3 strongly chondrogenic donors. Changes in BSP expression in the remaining strongly chondrogenic donor and in weakly chondrogenic MSCs were not significant. These data indicate that stimulation of β-catenin signaling has a suppressive effect on functional indicators of chondrocyte hypertrophy.

While DMSO had no effect on transcription of most of the genes evaluated, DMSO significantly suppressed expression of *MMP13*. Therefore, it is impossible to completely distinguish the effects of XAV939 and CHIR99021 from the effects of DMSO.

MMPs are Differentially Regulated by β-catenin

While gene expression is an indication of the changing phenotype of chondrogenic MSC pellets, functional hypertrophy can be identified via Col10 deposition, ALP activity, and MMP13 activity. However, no Col10 can be detected via immunohistochemistry on day 11, so alterations in Col10 deposition due to modulation of β-catenin signaling were not assessed in this case. Since ALP activity has been shown to correlate with changes in *ALP* expression, an ALP activity assay would be redundant here. Recently, MMPs have begun to be assessed in chondrogenic MSC pellets cultured with XAV939 and CHIR99021, but so far only pellets from one donor, 59M, have been analyzed. The results from that one donor are presented below.

MMP2 and MMP13 were secreted by chondrogenic pellets from all treatment groups. Conditioned media were analyzed by Western blot for the presence of MMP1, MMP2, and MMP13. While no MMP1 was detected in any conditioned medium, both MMP2 and MMP13 were present in the media of pellets from all treatment groups (Figure 6-7 A). The amount of secreted MMP2 appears to be increased in conditioned medium from the XAV939-treated pellets compared to its levels in the medium from control pellets. However, secreted MMP2 levels were unchanged in medium from CHIR99021-treated pellets. Less MMP13 was apparent in the medium from both treatment groups compared to control medium. The conditioned medium was also subjected to an MMP activity assay, but no MMP activity was detected, likely due to the presence of TIMPs, which are produced at high levels by MSCs [366]. However, at least at the level of secretion, β-catenin inhibition inhibited MMP13 and enhanced MMP2, while β-catenin stimulation had no effect on either one.
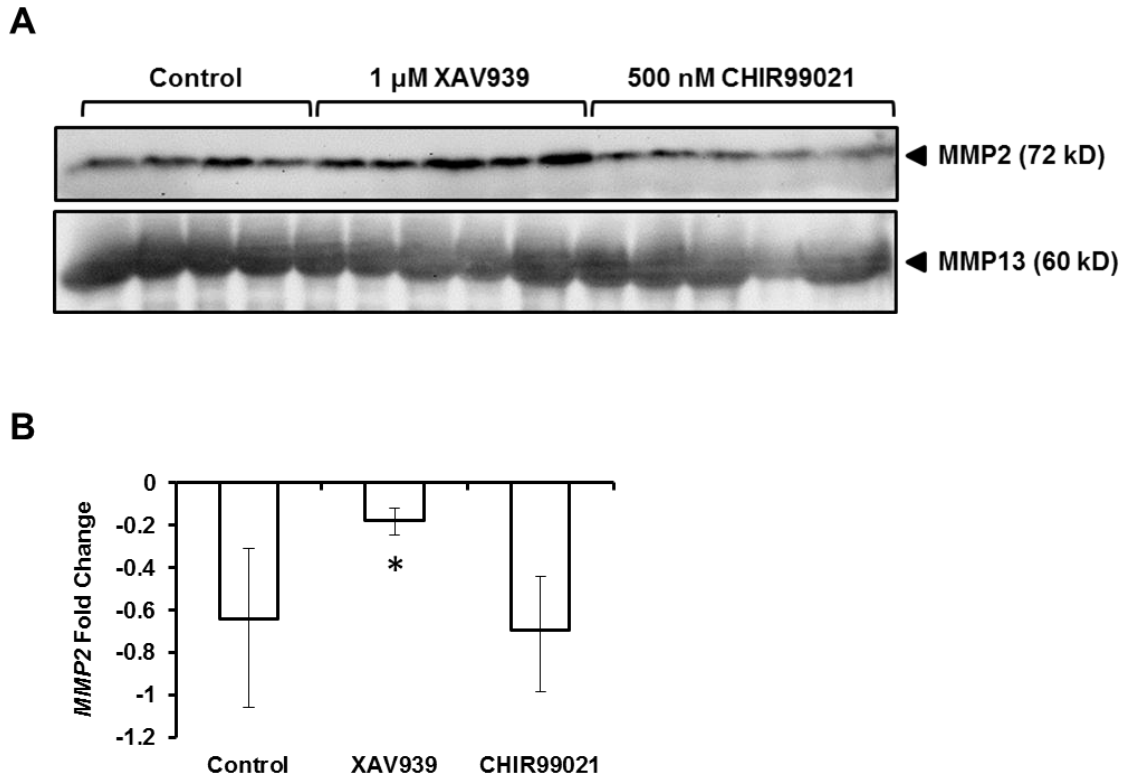
Figure 6-7. Inhibition of β-catenin signaling alters secretion of MMPs. Conditioned medium was collected from 59M pellets supplemented with 1 μM XAV939, 500 nM CHIR99021, or 0.1% DMSO (Control). (A) Western blot revealed increased MMP2 upon treatment with XAV939 and decreased MMP13 upon treatment with XAV939 and CHIR99021. (B) Alterations in MMP2 secretion were correlated with changes in *MMP2* expression. *$p<0.05$ (n=3).

The changes in secreted MMP13 and MMP2 with the different β-catenin treatments correlated with changes in their gene expression. As described previously, MMP13 was decreased with XAV939 treatment and unchanged by CHIR99021. Treatment with XAV939 led to increased expression of *MMP2*, while CHIR99021 had no significant effect, which correlated with its functional regulation (Figure 6-7 B). This indicates that in addition to MMP13, β-catenin signaling also regulates MMP2 during MSC chondrogenesis.

135

Chapter 7 Discussion

7.1 Summary

In Chapter 3, MSC chondrogenesis was characterized for two main purposes. The first was to identify a time point earlier than the commonly used day 21 at which chondrogenesis could be defined. The second aim was to map the development of hypertrophic characteristics, which are commonly overlooked in studies of MSC chondrogenesis, in order to better understand the hypertrophic character of chondrogenic MSCs. Toward the first aim, MSC pellets were cultured in CM, and sGAG deposition and relative expression of *Sox9*, *Col2a1*, and *Acan* were measured over the course of 21 days. Day 11 was identified as an earlier point at which chondrogenesis could be definitively established based on increased accumulation of GAG and increased expression of chondrogenic genes. The magnitude of GAG accumulation revealed a distinction between what were termed "strongly" and "weakly" chondrogenic MSC sources, and only the strongly chondrogenic cells were used for subsequent analyses. Unlike differentiating mesenchymal cells in the limb bud or in micromass culture, expression of hypertrophy genes during MSC chondrogenesis did not occur in a sequential pattern, but rather simultaneously with expression of articular cartilage specific genes, suggesting that MSCs undergoing chondrogenesis *in vitro* do not behave like neo-chondrocytes or hypertrophic chondrocytes, but rather like a hybrid of the two.

In Chapter 4, regulation of both the articular and hypertrophic aspects of chondrogenically differentiated MSCs by CHP was evaluated. Chondrogenic markers were enhanced on day 11 in MSC pellets exposed to daily CHP, while inhibitory effects

of CHP were seen for several markers of hypertrophy on day 21. Varying the days on which CHP was applied revealed diverse effects of loading during different phases of chondrogenic culture. Loading during the first 10 days of MSC chondrogenesis increased some markers of chondrogenesis, while loading during the latter half of chondrogenic culture was detrimental to chondrogenic markers. However, CHP applied during the second half of MSC chondrogenesis did inhibit expression of some hypertrophy marker genes. The canonical Wnt/β-catenin and MAPK signaling pathways were identified as mechanosensitive elements in MSCs exposed to CHP. β-Catenin signaling was selected as the focus of future studies on the regulation of the chondrogenic MSC phenotype because of its mechanosensitive nature and integral role in regulating developmental chondrogenesis, endochondral ossification, and the pathogenesis of OA.

In Chapter 5, regulation of β-catenin and canonical Wnt signaling was characterized in MSCs over the course of 11 days of chondrogenesis. β-Catenin was shown to be positively regulated at the level of transcription of *Ctnnb1* during MSC chondrogenesis. β-Catenin protein persisted at the membrane and in the nucleus after 11 days compared to day 1, and increased levels of dephosphorylated β-catenin correlated with increased canonical Wnt signaling. Elevated β-catenin signaling over the course of MSC chondrogenesis supported the previous conclusion that chondrogenic MSCs do not adhere to the phenotypic patterns observed in developmental chondrogenesis, where β-catenin signaling is decreased in regions of chondrogenic differentiation. The presence of β-catenin signaling in differentiating MSCs also confirmed that this pathway is a promising target through which to modify MSC chondrogenesis in order to improve the quality of engineered tissue.

In Chapter 6, the phenotypic effects of β-catenin modulation were assessed in MSCs after 11 days of chondrogenic culture. Inhibition of β-catenin enhanced GAG production and expression of chondrogenic genes, suggesting an inhibitory effect of β-catenin on MSC chondrogenesis. The decreased expression of many hypertrophic genes in response to β-catenin inhibition, suggests that β-catenin signaling is required for the development of hypertrophic characteristics in chondrogenic MSCs. The enhancement of chondrogenic genes and suppression of hypertrophy genes observed with β-catenin inhibition alleviates one of the major deficiencies of MSC chondrogenesis. Stimulation of β-catenin diminished GAG accumulation and *Col2a1* and *Acan* expression, suggesting an inhibitory effect of β-catenin on MSC chondrogenesis as before. However, while stimulation of β-catenin enhanced expression of Runx2, other hypertrophic genes were inhibited. These data suggest that overstimulation by β-catenin in MSCs actually prevents hypertrophy in these cells because they do not go through chondrogenesis, although we did not investigate whether these cells might actually be undergoing osteogenic differentiation. Thus, inhibition of β-catenin signaling during MSC chondrogenesis favored chondrogenesis over hypertrophy, while elevated β-catenin prevented any kind of chondrogenic differentiation.

Two of the recurring themes across multiple studies are the issue of donor variability and the idea of an "intermediate" MSC phenotype that falls somewhere between that of neo-chondrocytes and hypertrophic chondrocytes. Variability in the MSC response was observed in all studies in which MSCs from multiple donors were analyzed. Similarities between the phenotype of chondrogenic MSCs and other kinds of chondrocytes were discerned at many different levels. These themes will be fleshed out in

the following sections prior to describing the significance of the CHP and β-catenin studies.

7.2 Donor Variability

It is unsurprising that cells derived from different donors would exhibit varying capacities for chondrogenic differentiation. Firstly, MSC populations are themselves heterogeneous. MSCs derived from individual adherent cells vary as to their ability to undergo trilineage differentiation [2, 12]. Therefore, the proportion of MSCs capable of chondrogenic differentiation can vary by donor. Populations containing greater numbers of MSCs capable of chondrogenic differentiation will have a higher bulk chondrogenic capacity. Second, the degree to which cells from different colonies derived from a single donor exhibit signs of chondrogenic differentiation varies. Pittenger et al. noted that sometimes MSCs from an individual colony were only "weakly" positive for the chondrocyte phenotype compared to MSCs from other colonies from the same donor [2]. Thus, the proportion of cells capable of differing degrees of chondrogenic differentiation within an MSC population may give rise to differing overall levels of chondrogenic differentiation between donors. The inherent variability in the chondrogenic potential of MSCs from different donors must be taken into account when studying MSC chondrogenesis. Donor variability remains a major concern in the context of using autologous MSCs in cartilage repair therapies since not all MSCs from OA patients will be capable of strong chondrogenic differentiation. Recent attempts have been made to better define the osteogenic differentiation potential of clonal isolates of MSCs on the

basis of marker genes, and this paradigm can be applied to identify MSCs with strong chondrogenic potential [367].

In Chapter 3, a threshold was established to distinguish between strongly and weakly chondrogenic MSCs based on GAG production. In the initial characterization studies, MSCs from five donors were analyzed over the course of 21 days of chondrogenesis. The cells were easily segregated into groups based on the GAG content of their pellets on day 21: strongly chondrogenic pellets contained more than 12 μg GAG/μg DNA, and weakly chondrogenic pellets contained less than 6 μg GAG/μg DNA. In fact, quantitation of GAG was ultimately deemed unnecessary because GAG accumulation was easily visualized; the bigger the pellet under these conditions, the greater the GAG content. For the β-catenin and pathway modulation studies in Chapters 5 and 6, cultured pellets were classified as strongly or weakly chondrogenic based on gross examination. An attempt was made to use only strongly chondrogenic MSCs because the purpose of the pathway modulation studies was to discern the role of β-catenin in MSCs chondrogenesis, and weakly chondrogenic cells might not reflect the same signaling milieu present in strongly chondrogenic MSCs.

The division of MSCs into strongly and weakly chondrogenic groups was convenient for the purpose of this work, but these classifications do not completely or accurately reflect the spectrum of phenotypes found in chondrogenic MSCs. In addition to the absolute amount of extracellular matrix produced, MSCs from different donors exhibited varied temporal differentiation profiles. On day 11, MSC pellets from strongly chondrogenic donors exhibited disparate histological staining for sGAG, but staining was equally intense in pellets from all strongly chondrogenic donors by day 21, indicating that

some MSCs are merely delayed in their GAG synthesis program rather than deficient. The temporal progression of chondrogenic differentiation was especially important to consider in contextualizing the results in Chapter 6 because MSCs from different donors were indeed at different stages in their differentiation programs on day 11. Delayed chondrogenesis has been reported as the result of genetic mutations [368, 369], protein misexpression [170, 182], exogenous growth factor supplementation [370], and other chemical treatments [371] during chondrogenesis. Under these abnormal conditions, the signaling framework within differentiating cells is altered. In the case of MSCs, inherent disparities in the signaling programs of cells from different donors and different cells from individual donors, perhaps reflecting their biological state (e.g., cell cycle phase, epigenetics), may account for the variations in the temporal differentiation profiles.

Differential signaling activity between MSCs from different donors may help explain the variability observed in their responses to CHP. Other studies have also reported inconsistent responses to CHP by MSCs from different donors. Finger et al. subjected human marrow-derived MSCs in agarose gels to 4 hours of 1 Hz CHP at 7.5 MPa and observed varying fold changes in *Sox9* expression over 14 days [342]. Recently, Steward et al. reported that porcine marrow-derived MSCs in fibrin gels also exhibited donor variability in their biosynthetic response to 4 hours of 1 Hz CHP at 10 MPa after 21 days [338]. In this work, the wide range of GAG deposition and fold change values observed across donors is reflected in large standard deviations when measurements from multiple donors are averaged as in Chapter 4. Practically, this means that MSCs from large numbers of donors are required to yield significant results with p values of less than 0.05, even using paired statistical analyses. Therefore, trends across multiple patients

141

were evaluated as an indication of the effects of CHP and β-catenin modulation when statistical tests did not reveal significance.

Donor variability is also important to consider when interpreting quantitative RT-PCR results. Here, gene expression was calculated as a fold change relative to expression on the first day of chondrogenesis. The fold change value, therefore, depends on the initial expression levels of each gene. The magnitudes of the Sox9 fold changes were comparatively small, ranging from 0.4 to 3.3-fold, but it is important to note that during development skeletal precursors express *Sox9* even before overt chondrogenesis [125, 126]. If the same is true of MSCs, the relative expression of *Sox9* may not show significant changes even under induced chondrogenic conditions. A larger fold change may be indicative not of improved chondrogenesis, but of cells that had lower chondrogenic potential to begin with. In support of this theory, 51F and 56M MSCs deemed weakly chondrogenic by their inferior GAG production exhibited relatively high 3.2 and 4.4-fold increases in *Sox9* expression by day 21. Further, expression of *Sox9* is calculated relative to day 1 expression since the pellets are too loose to harvest before 24 hours. *Sox9* may be significantly upregulated during those first 24 hours of chondrogenic culture since it is induced early in chondrogenic differentiation. Subsequent modulation of Sox9 levels may be trivial compared to any early regulation. Thus, changes in *Sox9* expression need to be interpreted with care.

Conversely, increases in *Col2a1* and *Acan* should correlate with improved chondrogenesis. It is possible that any given population of MSCs will contain some number of chondrocyte precursors, which already express some amount of *Col2a1* and *Acan*. Again, differences in the fold change magnitudes between donors might be

indicative of their initial chondrogenic potential, with smaller fold changes corresponding to the MSCs that were already expressing some level of chondrocyte-specific genes. However, variability in fold change magnitudes might also reflect the inherent responsiveness of MSCs from a specific donor to chondrogenic induction. For example, 53M MSCs had the lowest *Col2a1* and *Acan* fold changes on day 21, which could indicate the presence of a high number of chondrocyte precursors among the primary MSCs or lower intrinsic sensitivity to the chondrogenic induction conditions used. Increased *Col2a1* and *Acan* expression was functionally reflected in deposition of Col2 and sGAG in pellets, although larger fold change magnitudes did not always correlate with greater extracellular matrix deposition. Thus, despite inter-donor differences in fold change magnitudes, increases in *Col2a1* and *Acan* are indicative of chondrogenic differentiation.

Increases and decreases in the hypertrophic genes during MSC chondrogenesis need to be similarly considered. Even though their populations are heterogeneous when it comes to the trilineage potential of individual cells, all MSCs are capable of osteogenic differentiation [12]. Since there is overlap between the genes expressed during chondrocyte hypertrophy and osteogenesis (i.e., *Runx2*, *ALP*, *BSP*), undifferentiated MSCs may be primed to express these genes or may already express them at low levels. In this work it was demonstrated that increases in *ALP* expression correlated with increased ALP activity (data not presented), so *ALP* expression data were viewed as a virtual measure of functional changes ALP activity. This is in agreement with a previous report of a correlation between transcription and activity of ALP in a bone marrow-derived stromal cell line [372]. MMP activity could not be detected in MSC-conditioned

medium, but MMP2 and MMP13 were both detected as secreted proteins. Changes in their expression patterns reflected alterations in secretion, but only one patient was analyzed so this correlation is inconclusive, but promising. The relationship between *PTHrP* and *BSP* expression and their functional parallels were not examined in this work.

Ultimately, fold changes in these genes are only an indication of chondrogenesis and hypertrophy, not a quantitation. Fold changes does not consider the possibility of starting with either high or low levels of a particular gene. Further, gene expression is calculated for whole pellets, so it is an average. Since pellets are formed from a heterogeneous population of cells, different regions sometimes display varying degrees of differentiation or different types of differentiation, and strong increasing expression in one region might mask moderate but significant decreasing expression in another. Therefore, gene expression and GAG data must be interpreted in parallel with functional measures of chondrogenesis like extracellular matrix accumulation.

Despite the magnitude differences observed in the chondrogenic differentiation of MSCs and their variable degrees of sensitivity to the mechanical and chemical treatments utilized, the results of these experiments clearly indicated effects of treatments. In addition, the studies provided clues to enrich our understanding of the phenotype of chondrogenic MSCs. In the next section, the behavior of chondrogenic MSCs will be evaluated against that of chondrogenic mesenchymal cells, hypertrophic chondrocytes, articular chondrocytes, and osteoarthritic chondrocytes.

7.3 The Hybrid Phenotype of Chondrogenic MSCs

The chondrogenesis studies in this work utilized a pellet culture configuration because it mimics the dense packing of mesenchymal cells that occurs before chondrogenesis *in vivo*. Recapitulation of the tight cell packing is sufficient to induce chondrogenic differentiation of isolated embryonic limb mesenchymal cells [100]. MSCs, however, require additional chondrogenic induction cues from TGF-β. As in articular cartilage, the MSCs in this work elaborated a matrix containing GAGs and Col2 to yield a tissue with cells residing in individual lacunae. MSCs also exhibited certain features of hypertrophic chondrocyte differentiation analogous to those observed during endochondral ossification, but how the phenotype observed during MSC chondrogenesis diverges from those observed in various naturally occurring chondrocytes is noteworthy.

The temporal course of MSC chondrogenesis was similar to that observed in micromass culture, which shares similarities with MSC pellets due to its high cell density. Signs of chondrogenesis were evident in micromasses as early as day 3 and maintained for at least 28 days [100]. The MSCs in this study began to detectably upregulate cartilage specific genes as early as day 5 and indisputably by day 11. The consistent upregulation of *Sox9*, *Col2a1*, and *Acan* on day 11 was the initial impetus for selecting day 11 as the endpoint in many of the studies in this work. GAG deposition was apparent throughout MSC pellets on day 11 and Col2 was detected on day 21 in regions overlapping with GAG, as in articular cartilage tissue. That GAG deposition on day 11 was indicative of regions of chondrogenic differentiation prior to detection of Col2, was another of the reasons that day 11 was deemed a suitable point at which to assess chondrogenesis despite the lack of Col2 staining.

After the onset of chondrogenesis in the developing limb, the majority of the chondrocytes continue the maturation process, and signs of chondrocyte maturation were evident in our MSCs as well. As described earlier, sequential chondrocyte maturation is characterized by the following changes: switch from production of Col2 to Col10, dramatic cell volume increase, matrix mineralization, matrix degradation, and apoptosis [184]. In micromass cultures, Col10 and ALP are detected as early as day 7, with matrix mineralization becoming apparent by day 14 [100]. Cell size and apoptotic cell death all increase over time. In the MSCs in this work, expression of hypertrophic genes was elevated as early as day 3 of culture, even before expression of chondrogenic genes. Other than *MMP13*, which experienced an early spike in expression, and *Runx2*, which decreased slightly, all hypertrophic genes continued to increase over time, indicating progressive advancement of hypertrophy in parallel with successful chondrogenesis. On day 21, Col10 accumulation in the extracellular matrix colocalized with that of GAG and Col2, indicating that the same cells are producing both types of collagen. Other characterizations of MSC chondrogenesis have also described hypertrophic gene expression and ALP activity [18]. These data indicate that the phenotype of chondrogenic MSCs actually encompasses both that of articular chondrocytes and hypertrophic ones.

One of the reasons for the observed hybrid phenotype is the defined chondrogenic culture medium. The MSCs in these studies were continuously supplemented with TGF-β3. Even if the natural tendency of MSC-derived chondrocytes is to undergo hypertrophy, under the influence of TGF-β, one would expect that tendency to hypertrophy would be suppressed and chondrogenesis would be amplified. In the growth plate, TGF-β reinforces the resting chondrocyte phenotype and prevents chondrocyte hypertrophy as

evidenced by the accelerated hypertrophy observed in the absence of TGF-β signaling [260]. Its effects are mediated in part through increased secretion of PTHrP by perichondrial cells [373]. While MSC pellets do not have a perichondrium, they do contain *PTHrP*-expressing cells. We showed that expression of *PTHrP* decreases with time, suggesting that MSCs might be less responsive to TGF-β as they differentiate, which may contribute to the progression of hypertrophy, or that MSCs do not upregulate *PTHrP* in response to TGF-β. Indeed, chondrogenic MSCs are inclined to hypertrophy. Pelttari et al. reported that when chondrogenic MSCs were withdrawn from a controlled environment and subcutaneously transplantated in SCID mice they underwent matrix calcification, vascular invasion, and microossicle formation [46]. Mueller and Tuan showed that under culture conditions that mirror some of those found in the growth plate, MSCs can undergo a differentiation program analogous to hypertrophy *in vitro* [323]. A combination of TGF-β withdrawal, dexamethasone reduction, and T3 and β-glycerophosphate supplementation after 14 days of traditional chondrogenic differentiation induced matrix mineralization and ALP activity in MSC pellets. Thus, MSCs can be induced to similar behavior to the transient chondrocytes found in the growth plate, but not under constant TGF-β stimulation.

The development of a dual articular-hypertrophy phenotype in MSCs under TGF-β stimulation recalls the phenotype of osteoarthritic chondrocytes. Since the role of articular chondrocytes is to maintain tissue integrity, it follows that the extracellular matrix molecules would be upregulated in response to tissue damage. Indeed, OA chondrocytes exhibit elevated transcription of *Col2a1*, *Col6*, *Col11a*, and other building blocks of normal cartilage tissue compared to normal chondrocytes [278]. However, they

also upregulate *Col1a1* and *Col3a1*, characteristic of dedifferentiation, and *Col10a1*, *Runx2*, *ALP*, and *MMP13* characteristic of hypertrophic differentiation [278, 280, 282, 292-295]. The coexpression of features from both varieties of chondrocytes is shared by OA chondrocytes and chondrogenic MSCs. The culprit in MSCs, as in OA chondrocytes, is signaling pathways that differ from those active in articular chondrocytes.

The arrest of chondrocyte differentiation at the articular stage is strongly tied to the internal signaling within the cells. Soluble factors can only induce transcriptional changes if the cells express the appropriate receptors and signaling components to respond to them. In addition, epigenetic modifications of select genes can block transcriptional changes even in the presence of the appropriate signals. Articular chondrocytes do not undergo hypertrophy even when removed from their native environment and implanted at an ectopic site [46]. Thus, the articular chondrocytes phenotype might be protected because the cells do not express the elements required to respond to hypertrophy-inducing signals or because hypertrophy genes are epigenetically silenced. However, MSCs may undergo hypertrophy because they do express the requisite signaling components or possess a different epigenetic signature. As described in the introductory chapter, the critical pathways regulating chondrocyte differentiation include TGF-β, Ihh/PTHrP, and canonical Wnt/β-catenin. Increasing or decreasing the activity of these pathways in MSCs is the key to controlling their phenotype. For reasons discussed previously, the β-catenin pathway was the focus of this work.

In Chapter 5, β-catenin signaling was characterized in chondrogenic MSCs. Not only is elevated β-catenin signaling absent in articular chondrocytes, but, along with loss of TGF-β signaling, resumption of β-catenin signaling has been identified as one of the

likely mechanisms in the pathogenesis of OA [296, 297, 374, 375]. Our results indicated that even under the pro-chondrogenic influence of TGF-β, the MSCs upregulated *Ctnnb1*, the gene encoding β-catenin, contained more active dephosphorylated β-catenin protein, and β-catenin was more transcriptionally active versus undifferentiated MSCs. On a transcriptional level, even though the MSCs are producing a fairly accurate cartilage tissue, they are not altering their expression of signaling molecules to reflect this transition. It is possible that the increase in dephosphorylated β-catenin protein was caused by an increase in cellular adhesions between cells and was not indicative of an increase in signaling. Even though most of the cells appear to reside in individual lacunae, there are still regions of high cell contact. Some lacunae contain multiple cells, and in regions of the pellets with lower levels of matrix production the cells remain in close contact. Further, chondrogenic MSC pellets retain a ring of fibroblast-like cells around the edge of the pellets that are stacked on top of each other. Western blot revealed that most of the β-catenin in the pellets was indeed localized at the membrane. However, the reporter gene results conclusively demonstrate that β-catenin signaling is more active in MSCs after 11 days of differentiation than in undifferentiated MSCs. Thus, not only did MSC-derived chondrocytes not adhere to the pattern of reduced β-catenin signaling observed in native chondrocyte differentiation, but they actively opposed it. Coupled with continuous TGF-β supplementation, this helps explain the hybrid phenotype observed as well as their other responses to culture modifications.

7.4 Mechanobiology of Hydrostatic Pressure Loading in Chondrogenic MSCs

The CHP studies in Chapter 4 suggested that at least until day 11, CHP has a pro-chondrogenic effect. This is agreement with many studies showing a stimulatory effect of physiological levels of CHP on MSC chondrogenesis at days 7 and 14 (see Table 4-1). Although the effects of static hydrostatic pressure on chondrocytes are dependent on culture condtions [61], increased pressure was shown to accelerate chondrogenesis in mouse limb bud as well [376]. No changes in the regulation of hypertrophic genes were observed in response to 11 days of CHP. This was counter to a mathematical model of intermittent joint loading, which predicted that hydrostatic pressures would oppose endochondral ossification [335]. Recent studies in porcine MSCs demonstrated decreased levels of *Col10a1* and *Ihh* after 14 days of CHP and decreased ALP activity after 21 days of CHP, suggesting that there might indeed be an inhibitory effect of CHP, but which might not be detected on day 11 [337]. On day 21, we observed a decrease in *Runx2* and *Col1a1* expression in CHP-loaded MSCs, but no changes in *Ihh*, *Col10a1*, or *BSP* expression were observed. However, by day 21, effects on chondrogenesis were absent. Consistent with this finding, no chondrosupportive effects of CHP were seen in porcine MSCs loaded for 21 days or longer [336, 338]. It seems, therefore, that the response of chondrogenic MSCs to CHP varies with time, likely due to their evolving differentiation state.

Varying the times of CHP application was performed to tease out effects of loading chondrogenic MSCs at different stages of differentiation. Loading during the first 10 days of MSC chondrogenesis was shown to favor increased expression of chondrogenic genes, while loading during the latter half of chondrogenic culture was

detrimental to these chondrogenic markers. When applied in the latter half of the culture period, CHP inhibited expression of some hypertrophic genes. This is consistent with effects on hypertrophic markers in other studies being observed at days 14 and 21 [337, 338], and with mathematical models [322, 335]. Therefore, the pro-chondrogenic effects of loading appear to occur only early during chondrogenic culture, while anti-hypertrophy effects happen at a more advanced stage of MSC differentiation.

Although the mechanisms by which hydrostatic pressure produces alterations in intracellular signaling have not been elucidated, there are several changes that develop over time that might interfere with CHP mechanotransduction. It is possible that as extracellular matrix is deposited, adhesions between the differentiating MSCs and their new matrix alter their response to CHP. Another possibility is that as the cells are pushed apart due to matrix accumulation, a reduction in cell to cell adhesions changes the organization of potential CHP-responsive elements such as membrane-bound receptors, cytoskeletal filaments, and other associated proteins. Or else, CHP itself may alter signaling such that the sensitivity of MSCs to CHP is reduced the longer CHP is applied. While these questions were not answered in this work, we did examine changes in intracellular signaling caused by CHP. Since the results of the CHP studies indicated that CHP was beneficial to MSC chondrogenesis at the levels of both promoting an articular phenotype and suppressing a hypertrophic phenotype, the molecular mechanisms that could be responsible for these effects was investigated. It was found that CHP suppressed both extracellular regulated kinase (ERK)1/2 and β-catenin activation in chondrogenic MSCs after only a single 4 hour application.

The extracellular regulated kinase (ERK)1/2 signaling pathway is one of three major mitogen-activated protein kinase (MAPK) cascades, and it can be initiated by integrins, receptor tyrosine kinases, G-protein coupled receptors, and ion channels [377]. Reports indicate that while ERK1/2 inhibits developmental chondrogenesis, its role in chondrocyte hypertrophy is less clear with one study demonstrating inhibition of hypertrophy under constitutive ERK signaling in transgenic mice and another showing inhibition of hypertrophy with an ERK inhibitor in organ culture [377]. The role of ERK1/2 in MSCs was similarly unclear. In one study, ERK1/2 inhibition enhanced GAG synthesis and expression of *Sox9* and *Col2a1* in chondrogenic MSC pellets, while expression of *Runx2* and *Col10a1* were decreased [378]. In another study, the same inhibitor blocked TGF-β1-induced expression of *Sox9*, *Col2a1*, and *Acan* in MSC pellets [379]. Activation of ERK1/2 induced phosphorylation of Runx2 and transcription of Runx2 target genes in osteogenic MSCs [380]. In yet another study, dynamic compression of MSCs in fibrin gels enhanced chondrogenesis in an ERK1/2-dependent manner, but hypertrophy/osteogenic characteristics were further augmented by ERK1/2 inhibition [381]. These studies indicate that the targets of ERK1/2 signaling are highly context dependent.

The mechanosensitivity of β-catenin has been previously described elsewhere. Cyclic stretch, compression, and fluid flow have all been shown to increase β-catenin signaling activity in various cell types, primarily in the context of supporting osteogenesis [382-389]. In contrast, CHP had an inhibitory effect on β-catenin in the MSCs used in this study. Thus, this cartilage-specific force was able to modify β-catenin in a manner antagonistic to osteogenesis, and this regulation might be responsible for the

pro-chondrogenic effects of CHP. Based on this result, we went on to examine the role of β-catenin in MSC chondrogenesis. The regulatory role of β-catenin in developmental chondrogenesis was described extensively in Chapter 1. Briefly, β-catenin signaling negatively regulates chondrogenesis [181-183], positively regulates endochondral ossification [169, 236], and has been implicated in the pathogenesis of OA [296, 297, 374, 375]. We found that these functions were duplicated in MSC chondrogenesis. Coupled with evidence that CHP inhibits β-catenin in MSCs, this means that it is possible that β-catenin inhibition by CHP is responsible for the pro-chondrogenic and anti-hypertrophy effects observed in MSCs exposed to CHP. Additional studies using CHP in combination with β-catenin inhibitors are necessary to confirm this hypothesis.

7.5 β-Catenin Regulates MSC Chondrogenesis

We observed an increase in membrane-associated β-catenin as well as an increase in β-catenin-mediated transcription after 11 days of MSC chondrogenesis. The increase in β-catenin at the membrane is troubling because enhanced cell-cell adhesions are associated with inhibition of chondrogenesis. However, MSCs in pellet culture do undergo extensive chondrogenesis, indicating either that TGF-β supplementation is able to overcome the effects of increased cell adhesions, or that increased adhesions are an artifact of cell packing and are not indicative of greater phenotypic modulation. The increased signaling activity, however, is of particular concern because during development it corresponds with a transition to hypertrophy. It is possible that the increased cellular adhesions are partially responsible for the increased signaling-competent β-catenin, in which case this pathway might not be of great concern in less

dense culture systems, but the canonical Wnt/β-catenin pathway remains of great interest in MSC pellet culture and of great relevance to treating OA.

The studies in Chapter 6 demonstrated that inhibition of β-catenin signaling with the small molecule XAV939 enhanced MSC chondrogenesis. This effect mirrors the role of β-catenin in embryonic limb development, in which conditional knockout of β-catenin in the mesenchymal condensation results in ectopic cartilage formation and inhibition of endochondral ossification [168, 271]. Also consistent with our findings, Im et al. reported that the Wnt inhibitors Dickkopf (Dkk)-1 and secreted Frizzled-related protein (sFRP)-1 enhanced GAG synthesis and expression of *Sox9* and *Col2a1* in MSC pellets in the absence of TGF-β [358, 359]. However, they also found that the effects of the Wnt inhibitors were abolished in the presence of TGF-β, while we continued to observe difference [359]. One explanation for this disparity is based on their choice of inhibitor. Dkk-1 is a secreted protein that complexes with LRP5/6 and the transmembrane protein Kremen [390]. Formation of this tertiary complex results in the endocytosis of LRP5/6 and inhibition of Wnt signaling at the membrane. Similarly, sFRPs are secreted proteins with a cysteine rich domain that compete with Fz for Wnt binding, inhibiting Wnt activation of Fz [390]. These molecules both inhibit Wnt signaling upstream of β-catenin. However, TGF-β/Smad3 signaling is able to bypass the canonical Wnt pathway and activate β-catenin directly [324, 391]. Thus, the addition of TGF-β to the culture medium in the studies by Im et al. could have effectively negated the β-catenin-inhibitory effects Dkk-1 and sFRP-1 by providing an alternate stimulus to activate β-catenin. In contrast, XAV939 inhibits β-catenin signaling downstream of Wnt by stabilizing it within the Axin complex, which is not overcome by TGF-β signaling. Therefore, the synergistic

effects of TGF-β and β-catenin inhibition on MSC chondrogenesis could still be distinguished here. Future studies directly comparing XAV939 with Dkk-1 and/or sFRP-1 would be necessary to confirm this hypothesis.

The role of β-catenin in chondrogenesis is inextricably linked with that of Sox9, and inhibition of β-catenin resulted in increased expression of *Sox9* in this work. Several studies have demonstrated that Sox9 and β-catenin each represses transcriptional activity and induce degradation of the other [134, 182, 236]. Akiyama et al. also showed that their effects are virtually opposite in developmental chondrogenesis [182]. Thus, the balance between β-catenin and Sox9 seems to be of critical importance. In the MSC pellets described in this work, that β-catenin inhibition promotes chondrogenesis would be expected to result at least in part by abolishing β-catenin-driven degradation of Sox9. Coupled with increased expression of *Sox9* mRNA, this suggests that the effects of β-catenin inhibition likely occur at both transcriptional and protein levels. Shifting the balance between Sox9 and β-catenin also has implications for hypertrophy. Although Sox9 is required for chondrocytes to reach hypertrophy as well as for expression of *Col10a1* [236], the other aspects of hypertrophy are mediated by Runx2, the transcription of which is induced by β-catenin and opposed by Sox9 [231, 236-238]. In chondrogenic MSCs then, inhibition of β-catenin should curtail expression of *Runx2* and the rest of the hypertrophic program, consistent with our observations.

In addition to its role in modulating chondrogenesis, we found that XAV939 indeed inhibited expression of hypertrophy genes, but not *Col10a1*, which was upregulated. Induction of *Col10a1* expression in chondrogenic MSCs may not indicate hypertrophy as it does in the growth plate. The *Col10a1* promoter contains a binding site

for Sox9, which positively regulates expression of *Col10a1* during chondrocyte hypertrophy [236]. However, despite the prevalence of Sox9, *Col10* is not expressed in articular chondrocytes. The finding that expression of *Col10* is also controlled at an epigenetic level helps explain this discrepancy. Zimmermann et al. showed that in articular chondrocytes, all 9 CpG sites in the *Col10a1* promoter were methylated, compared to only 60-80% methylation in MSCs [392]. Methylation was further reduced upon chondrogenic differentiation of MSCs and correlated with increased expression of *Col10a1*. Since *Col10* is not epigenetically silenced in MSCs as in articular chondrocytes, Col10 accumulation in MSC chondrogenesis might be induced as a byproduct of increased Sox9 transcriptional activity rather than as part of a larger hypertrophic program.

If Col10 does not portend the degradation of cartilage tissue, then its expression may not be of great significance in chondrogenic MSC pellets. One of the main concerns in cartilage regeneration is that the mechanical properties of the regenerated tissue are sufficient to withstand the rigorous loading environment in the joint. Many repair strategies use biocompatible materials to aid in the development of adequate mechanical properties. The use of materials like fibrin glue with inferior biomechanical properties has been shown to result in fissures and insufficient integration despite the formation of cartilage-like neotissue [393]. The mechanical properties of growth plate cartilage are similar to those of mature articular cartilage, suggesting that the presence of Col10 in chondrogenic MSC tissue would not necessarily compromise its mechanical integrity [394, 395].

The other main concern is that Col10 may be able to itself activate hypertrophy in chondrogenic MSCs. Col10 and other fibrillar collagens are ligands of the discoidin domain receptor (DDR) 2 found on chondrocytes [396-398]. Activation of DDR2 signaling is required for normal chondrocyte proliferation both *in vivo* and *in vitro* [396], and has been shown to activate MMP13 in chondrocytes [398] and induce Runx2 phosphorylation and activation in ATDC5 cells [399]. These disparate activities may be caused by the binding of different collagens as Col10 activates DDR2 through a different binding site than Col1 and Col2 [397]. For example, if Col2 binding activates DDR-dependent proliferation and Col10 binding activates DDR-dependent hypertrophy, the transition from Col2 to Col10 producing chondrocytes would positively regulate the progression of hypertrophy. In chondrogenic MSCs that simultaneously express both Col2 and Col10, competitive binding would attenuate activation of DDR-dependent hypertrophy. However, the role of DDR2 in MSCs has not yet been described. Based on the evidence in this work, there is no indication that Col10 is accompanied by or a trigger for hypertrophy in chondrogenic MSCs. However, before concluding that Col10 is benign in this context, further studies are needed.

This study examined the effects of β-catenin inhibition on MMP secretion and found decreased levels of MMP13, but increased secretion of MMP2 in MSCs from a single donor. A decrease in MMP13 secretion is consistent with the observed suppression of hypertrophy, as it is the primary collagenase expressed by both hypertrophic and OA chondrocytes. The significance of increased MMP2 secretion in these cells, however, is less clear because it is not well characterized in chondrocytes. Unlike *MMP13*, which is expressed at low levels in articular chondrocytes and at high levels in OA chondrocytes,

MMP2 is expressed at high levels in both [400, 401]. Although it is upregulated in OA chondrocytes, the role of MMP2 in OA is unknown. However, since chondrocytes already express high levels of *MMP2*, its effects are not necessarily destructive. In their study on the tenogenic differentiation of MSCs, Kuo and Tuan suggest that because MMPs are required for maintenance of tissue integrity by matrix remodeling, increases in MMPs may indicate active extracellular matrix remodeling rather than degradation [402]. Another possibility is that MMP2 is not exerting its effects at the level of tissue breakdown. Though it is a gelatinase, MMP2 can cleave the pro-region of TGF-β, releasing the active molecule [403]. In fact, one of the essential functions of gelatinases is thought to be the release of bound bioactive factors and cryptic domains via matrix degradation [404]. In OA, increased levels of MMP2 could reflect an attempt to release more TGF-β (i.e., an anabolic step) and restore the proper signaling balance in the tissue. In these MSCs, an increase in MMP2 might have a similar pro-chondrogenic objective, although this requires further investigation.

While stimulation of β-catenin signaling with the GSK-3β inhibitor CHIR99021 led to inhibition of chondrogenesis in MSCs, it did not enhance hypertrophy as expected. *Runx2*, *Col10a1*, and *BSP* expression were reduced, and ALP was also reduced in MSCs from the majority of donors, while *PTHrP* and *MMP13* were unchanged. This suggests that stimulation of β-catenin actually inhibits both types of chondrocyte differentiation since chondrogenesis is required in order for hypertrophy to proceed. Upon gross examination, CHIR99021-treated pellets did not differ in size, indicating the elaboration of an extracellular matrix, albeit one lacking the characteristic constituents of a cartilage matrix. Similar to our observations, expression of a constitutively active β-catenin in

Col2a1-expressing chondrocyte precursors severely inhibited chondrogenesis, which in turn compromised hypertrophy [181, 182]. Conversely, when constitutively active β-catenin is expressed in growth plate chondrocytes, hypertrophic differentiation is accelerated [169, 236]. Thus, in response to β-catenin stimulation, MSCs behave like undifferentiated precursors rather than chondrocytes and do not undergo chondrogenic differentiation or maturation.

In opposition to our results, Yang et al. recently reported that activation of β-catenin signaling with LiCl enhances chondrogenesis in concert with TGF-β [360]. In addition to undesirable effects of LiCl in long-term cell culture, observed effects cannot be definitively attributed to alterations in β-catenin since LiCl is a non-specific inhibitor of GSK-3β [363]. Nonetheless, they demonstrated increased GAG and Col2 deposition after 28 days of culture, and a less advanced hypertrophic phenotype after 35 days of preconditioning followed by 8 weeks of subcutaneous implantation compared to TGF-β conditioning alone. However, most of the co-treated samples could not be retrieved, indicating that these had not actually achieved a differentiated state even after 35 days in the presence of LiCl and were resorbed into the surrounding tissue. In the few co-treated samples that were examined, differentiation may have lagged behind the TGF-β group simply because their differentiation was repressed with LiCl treatment prior to implantation. Inhibition of chondrogenic differentiation by β-catenin stimulation is consistent with our results.

That β-catenin stimulation inhibits MSC differentiation as in mesenchymal cells rather than enhancing hypertrophy as in OA chondrocytes, despite the phenotypic similarities between MSCs and OA chondrocytes, is not unprecedented. In their

characterization of induced hypertrophy in MSC pellet cultures, Mueller and Tuan observed heterogeneous morphology with areas of hypertrophy and areas of dedifferentiation, and they postulated that the MSCs needed to reach a certain degree of chondrogenic differentiation before true hypertrophic differentiation could proceed [323]. Based on this protocol, Scotti et al. showed that week-old chondrogenic MSC neotissue was resorbed upon subcutaneous implantation in mice, while hypertrophic tissue was converted to bone via endochondral ossification [405]. These findings suggest that even though chondrogenic MSCs are functionally similar to chondrocytes, there is a threshold of differentiation before which they still require external differentiation cues in order for differentiation to proceed. The aforementioned studies both utilized a threshold of 14 days, and it remains to be determined whether day 11 would fall above or below this critical point. Before reaching this threshold, MSCs would be expected to respond to alterations in signaling more like chondrocyte precursors than mature chondrocytes. Future studies that investigate the effects of β-catenin stimulation beyond this differentiation threshold by adding CHIR99021 to the culture medium after an initial period of chondrogenic induction might show that β-catenin does indeed favor hypertrophic differentiation of chondrogenic MSCs.

7.6 Global Implications and Conclusion

In this work, we have examined the mechanisms involved in mechanical and molecular regulation of chondrogenic MSCs. While MSCs are an abundant and promising cell source for cartilage tissue engineering and regenerative medicine strategies, precise control of their phenotype continues to present a challenge. Previously,

chondrogenic MSCs have been compared to chondrocytes proceeding through the process of terminal differentiation as in endochondral development, thus necessitating arrest of differentiation before appearance of the undesirable features of the hypertrophic phenotype. However, in this work we have shown that the development of hypertrophic characteristics coincides with chondrogenesis rather than occurring in a sequential manner. Thus, if chondrogenic MSCs resemble OA chondrocytes, then phenotypic modulation rather than differentiation arrest is required for articular cartilage engineering. Furthermore, because their behavior is similar to OA chondrocytes, chondrogenic MSCs represent an ideal cell type for evaluating therapies for the treatment of OA.

We have shown that the canonical Wnt/β-catenin signaling pathway is an attractive target for achieving the desired phenotypic adjustments in chondrogenic MSCs. Like OA chondrocytes, chondrogenic MSCs exhibit abnormal activation of β-catenin signaling. Here, we have shown that inhibition of this pathway not only enhances chondrogenic differentiation, but suppresses many of the undesirable traits typically observed during MSC chondrogenesis. There are several ways in which this result can inform cartilage regeneration therapies. First, β-catenin inhibitors could be added to defined chondrogenic media formulations used for *in vitro* tissue engineering to improve the tissue outcome. For *in vivo* applications, implanted MSCs or even autologous chondrocytes could be genetically engineered to be unresponsive to β-catenin signaling in order to improve their function and shield them from adverse signals in the OA joint. This might also protect them from cancers, as constitutive activation of Wnt/β-catenin signaling has been implicated in many types of cancer [406]. Finally, β-catenin inhibitors might be useful for targeted drug or gene therapy approaches.

In conclusion, by demonstrating the regulation of chondrogenic MSCs by β-catenin, we have begun to unravel the complex signaling networks responsible for their OA-like phenotype. While further studies are needed to continue exploring the functional consequences of β-catenin modulation both in this system and *in vivo*, this work represents a foundation upon which successful cartilage repair therapies can be built.

Chapter 8 References

1.   Dominici, M., et al., *Minimal criteria for defining multipotent mesenchymal stromal cells. The International Society for Cellular Therapy position statement.* Cytotherapy, 2006. **8**(4): p. 315-7.

2.   Pittenger, M.F., et al., *Multilineage potential of adult human mesenchymal stem cells.* Science, 1999. **284**(5411): p. 143-7.

3.   Friedenstein, A.J., R.K. Chailakhjan, and K.S. Lalykina, *The development of fibroblast colonies in monolayer cultures of guinea-pig bone marrow and spleen cells.* Cell Tissue Kinet, 1970. **3**(4): p. 393-403.

4.   Zuk, P.A., et al., *Multilineage cells from human adipose tissue: implications for cell-based therapies.* Tissue Eng, 2001. **7**(2): p. 211-28.

5.   Qu-Petersen, Z., et al., *Identification of a novel population of muscle stem cells in mice: potential for muscle regeneration.* J Cell Biol, 2002. **157**(5): p. 851-64.

6.   Sakaguchi, Y., et al., *Comparison of human stem cells derived from various mesenchymal tissues: superiority of synovium as a cell source.* Arthritis Rheum, 2005. **52**(8): p. 2521-9.

7.   Gronthos, S., et al., *Postnatal human dental pulp stem cells (DPSCs) in vitro and in vivo.* Proc Natl Acad Sci U S A, 2000. **97**(25): p. 13625-30.

8.   Romanov, Y.A., V.A. Svintsitskaya, and V.N. Smirnov, *Searching for alternative sources of postnatal human mesenchymal stem cells: candidate MSC-like cells from umbilical cord.* Stem Cells, 2003. **21**(1): p. 105-10.

9.   Charbord, P., *Bone marrow mesenchymal stem cells: historical overview and concepts.* Hum Gene Ther, 2010. **21**(9): p. 1045-56.

10.   Pevsner-Fischer, M., S. Levin, and D. Zipori, *The origins of mesenchymal stromal cell heterogeneity.* Stem Cell Rev, 2011. **7**(3): p. 560-8.

11.   Haynesworth, S.E., M.A. Baber, and A.I. Caplan, *Cell surface antigens on human marrow-derived mesenchymal cells are detected by monoclonal antibodies.* Bone, 1992. **13**(1): p. 69-80.

12.   Muraglia, A., R. Cancedda, and R. Quarto, *Clonal mesenchymal progenitors from human bone marrow differentiate in vitro according to a hierarchical model.* J Cell Sci, 2000. **113 (Pt 7)**: p. 1161-6.

13.   Song, L. and R.S. Tuan, *Transdifferentiation potential of human mesenchymal stem cells derived from bone marrow.* FASEB J, 2004. **18**(9): p. 980-2.

14.   *Prevalence of doctor-diagnosed arthritis and arthritis-attributable activity limitation --- United States, 2007-2009.* MMWR Morb Mortal Wkly Rep, 2010. **59**(39): p. 1261-5.

15.   *National and state medical expenditures and lost earnings attributable to arthritis and other rheumatic conditions--United States, 2003.* MMWR Morb Mortal Wkly Rep, 2007. **56**(1): p. 4-7.

16.   Lawrence, R.C., et al., *Estimates of the prevalence of arthritis and other rheumatic conditions in the United States. Part II.* Arthritis Rheum, 2008. **58**(1): p. 26-35.

17.   Rogmark, C., et al., *A prospective randomised trial of internal fixation versus arthroplasty for displaced fractures of the neck of the femur. Functional outcome for 450 patients at two years.* J Bone Joint Surg Br, 2002. **84**(2): p. 183-8.

18. Pelttari, K., E. Steck, and W. Richter, *The use of mesenchymal stem cells for chondrogenesis.* Injury, 2008. **39 Suppl 1**: p. S58-65.

19. Caplan, A.I., *Why are MSCs therapeutic? New data: new insight.* J Pathol, 2009. **217**(2): p. 318-24.

20. Cohen, N.P., R.J. Foster, and V.C. Mow, *Composition and dynamics of articular cartilage: structure, function, and maintaining healthy state.* J Orthop Sports Phys Ther, 1998. **28**(4): p. 203-15.

21. Poole, A.R., et al., *Composition and structure of articular cartilage: a template for tissue repair.* Clin Orthop Relat Res, 2001(391 Suppl): p. S26-33.

22. Poole, C.A., *Articular cartilage chondrons: form, function and failure.* J Anat, 1997. **191 (Pt 1)**: p. 1-13.

23. Oegema, T.R., Jr., et al., *The interaction of the zone of calcified cartilage and subchondral bone in osteoarthritis.* Microsc Res Tech, 1997. **37**(4): p. 324-32.

24. Gannon, J.M., et al., *Localization of type X collagen in canine growth plate and adult canine articular cartilage.* J Orthop Res, 1991. **9**(4): p. 485-94.

25. Havelka, S., et al., *The calcified-noncalcified cartilage interface: the tidemark.* Acta Biol Hung, 1984. **35**(2-4): p. 271-9.

26. Ogata, K. and L.A. Whiteside, *Barrier to material transfer at the bone-cartilage interface: measurement with hydrogen gas in vivo.* Clin Orthop Relat Res, 1979(145): p. 273-6.

27. Holtzer, H., et al., *The Loss of Phenotypic Traits by Differentiated Cells in Vitro, I. Dedifferentiation of Cartilage Cells.* Proc Natl Acad Sci U S A, 1960. **46**(12): p. 1533-42.

28. Johnstone, B., et al., *In VitroChondrogenesis of Bone Marrow-Derived Mesenchymal Progenitor Cells.* Experimental Cell Research, 1998. **238**(1): p. 265-272.

29. Barry, F., et al., *Chondrogenic Differentiation of Mesenchymal Stem Cells from Bone Marrow: Differentiation-Dependent Gene Expression of Matrix Components.* Experimental Cell Research, 2001. **268**(2): p. 189-200.

30. Sekiya, I., D.C. Colter, and D.J. Prockop, *BMP-6 enhances chondrogenesis in a subpopulation of human marrow stromal cells.* Biochem Biophys Res Commun, 2001. **284**(2): p. 411-8.

31. Bosnakovski, D., et al., *Chondrogenic differentiation of bovine bone marrow mesenchymal stem cells in pellet cultural system.* Experimental Hematology, 2004. **32**(5): p. 502-509.

32. Yoneno, K., et al., *Multidifferentiation potential of mesenchymal stem cells in three-dimensional collagen gel cultures.* J Biomed Mater Res A, 2005. **75**(3): p. 733-41.

33. Mauck, R.L., X. Yuan, and R.S. Tuan, *Chondrogenic differentiation and functional maturation of bovine mesenchymal stem cells in long-term agarose culture.* Osteoarthritis and Cartilage, 2006. **14**(2): p. 179-189.

34. Caterson, E.J., et al., *Polymer/alginate amalgam for cartilage-tissue engineering.* Ann N Y Acad Sci, 2002. **961**: p. 134-8.

35. Bosnakovski, D., et al., *Chondrogenic differentiation of bovine bone marrow mesenchymal stem cells (MSCs) in different hydrogels: influence of collagen type*

II extracellular matrix on MSC chondrogenesis. Biotechnol Bioeng, 2006. **93**(6): p. 1152-63.

36. Li, W.-J., et al., *A three-dimensional nanofibrous scaffold for cartilage tissue engineering using human mesenchymal stem cells.* Biomaterials, 2005. **26**(6): p. 599-609.

37. Wang, Y., et al., *In vitro cartilage tissue engineering with 3D porous aqueous-derived silk scaffolds and mesenchymal stem cells.* Biomaterials, 2005. **26**(34): p. 7082-7094.

38. Markway, B.D., et al., *Enhanced chondrogenic differentiation of human bone marrow-derived mesenchymal stem cells in low oxygen environment micropellet cultures.* Cell Transplant, 2010. **19**(1): p. 29-42.

39. Engler, A.J., et al., *Matrix elasticity directs stem cell lineage specification.* Cell, 2006. **126**(4): p. 677-89.

40. Puetzer, J.L., J.N. Petitte, and E.G. Loboa, *Comparative review of growth factors for induction of three-dimensional in vitro chondrogenesis in human mesenchymal stem cells isolated from bone marrow and adipose tissue.* Tissue Eng Part B Rev, 2010. **16**(4): p. 435-44.

41. Kelly, D.J. and C.R. Jacobs, *The role of mechanical signals in regulating chondrogenesis and osteogenesis of mesenchymal stem cells.* Birth Defects Res C Embryo Today, 2010. **90**(1): p. 75-85.

42. Karlsson, C., et al., *Differentiation of human mesenchymal stem cells and articular chondrocytes: analysis of chondrogenic potential and expression pattern of differentiation-related transcription factors.* J Orthop Res, 2007. **25**(2): p. 152-63.

43. Indrawattana, N., et al., *Growth factor combination for chondrogenic induction from human mesenchymal stem cell.* Biochemical and Biophysical Research Communications, 2004. **320**(3): p. 914-919.

44. Dickhut, A., et al., *Calcification or dedifferentiation: requirement to lock mesenchymal stem cells in a desired differentiation stage.* J Cell Physiol, 2009. **219**(1): p. 219-26.

45. Weiss, S., et al., *Impact of growth factors and PTHrP on early and late chondrogenic differentiation of human mesenchymal stem cells.* J Cell Physiol, 2010. **223**(1): p. 84-93.

46. Pelttari, K., et al., *Premature induction of hypertrophy during in vitro chondrogenesis of human mesenchymal stem cells correlates with calcification and vascular invasion after ectopic transplantation in SCID mice.* Arthritis Rheum, 2006. **54**(10): p. 3254-66.

47. Mueller, M.B., et al., *Hypertrophy in mesenchymal stem cell chondrogenesis: effect of TGF-beta isoforms and chondrogenic conditioning.* Cells Tissues Organs, 2010. **192**(3): p. 158-66.

48. Bertram, H., et al., *Matrix metalloprotease inhibitors suppress initiation and progression of chondrogenic differentiation of mesenchymal stromal cells in vitro.* Stem Cells Dev, 2009. **18**(6): p. 881-92.

49. Fuerst, M., et al., *Calcification of articular cartilage in human osteoarthritis.* Arthritis Rheum, 2009. **60**(9): p. 2694-703.

50. Walsh, D.A., et al., *Angiogenesis in the synovium and at the osteochondral junction in osteoarthritis.* Osteoarthritis Cartilage, 2007. **15**(7): p. 743-51.

51. Rogers, B.A., et al., *Topographical variation in glycosaminoglycan content in human articular cartilage.* J Bone Joint Surg Br, 2006. **88**(12): p. 1670-4.

52. Brama, P.A., et al., *Topographical mapping of biochemical properties of articular cartilage in the equine fetlock joint.* Equine Vet J, 2000. **32**(1): p. 19-26.

53. Sah, R.L., et al., *Biosynthetic response of cartilage explants to dynamic compression.* J Orthop Res, 1989. **7**(5): p. 619-36.

54. Larsson, T., R.M. Aspden, and D. Heinegard, *Effects of mechanical load on cartilage matrix biosynthesis in vitro.* Matrix, 1991. **11**(6): p. 388-94.

55. Saadat, E., et al., *Long-term cyclical in vivo loading increases cartilage proteoglycan content in a spatially specific manner: an infrared microspectroscopic imaging and polarized light microscopy study.* Arthritis Res Ther, 2006. **8**(5): p. R147.

56. Mow, V.C., G.A. Ateshian, and R.L. Spilker, *Biomechanics of diarthrodial joints: a review of twenty years of progress.* J Biomech Eng, 1993. **115**(4B): p. 460-7.

57. Urban, J.P., *The chondrocyte: a cell under pressure.* Br J Rheumatol, 1994. **33**(10): p. 901-8.

58. Mow, V.C., W.Y. Gu, and F.H. Chen, *Structure and Function of Articular Cartilage and Meniscus*, in *Basic Orthopaedic Biomechanics and Mechano-Biology*, V.C. Mow and R. Huiskes, Editors. 2005, Lippincott Williams & Wilkins: Philadelphia. p. 181-258.

59. Wong, M. and D.R. Carter, *Articular cartilage functional histomorphology and mechanobiology: a research perspective.* Bone, 2003. **33**(1): p. 1-13.

60. Wilkins, R.J., J.A. Browning, and J.P. Urban, *Chondrocyte regulation by mechanical load.* Biorheology, 2000. **37**(1-2): p. 67-74.

61. Elder, B.D. and K.A. Athanasiou, *Hydrostatic pressure in articular cartilage tissue engineering: from chondrocytes to tissue regeneration.* Tissue Eng Part B Rev, 2009. **15**(1): p. 43-53.

62. Schumann, D., et al., *Mechanobiological conditioning of stem cells for cartilage tissue engineering.* Biomed Mater Eng, 2006. **16**(4 Suppl): p. S37-52.

63. Ingber, D.E., *Tensegrity I. Cell structure and hierarchical systems biology.* J Cell Sci, 2003. **116**(Pt 7): p. 1157-73.

64. Ingber, D.E., *Tensegrity II. How structural networks influence cellular information processing networks.* J Cell Sci, 2003. **116**(Pt 8): p. 1397-408.

65. Woods, A., G. Wang, and F. Beier, *Regulation of chondrocyte differentiation by the actin cytoskeleton and adhesive interactions.* J Cell Physiol, 2007. **213**(1): p. 1-8.

66. Ragan, P.M., et al., *Down-regulation of chondrocyte aggrecan and type-II collagen gene expression correlates with increases in static compression magnitude and duration.* J Orthop Res, 1999. **17**(6): p. 836-42.

67. Loening, A.M., et al., *Injurious mechanical compression of bovine articular cartilage induces chondrocyte apoptosis.* Arch Biochem Biophys, 2000. **381**(2): p. 205-12.

68.   Hunter, C.J., et al., *Mechanical compression alters gene expression and extracellular matrix synthesis by chondrocytes cultured in collagen I gels.* Biomaterials, 2002. **23**(4): p. 1249-59.

69.   Lee, D.A., et al., *The influence of mechanical loading on isolated chondrocytes seeded in agarose constructs.* Biorheology, 2000. **37**(1-2): p. 149-61.

70.   Mauck, R.L., et al., *Functional tissue engineering of articular cartilage through dynamic loading of chondrocyte-seeded agarose gels.* J Biomech Eng, 2000. **122**(3): p. 252-60.

71.   Mauck, R.L., et al., *Regulation of cartilaginous ECM gene transcription by chondrocytes and MSCs in 3D culture in response to dynamic loading.* Biomech Model Mechanobiol, 2007. **6**(1-2): p. 113-25.

72.   Gemmiti, C.V. and R.E. Guldberg, *Fluid flow increases type II collagen deposition and tensile mechanical properties in bioreactor-grown tissue-engineered cartilage.* Tissue Eng, 2006. **12**(3): p. 469-79.

73.   Cohen, I., et al., *Storing live embryonic and adult human cartilage grafts for transplantation using a joint simulating device.* Biomaterials, 2000. **21**(21): p. 2117-23.

74.   Smith, R.L., et al., *Effects of fluid-induced shear on articular chondrocyte morphology and metabolism in vitro.* J Orthop Res, 1995. **13**(6): p. 824-31.

75.   Smith, R.L., D.R. Carter, and D.J. Schurman, *Pressure and shear differentially alter human articular chondrocyte metabolism: a review.* Clin Orthop Relat Res, 2004(427 Suppl): p. S89-95.

76.   Toyoda, T., et al., *Upregulation of aggrecan and type II collagen mRNA expression in bovine chondrocytes by the application of hydrostatic pressure.* Biorheology, 2003. **40**(1-3): p. 79-85.

77.   Parkkinen, J.J., et al., *Effects of cyclic hydrostatic pressure on proteoglycan synthesis in cultured chondrocytes and articular cartilage explants.* Arch Biochem Biophys, 1993. **300**(1): p. 458-65.

78.   Smith, R.L., et al., *Time-dependent effects of intermittent hydrostatic pressure on articular chondrocyte type II collagen and aggrecan mRNA expression.* J Rehabil Res Dev, 2000. **37**(2): p. 153-61.

79.   Ikenoue, T., et al., *Mechanoregulation of human articular chondrocyte aggrecan and type II collagen expression by intermittent hydrostatic pressure in vitro.* J Orthop Res, 2003. **21**(1): p. 110-6.

80.   Ramage, L., G. Nuki, and D.M. Salter, *Signalling cascades in mechanotransduction: cell-matrix interactions and mechanical loading.* Scand J Med Sci Sports, 2009. **19**(4): p. 457-69.

81.   Fell, H.B., *The histogenesis of cartilage and bone in the long bones of the embryonic fowl.* Journal of Morphology, 1925. **40**(3): p. 417-459.

82.   Goel, S.C., *Electron microscopic studies on developing cartilage. I. The membrane system related to the synthesis and secretion of extracellular materials.* J Embryol Exp Morphol, 1970. **23**(1): p. 169-84.

83.   Searls, R.L., S.R. Hilfer, and S.M. Mirow, *An ultrastructural study of early chondrogenesis in the chick wing bud.* Dev Biol, 1972. **28**(1): p. 123-37.

84. Neubert, D., H.J. Merker, and S. Tapken, *Comparative studies on the prenatal development of mouse extremities in vivo and in organ culture.* Naunyn Schmiedebergs Arch Pharmacol, 1974. **286**(3): p. 251-70.

85. Thorogood, P.V. and J.R. Hinchliffe, *An analysis of the condensation process during chondrogenesis in the embryonic chick hind limb.* J Embryol Exp Morphol, 1975. **33**(3): p. 581-606.

86. Zimmermann, B., E. Scharlach, and R. Kaatz, *Cell contact and surface coat alterations of limb-bud mesenchymal cells during differentiation.* J Embryol Exp Morphol, 1982. **72**: p. 1-18.

87. Zimmermann, B., *Assembly and disassembly of gap junctions during mesenchymal cell condensation and early chondrogenesis in limb buds of mouse embryos.* J Anat, 1984. **138 (Pt 2)**: p. 351-63.

88. Silver, M.H., J.M. Foidart, and R.M. Pratt, *Distribution of fibronectin and collagen during mouse limb and palate development.* Differentiation, 1981. **18**(3): p. 141-9.

89. Mallein-Gerin, F., et al., *Temporal and spatial analysis of cartilage proteoglycan core protein gene expression during limb development by in situ hybridization.* Dev Biol, 1988. **126**(2): p. 337-45.

90. Dessau, W., et al., *Changes in the patterns of collagens and fibronectin during limb-bud chondrogenesis.* J Embryol Exp Morphol, 1980. **57**: p. 51-60.

91. Melnick, M., et al., *Spatiotemporal patterns of fibronectin distribution during embryonic development. I. Chick limbs.* J Embryol Exp Morphol, 1981. **63**: p. 193-206.

92. Singley, C.T. and M. Solursh, *The spatial distribution of hyaluronic acid and mesenchymal condensation in the embryonic chick wing.* Dev Biol, 1981. **84**(1): p. 102-20.

93. Shinomura, T., et al., *The distribution of mesenchyme proteoglycan (PG-M) during wing bud outgrowth.* Anat Embryol (Berl), 1990. **181**(3): p. 227-33.

94. Kosher, R.A., W.M. Kulyk, and S.W. Gay, *Collagen gene expression during limb cartilage differentiation.* J Cell Biol, 1986. **102**(4): p. 1151-6.

95. Tacchetti, C., et al., *Cell condensation in chondrogenic differentiation.* Exp Cell Res, 1992. **200**(1): p. 26-33.

96. Knudson, C.B. and W. Knudson, *Cartilage proteoglycans.* Semin Cell Dev Biol, 2001. **12**(2): p. 69-78.

97. Wardale, R.J. and V.C. Duance, *Quantification and immunolocalisation of porcine articular and growth plate cartilage collagens.* J Cell Sci, 1993. **105 (Pt 4)**: p. 975-84.

98. Shibata, S., et al., *In situ hybridization and immunohistochemistry of versican, aggrecan and link protein, and histochemistry of hyaluronan in the developing mouse limb bud cartilage.* J Anat, 2003. **203**(4): p. 425-32.

99. Ahrens, P.B., M. Solursh, and R.S. Reiter, *Stage-related capacity for limb chondrogenesis in cell culture.* Dev Biol, 1977. **60**(1): p. 69-82.

100. Mello, M.A. and R.S. Tuan, *High density micromass cultures of embryonic limb bud mesenchymal cells: an in vitro model of endochondral skeletal development.* In Vitro Cell Dev Biol Anim, 1999. **35**(5): p. 262-9.

101. Caplan, A.I., *Effects of the nicotinamide-sensitive teratogen3-acetylpyridine on chick limb cells in culture.* Exp Cell Res, 1970. **62**(2): p. 341-55.
102. von der Mark, K. and H. von der Mark, *Immunological and biochemical studies of collagen type transition during in vitro chrondrogenesis of chick limb mesodermal cells.* J Cell Biol, 1977. **73**(3): p. 736-47.
103. Oberlender, S.A. and R.S. Tuan, *Expression and functional involvement of N-cadherin in embryonic limb chondrogenesis.* Development, 1994. **120**(1): p. 177-87.
104. Oberlender, S.A. and R.S. Tuan, *Spatiotemporal profile of N-cadherin expression in the developing limb mesenchyme.* Cell Adhes Commun, 1994. **2**(6): p. 521-37.
105. Woodward, W.A. and R.S. Tuan, *N-Cadherin expression and signaling in limb mesenchymal chondrogenesis: stimulation by poly-L-lysine.* Dev Genet, 1999. **24**(1-2): p. 178-87.
106. Delise, A.M. and R.S. Tuan, *Analysis of N-cadherin function in limb mesenchymal chondrogenesis in vitro.* Dev Dyn, 2002. **225**(2): p. 195-204.
107. DeLise, A.M. and R.S. Tuan, *Alterations in the spatiotemporal expression pattern and function of N-cadherin inhibit cellular condensation and chondrogenesis of limb mesenchymal cells in vitro.* J Cell Biochem, 2002. **87**(3): p. 342-59.
108. Coleman, C.M. and R.S. Tuan, *Functional role of growth/differentiation factor 5 in chondrogenesis of limb mesenchymal cells.* Mech Dev, 2003. **120**(7): p. 823-36.
109. Kelley, R.O. and J.F. Fallon, *Identification and distribution of gap junctions in the mesoderm of the developing chick limb bud.* J Embryol Exp Morphol, 1978. **46**: p. 99-110.
110. Coelho, C.N. and R.A. Kosher, *Gap junctional communication during limb cartilage differentiation.* Dev Biol, 1991. **144**(1): p. 47-53.
111. Zhang, W., C. Green, and N.S. Stott, *Bone morphogenetic protein-2 modulation of chondrogenic differentiation in vitro involves gap junction-mediated intercellular communication.* J Cell Physiol, 2002. **193**(2): p. 233-43.
112. White, D.G., et al., *Functional analysis of fibronectin isoforms in chondrogenesis: Full-length recombinant mesenchymal fibronectin reduces spreading and promotes condensation and chondrogenesis of limb mesenchymal cells.* Differentiation, 2003. **71**(4-5): p. 251-61.
113. Frenz, D.A., N.S. Jaikaria, and S.A. Newman, *The mechanism of precartilage mesenchymal condensation: a major role for interaction of the cell surface with the amino-terminal heparin-binding domain of fibronectin.* Dev Biol, 1989. **136**(1): p. 97-103.
114. Gehris, A.L., et al., *The region encoded by the alternatively spliced exon IIIA in mesenchymal fibronectin appears essential for chondrogenesis at the level of cellular condensation.* Dev Biol, 1997. **190**(2): p. 191-205.
115. Mackie, E.J., I. Thesleff, and R. Chiquet-Ehrismann, *Tenascin is associated with chondrogenic and osteogenic differentiation in vivo and promotes chondrogenesis in vitro.* J Cell Biol, 1987. **105**(6 Pt 1): p. 2569-79.
116. Koyama, E., et al., *Syndecan-3, tenascin-C, and the development of cartilaginous skeletal elements and joints in chick limbs.* Dev Dyn, 1995. **203**(2): p. 152-62.

117. Mackie, E.J. and L.I. Murphy, *The role of tenascin-C and related glycoproteins in early chondrogenesis.* Microsc Res Tech, 1998. **43**(2): p. 102-10.

118. Murphy, L.I., et al., *Tenascin-C induced stimulation of chondrogenesis is dependent on the presence of the C-terminal fibrinogen-like globular domain.* FEBS Lett, 2000. **480**(2-3): p. 189-92.

119. Chuong, C.M., et al., *Roles of adhesion molecules NCAM and tenascin in limb skeletogenesis: analysis with antibody perturbation, exogenous gene expression, talpid mutants and activin stimulation.* Prog Clin Biol Res, 1993. **383B**: p. 465-74.

120. Chiquet-Ehrismann, R., et al., *Tenascin interferes with fibronectin action.* Cell, 1988. **53**(3): p. 383-90.

121. Conacci-Sorrell, M., J. Zhurinsky, and A. Ben-Ze'ev, *The cadherin-catenin adhesion system in signaling and cancer.* J Clin Invest, 2002. **109**(8): p. 987-91.

122. Hatta, K. and M. Takeichi, *Expression of N-cadherin adhesion molecules associated with early morphogenetic events in chick development.* Nature, 1986. **320**(6061): p. 447-9.

123. Cho, S.H., et al., *Retinoic acid inhibits chondrogenesis of mesenchymal cells by sustaining expression of N-cadherin and its associated proteins.* J Cell Biochem, 2003. **89**(4): p. 837-47.

124. Widelitz, R.B., et al., *Adhesion molecules in skeletogenesis: II. Neural cell adhesion molecules mediate precartilaginous mesenchymal condensations and enhance chondrogenesis.* J Cell Physiol, 1993. **156**(2): p. 399-411.

125. Wright, E., et al., *The Sry-related gene Sox9 is expressed during chondrogenesis in mouse embryos.* Nature genetics, 1995. **9**(1): p. 15-20.

126. Healy, C., D. Uwanogho, and P.T. Sharpe, *Regulation and role of Sox9 in cartilage formation.* Dev Dyn, 1999. **215**(1): p. 69-78.

127. Ng, L.J., et al., *SOX9 binds DNA, activates transcription, and coexpresses with type II collagen during chondrogenesis in the mouse.* Dev Biol, 1997. **183**(1): p. 108-21.

128. Lefebvre, V., R.R. Behringer, and B. de Crombrugghe, *L-Sox5, Sox6 and Sox9 control essential steps of the chondrocyte differentiation pathway.* Osteoarthritis Cartilage, 2001. **9 Suppl A**: p. S69-75.

129. Bi, W., et al., *Haploinsufficiency of Sox9 results in defective cartilage primordia and premature skeletal mineralization.* Proc Natl Acad Sci U S A, 2001. **98**(12): p. 6698-703.

130. Akiyama, H., et al., *The transcription factor Sox9 has essential roles in successive steps of the chondrocyte differentiation pathway and is required for expression of Sox5 and Sox6.* Genes Dev, 2002. **16**(21): p. 2813-28.

131. Bi, W., et al., *Sox9 is required for cartilage formation.* Nature genetics, 1999. **22**(1): p. 85-9.

132. Ikegami, D., et al., *Sox9 sustains chondrocyte survival and hypertrophy in part through Pik3ca-Akt pathways.* Development, 2011. **138**(8): p. 1507-19.

133. Kawakami, Y., et al., *Transcriptional coactivator PGC-1alpha regulates chondrogenesis via association with Sox9.* Proc Natl Acad Sci U S A, 2005. **102**(7): p. 2414-9.

134. Topol, L., et al., *Sox9 inhibits Wnt signaling by promoting beta-catenin phosphorylation in the nucleus.* J Biol Chem, 2009. **284**(5): p. 3323-33.

135. Lefebvre, V., et al., *SOX9 is a potent activator of the chondrocyte-specific enhancer of the pro alpha1(II) collagen gene.* Mol Cell Biol, 1997. **17**(4): p. 2336-46.

136. Lefebvre, V., P. Li, and B. de Crombrugghe, *A new long form of Sox5 (L-Sox5), Sox6 and Sox9 are coexpressed in chondrogenesis and cooperatively activate the type II collagen gene.* EMBO J, 1998. **17**(19): p. 5718-33.

137. Sekiya, I., et al., *SOX9 enhances aggrecan gene promoter/enhancer activity and is up-regulated by retinoic acid in a cartilage-derived cell line, TC6.* J Biol Chem, 2000. **275**(15): p. 10738-44.

138. Kent, J., et al., *A male-specific role for SOX9 in vertebrate sex determination.* Development, 1996. **122**(9): p. 2813-22.

139. Han, Y. and V. Lefebvre, *L-Sox5 and Sox6 drive expression of the aggrecan gene in cartilage by securing binding of Sox9 to a far-upstream enhancer.* Molecular and cellular biology, 2008. **28**(16): p. 4999-5013.

140. Feng, X.H. and R. Derynck, *Specificity and versatility in tgf-beta signaling through Smads.* Annu Rev Cell Dev Biol, 2005. **21**: p. 659-93.

141. Pogue, R. and K. Lyons, *BMP signaling in the cartilage growth plate.* Curr Top Dev Biol, 2006. **76**: p. 1-48.

142. Blaney Davidson, E.N., et al., *Increase in ALK1/ALK5 ratio as a cause for elevated MMP-13 expression in osteoarthritis in humans and mice.* J Immunol, 2009. **182**(12): p. 7937-45.

143. Ferguson, C.M., et al., *Smad2 and 3 mediate transforming growth factor-beta1-induced inhibition of chondrocyte maturation.* Endocrinology, 2000. **141**(12): p. 4728-35.

144. Furumatsu, T., et al., *Smad3 induces chondrogenesis through the activation of SOX9 via CREB-binding protein/p300 recruitment.* J Biol Chem, 2005. **280**(9): p. 8343-50.

145. Iwai, T., et al., *Smad7 Inhibits chondrocyte differentiation at multiple steps during endochondral bone formation and down-regulates p38 MAPK pathways.* J Biol Chem, 2008. **283**(40): p. 27154-64.

146. Baffi, M.O., et al., *Conditional deletion of the TGF-beta type II receptor in Col2a expressing cells results in defects in the axial skeleton without alterations in chondrocyte differentiation or embryonic development of long bones.* Dev Biol, 2004. **276**(1): p. 124-42.

147. Yoon, B.S., et al., *Bmpr1a and Bmpr1b have overlapping functions and are essential for chondrogenesis in vivo.* Proc Natl Acad Sci U S A, 2005. **102**(14): p. 5062-7.

148. Leonard, C.M., et al., *Role of transforming growth factor-beta in chondrogenic pattern formation in the embryonic limb: stimulation of mesenchymal condensation and fibronectin gene expression by exogenenous TGF-beta and evidence for endogenous TGF-beta-like activity.* Dev Biol, 1991. **145**(1): p. 99-109.

149.   Taipaleenmaki, H., et al., *The crosstalk between transforming growth factor-beta1 and delta like-1 mediates early chondrogenesis during embryonic endochondral ossification.* Stem Cells, 2012. **30**(2): p. 304-13.

150.   Downie, S.A. and S.A. Newman, *Morphogenetic Differences between Fore and Hind Limb Precartilage Mesenchyme: Relation to Mechanisms of Skeletal Pattern Formation.* Developmental Biology, 1994. **162**(1): p. 195-208.

151.   Chimal-Monroy, J., et al., *Analysis of the molecular cascade responsible for mesodermal limb chondrogenesis: Sox genes and BMP signaling.* Dev Biol, 2003. **257**(2): p. 292-301.

152.   Roark, E.F. and K. Greer, *Transforming growth factor-beta and bone morphogenetic protein-2 act by distinct mechanisms to promote chick limb cartilage differentiation in vitro.* Dev Dyn, 1994. **200**(2): p. 103-16.

153.   Stott, N.S., T.X. Jiang, and C.M. Chuong, *Successive formative stages of precartilaginous mesenchymal condensations in vitro: modulation of cell adhesion by Wnt-7A and BMP-2.* J Cell Physiol, 1999. **180**(3): p. 314-24.

154.   Fischer, L., G. Boland, and R.S. Tuan, *Wnt signaling during BMP-2 stimulation of mesenchymal chondrogenesis.* J Cell Biochem, 2002. **84**(4): p. 816-31.

155.   Haas, A.R. and R.S. Tuan, *Chondrogenic differentiation of murine C3H10T1/2 multipotential mesenchymal cells: II. Stimulation by bone morphogenetic protein-2 requires modulation of N-cadherin expression and function.* Differentiation, 1999. **64**(2): p. 77-89.

156.   Denker, A.E., et al., *Chondrogenic differentiation of murine C3H10T1/2 multipotential mesenchymal cells: I. Stimulation by bone morphogenetic protein-2 in high-density micromass cultures.* Differentiation, 1999. **64**(2): p. 67-76.

157.   Zou, H., et al., *Distinct roles of type I bone morphogenetic protein receptors in the formation and differentiation of cartilage.* Genes Dev, 1997. **11**(17): p. 2191-203.

158.   Pizette, S. and L. Niswander, *BMPs are required at two steps of limb chondrogenesis: formation of prechondrogenic condensations and their differentiation into chondrocytes.* Dev Biol, 2000. **219**(2): p. 237-49.

159.   Enomoto-Iwamoto, M., et al., *Bone morphogenetic protein signaling is required for maintenance of differentiated phenotype, control of proliferation, and hypertrophy in chondrocytes.* J Cell Biol, 1998. **140**(2): p. 409-18.

160.   Furumatsu, T., T. Ozaki, and H. Asahara, *Smad3 activates the Sox9-dependent transcription on chromatin.* Int J Biochem Cell Biol, 2009. **41**(5): p. 1198-204.

161.   Pan, Q., et al., *Sox9, a key transcription factor of bone morphogenetic protein-2-induced chondrogenesis, is activated through BMP pathway and a CCAAT box in the proximal promoter.* J Cell Physiol, 2008. **217**(1): p. 228-41.

162.   Akiyama, T., *Wnt/beta-catenin signaling.* Cytokine Growth Factor Rev, 2000. **11**(4): p. 273-82.

163.   Barker, N., *The canonical Wnt/beta-catenin signalling pathway.* Methods Mol Biol, 2008. **468**: p. 5-15.

164.   Logan, C.Y. and R. Nusse, *The Wnt signaling pathway in development and disease.* Annu Rev Cell Dev Biol, 2004. **20**: p. 781-810.

165.   Shapiro, L. and W.I. Weis, *Structure and biochemistry of cadherins and catenins.* Cold Spring Harb Perspect Biol, 2009. **1**(3): p. a003053.

166. Semenov, M.V., et al., *SnapShot: Noncanonical Wnt Signaling Pathways.* Cell, 2007. **131**(7): p. 1378.

167. De, A., *Wnt/Ca2+ signaling pathway: a brief overview.* Acta Biochim Biophys Sin (Shanghai), 2011. **43**(10): p. 745-56.

168. Day, T.F., et al., *Wnt/beta-catenin signaling in mesenchymal progenitors controls osteoblast and chondrocyte differentiation during vertebrate skeletogenesis.* Dev Cell, 2005. **8**(5): p. 739-50.

169. Hartmann, C. and C.J. Tabin, *Dual roles of Wnt signaling during chondrogenesis in the chicken limb.* Development, 2000. **127**(14): p. 3141-59.

170. Tufan, A.C., K.M. Daumer, and R.S. Tuan, *Frizzled-7 and limb mesenchymal chondrogenesis: effect of misexpression and involvement of N-cadherin.* Dev Dyn, 2002. **223**(2): p. 241-53.

171. Ryu, J.H., et al., *Regulation of the chondrocyte phenotype by beta-catenin.* Development, 2002. **129**(23): p. 5541-50.

172. Wada, N., et al., *Involvement of Frzb-1 in mesenchymal condensation and cartilage differentiation in the chick limb bud.* Int J Dev Biol, 1999. **43**(6): p. 495-500.

173. Tufan, A.C. and R.S. Tuan, *Wnt regulation of limb mesenchymal chondrogenesis is accompanied by altered N-cadherin-related functions.* FASEB J, 2001. **15**(8): p. 1436-8.

174. Kawakami, Y., et al., *Involvement of Wnt-5a in chondrogenic pattern formation in the chick limb bud.* Dev Growth Differ, 1999. **41**(1): p. 29-40.

175. Topol, L., et al., *Wnt-5a inhibits the canonical Wnt pathway by promoting GSK-3-independent beta-catenin degradation.* J Cell Biol, 2003. **162**(5): p. 899-908.

176. Meyer, R.A., et al., *Developmental regulation and asymmetric expression of the gene encoding Cx43 gap junctions in the mouse limb bud.* Dev Genet, 1997. **21**(4): p. 290-300.

177. Rudnicki, J.A. and A.M. Brown, *Inhibition of chondrogenesis by Wnt gene expression in vivo and in vitro.* Dev Biol, 1997. **185**(1): p. 104-18.

178. Bradley, E.W. and M.H. Drissi, *Wnt5b regulates mesenchymal cell aggregation and chondrocyte differentiation through the planar cell polarity pathway.* J Cell Physiol, 2011. **226**(6): p. 1683-93.

179. Hartmann, C. and C.J. Tabin, *Wnt-14 plays a pivotal role in inducing synovial joint formation in the developing appendicular skeleton.* Cell, 2001. **104**(3): p. 341-51.

180. Joeng, K.S., et al., *Lrp5 and Lrp6 redundantly control skeletal development in the mouse embryo.* Dev Biol, 2011. **359**(2): p. 222-9.

181. Tamamura, Y., et al., *Developmental regulation of Wnt/beta-catenin signals is required for growth plate assembly, cartilage integrity, and endochondral ossification.* J Biol Chem, 2005. **280**(19): p. 19185-95.

182. Akiyama, H., et al., *Interactions between Sox9 and beta-catenin control chondrocyte differentiation.* Genes Dev, 2004. **18**(9): p. 1072-87.

183. Miclea, R.L., et al., *Adenomatous polyposis coli-mediated control of beta-catenin is essential for both chondrogenic and osteogenic differentiation of skeletal precursors.* BMC Dev Biol, 2009. **9**: p. 26.

184. Mackie, E.J., et al., *Endochondral ossification: how cartilage is converted into bone in the developing skeleton.* Int J Biochem Cell Biol, 2008. **40**(1): p. 46-62.

185. Ballock, R.T. and R.J. O'Keefe, *Physiology and pathophysiology of the growth plate.* Birth Defects Res C Embryo Today, 2003. **69**(2): p. 123-43.

186. Mackie, E.J., L. Tatarczuch, and M. Mirams, *The skeleton: a multi-functional complex organ: the growth plate chondrocyte and endochondral ossification.* J Endocrinol, 2011. **211**(2): p. 109-21.

187. Vortkamp, A., et al., *Regulation of rate of cartilage differentiation by Indian hedgehog and PTH-related protein.* Science, 1996. **273**(5275): p. 613-22.

188. Hunziker, E.B., R.K. Schenk, and L.M. Cruz-Orive, *Quantitation of chondrocyte performance in growth-plate cartilage during longitudinal bone growth.* J Bone Joint Surg Am, 1987. **69**(2): p. 162-73.

189. Lee, K., J.D. Deeds, and G.V. Segre, *Expression of parathyroid hormone-related peptide and its receptor messenger ribonucleic acids during fetal development of rats.* Endocrinology, 1995. **136**(2): p. 453-63.

190. Lee, K., et al., *Parathyroid hormone-related peptide delays terminal differentiation of chondrocytes during endochondral bone development.* Endocrinology, 1996. **137**(11): p. 5109-18.

191. St-Jacques, B., M. Hammerschmidt, and A.P. McMahon, *Indian hedgehog signaling regulates proliferation and differentiation of chondrocytes and is essential for bone formation.* Genes Dev, 1999. **13**(16): p. 2072-86.

192. Long, F., et al., *Genetic manipulation of hedgehog signaling in the endochondral skeleton reveals a direct role in the regulation of chondrocyte proliferation.* Development, 2001. **128**(24): p. 5099-108.

193. Kobayashi, T., et al., *Indian hedgehog stimulates periarticular chondrocyte differentiation to regulate growth plate length independently of PTHrP.* J Clin Invest, 2005. **115**(7): p. 1734-42.

194. Ehlen, H.W., L.A. Buelens, and A. Vortkamp, *Hedgehog signaling in skeletal development.* Birth Defects Res C Embryo Today, 2006. **78**(3): p. 267-79.

195. Koziel, L., et al., *Ext1-dependent heparan sulfate regulates the range of Ihh signaling during endochondral ossification.* Dev Cell, 2004. **6**(6): p. 801-13.

196. Day, T.F. and Y. Yang, *Wnt and hedgehog signaling pathways in bone development.* J Bone Joint Surg Am, 2008. **90 Suppl 1**: p. 19-24.

197. Koziel, L., et al., *Gli3 acts as a repressor downstream of Ihh in regulating two distinct steps of chondrocyte differentiation.* Development, 2005. **132**(23): p. 5249-60.

198. Dai, P., et al., *Sonic Hedgehog-induced activation of the Gli1 promoter is mediated by GLI3.* J Biol Chem, 1999. **274**(12): p. 8143-52.

199. Wang, B., J.F. Fallon, and P.A. Beachy, *Hedgehog-regulated processing of Gli3 produces an anterior/posterior repressor gradient in the developing vertebrate limb.* Cell, 2000. **100**(4): p. 423-34.

200. Hilton, M.J., et al., *Ihh controls cartilage development by antagonizing Gli3, but requires additional effectors to regulate osteoblast and vascular development.* Development, 2005. **132**(19): p. 4339-51.

201. Iwasaki, M., A.X. Le, and J.A. Helms, *Expression of indian hedgehog, bone morphogenetic protein 6 and gli during skeletal morphogenesis.* Mech Dev, 1997. **69**(1-2): p. 197-202.

202. Delezoide, A.L., et al., *Spatio-temporal expression of FGFR 1, 2 and 3 genes during human embryo-fetal ossification.* Mech Dev, 1998. **77**(1): p. 19-30.

203. Peters, K., et al., *Unique expression pattern of the FGF receptor 3 gene during mouse organogenesis.* Dev Biol, 1993. **155**(2): p. 423-30.

204. Segev, O., et al., *Restrained chondrocyte proliferation and maturation with abnormal growth plate vascularization and ossification in human FGFR-3(G380R) transgenic mice.* Hum Mol Genet, 2000. **9**(2): p. 249-58.

205. Chen, L., et al., *A Ser(365)-->Cys mutation of fibroblast growth factor receptor 3 in mouse downregulates Ihh/PTHrP signals and causes severe achondroplasia.* Hum Mol Genet, 2001. **10**(5): p. 457-65.

206. Wang, Q., et al., *Differential regulation of endochondral bone growth and joint development by FGFR1 and FGFR3 tyrosine kinase domains.* Development, 2001. **128**(19): p. 3867-76.

207. Krejci, P., et al., *FGF2 inhibits proliferation and alters the cartilage-like phenotype of RCS cells.* Exp Cell Res, 2004. **297**(1): p. 152-64.

208. Su, W.C., et al., *Activation of Stat1 by mutant fibroblast growth-factor receptor in thanatophoric dysplasia type II dwarfism.* Nature, 1997. **386**(6622): p. 288-92.

209. Krejci, P., et al., *FGFR3 signaling induces a reversible senescence phenotype in chondrocytes similar to oncogene-induced premature senescence.* Bone, 2010. **47**(1): p. 102-10.

210. Sahni, M., et al., *FGF signaling inhibits chondrocyte proliferation and regulates bone development through the STAT-1 pathway.* Genes Dev, 1999. **13**(11): p. 1361-6.

211. Colvin, J.S., et al., *Skeletal overgrowth and deafness in mice lacking fibroblast growth factor receptor 3.* Nature genetics, 1996. **12**(4): p. 390-7.

212. Liu, J.P., et al., *Mice carrying null mutations of the genes encoding insulin-like growth factor I (Igf-1) and type 1 IGF receptor (Igf1r).* Cell, 1993. **75**(1): p. 59-72.

213. Wang, J., et al., *Evidence supporting dual, IGF-I-independent and IGF-I-dependent, roles for GH in promoting longitudinal bone growth.* J Endocrinol, 2004. **180**(2): p. 247-55.

214. Wang, J., J. Zhou, and C.A. Bondy, *Igf1 promotes longitudinal bone growth by insulin-like actions augmenting chondrocyte hypertrophy.* FASEB J, 1999. **13**(14): p. 1985-90.

215. Ohlsson, C., et al., *Growth hormone induces multiplication of the slowly cycling germinal cells of the rat tibial growth plate.* Proc Natl Acad Sci U S A, 1992. **89**(20): p. 9826-30.

216. Reinecke, M., et al., *Effect of growth hormone and insulin-like growth factor I (IGF-I) on the expression of IGF-I messenger ribonucleic acid and peptide in rat tibial growth plate and articular chondrocytes in vivo.* Endocrinology, 2000. **141**(8): p. 2847-53.

217. Hunziker, E.B., J. Wagner, and J. Zapf, *Differential effects of insulin-like growth factor I and growth hormone on developmental stages of rat growth plate chondrocytes in vivo.* J Clin Invest, 1994. **93**(3): p. 1078-86.

218. Sims, N.A., et al., *Bone homeostasis in growth hormone receptor-null mice is restored by IGF-I but independent of Stat5.* J Clin Invest, 2000. **106**(9): p. 1095-103.

219. Stevens, D.A., et al., *Thyroid hormones regulate hypertrophic chondrocyte differentiation and expression of parathyroid hormone-related peptide and its receptor during endochondral bone formation.* J Bone Miner Res, 2000. **15**(12): p. 2431-42.

220. Wang, Y., et al., *IGF-1R signaling in chondrocytes modulates growth plate development by interacting with the PTHrP/Ihh pathway.* J Bone Miner Res, 2011. **26**(7): p. 1437-46.

221. Takeda, S., et al., *Continuous expression of Cbfa1 in nonhypertrophic chondrocytes uncovers its ability to induce hypertrophic chondrocyte differentiation and partially rescues Cbfa1-deficient mice.* Genes Dev, 2001. **15**(4): p. 467-81.

222. Inada, M., et al., *Maturational disturbance of chondrocytes in Cbfa1-deficient mice.* Dev Dyn, 1999. **214**(4): p. 279-90.

223. Kim, I.S., et al., *Regulation of chondrocyte differentiation by Cbfa1.* Mech Dev, 1999. **80**(2): p. 159-70.

224. Stricker, S., et al., *Role of Runx genes in chondrocyte differentiation.* Dev Biol, 2002. **245**(1): p. 95-108.

225. Otto, F., et al., *Cbfa1, a candidate gene for cleidocranial dysplasia syndrome, is essential for osteoblast differentiation and bone development.* Cell, 1997. **89**(5): p. 765-71.

226. Guo, J., et al., *PTH/PTHrP receptor delays chondrocyte hypertrophy via both Runx2-dependent and -independent pathways.* Dev Biol, 2006. **292**(1): p. 116-28.

227. Enomoto, H., et al., *Cbfa1 is a positive regulatory factor in chondrocyte maturation.* J Biol Chem, 2000. **275**(12): p. 8695-702.

228. Karsenty, G., *Role of Cbfa1 in osteoblast differentiation and function.* Semin Cell Dev Biol, 2000. **11**(5): p. 343-6.

229. Yoshida, C.A., et al., *Runx2 and Runx3 are essential for chondrocyte maturation, and Runx2 regulates limb growth through induction of Indian hedgehog.* Genes Dev, 2004. **18**(8): p. 952-63.

230. Zheng, Q., et al., *Type X collagen gene regulation by Runx2 contributes directly to its hypertrophic chondrocyte-specific expression in vivo.* J Cell Biol, 2003. **162**(5): p. 833-42.

231. Dong, Y.F., et al., *Wnt induction of chondrocyte hypertrophy through the Runx2 transcription factor.* J Cell Physiol, 2006. **208**(1): p. 77-86.

232. Selvamurugan, N., et al., *Identification and characterization of Runx2 phosphorylation sites involved in matrix metalloproteinase-13 promoter activation.* FEBS Lett, 2009. **583**(7): p. 1141-6.

233. Roca, H., et al., *Cooperative interactions between RUNX2 and homeodomain protein-binding sites are critical for the osteoblast-specific expression of the bone sialoprotein gene.* J Biol Chem, 2005. **280**(35): p. 30845-55.

234. Dong, Y.F., et al., *Transforming growth factor-beta and Wnt signals regulate chondrocyte differentiation through Twist1 in a stage-specific manner.* Mol Endocrinol, 2007. **21**(11): p. 2805-20.

235. Bi, W., et al., *Sox9 is required for cartilage formation.* Nat Genet, 1999. **22**(1): p. 85-9.

236. Dy, P., et al., *Sox9 directs hypertrophic maturation and blocks osteoblast differentiation of growth plate chondrocytes.* Dev Cell, 2012. **22**(3): p. 597-609.

237. Cheng, A. and P.G. Genever, *SOX9 determines RUNX2 transactivity by directing intracellular degradation.* J Bone Miner Res, 2010. **25**(12): p. 2680-9.

238. Eames, B.F., P.T. Sharpe, and J.A. Helms, *Hierarchy revealed in the specification of three skeletal fates by Sox9 and Runx2.* Dev Biol, 2004. **274**(1): p. 188-200.

239. Amizuka, N., et al., *Programmed cell death of chondrocytes and aberrant chondrogenesis in mice homozygous for parathyroid hormone-related peptide gene deletion.* Endocrinology, 1996. **137**(11): p. 5055-67.

240. Karaplis, A.C., et al., *Lethal skeletal dysplasia from targeted disruption of the parathyroid hormone-related peptide gene.* Genes Dev, 1994. **8**(3): p. 277-89.

241. Lanske, B., et al., *PTH/PTHrP receptor in early development and Indian hedgehog-regulated bone growth.* Science, 1996. **273**(5275): p. 663-6.

242. Karp, S.J., et al., *Indian hedgehog coordinates endochondral bone growth and morphogenesis via parathyroid hormone related-protein-dependent and - independent pathways.* Development, 2000. **127**(3): p. 543-8.

243. Weir, E.C., et al., *Targeted overexpression of parathyroid hormone-related peptide in chondrocytes causes chondrodysplasia and delayed endochondral bone formation.* Proc Natl Acad Sci U S A, 1996. **93**(19): p. 10240-5.

244. Schipani, E., et al., *Targeted expression of constitutively active receptors for parathyroid hormone and parathyroid hormone-related peptide delays endochondral bone formation and rescues mice that lack parathyroid hormone-related peptide.* Proc Natl Acad Sci U S A, 1997. **94**(25): p. 13689-94.

245. Chung, U.I., et al., *The parathyroid hormone/parathyroid hormone-related peptide receptor coordinates endochondral bone development by directly controlling chondrocyte differentiation.* Proc Natl Acad Sci U S A, 1998. **95**(22): p. 13030-5.

246. Li, T.F., et al., *Parathyroid hormone-related peptide (PTHrP) inhibits Runx2 expression through the PKA signaling pathway.* Exp Cell Res, 2004. **299**(1): p. 128-36.

247. Zhang, M., et al., *PTHrP prevents chondrocyte premature hypertrophy by inducing cyclin-D1-dependent Runx2 and Runx3 phosphorylation, ubiquitylation and proteasomal degradation.* J Cell Sci, 2009. **122**(Pt 9): p. 1382-9.

248. Harvey, C.B., et al., *Molecular mechanisms of thyroid hormone effects on bone growth and function.* Mol Genet Metab, 2002. **75**(1): p. 17-30.

249. Miura, M., et al., *Thyroid hormones promote chondrocyte differentiation in mouse ATDC5 cells and stimulate endochondral ossification in fetal mouse tibias through iodothyronine deiodinases in the growth plate.* J Bone Miner Res, 2002. **17**(3): p. 443-54.

250. Robson, H., et al., *Thyroid hormone acts directly on growth plate chondrocytes to promote hypertrophic differentiation and inhibit clonal expansion and cell proliferation.* Endocrinology, 2000. **141**(10): p. 3887-97.

251. Burch, W.M. and H.E. Lebovitz, *Triiodothyronine stimulates maturation of porcine growth-plate cartilage in vitro.* J Clin Invest, 1982. **70**(3): p. 496-504.

252. Mello, M.A. and R.S. Tuan, *Effects of TGF-β1 and triiodothyronine on cartilage maturation: In vitro analysis using long-term high-density micromass cultures of chick embryonic limb mesenchymal cells.* Journal of Orthopaedic Research, 2006. **24**(11): p. 2095-2105.

253. Kang, J.S., et al., *Repression of Runx2 function by TGF-beta through recruitment of class II histone deacetylases by Smad3.* EMBO J, 2005. **24**(14): p. 2543-55.

254. Chen, C.G., et al., *Chondrocyte-intrinsic Smad3 represses Runx2-inducible MMP-13 expression to maintain articular cartilage and prevent osteoarthritis.* Arthritis Rheum, 2012.

255. Serra, R., A. Karaplis, and P. Sohn, *Parathyroid hormone-related peptide (PTHrP)-dependent and -independent effects of transforming growth factor beta (TGF-beta) on endochondral bone formation.* J Cell Biol, 1999. **145**(4): p. 783-94.

256. Shu, B., et al., *BMP2, but not BMP4, is crucial for chondrocyte proliferation and maturation during endochondral bone development.* J Cell Sci, 2011. **124**(Pt 20): p. 3428-40.

257. Olney, R.C., et al., *Growth factor regulation of human growth plate chondrocyte proliferation in vitro.* Biochem Biophys Res Commun, 2004. **317**(4): p. 1171-82.

258. Minina, E., et al., *BMP and Ihh/PTHrP signaling interact to coordinate chondrocyte proliferation and differentiation.* Development, 2001. **128**(22): p. 4523-34.

259. Yang, X., et al., *TGF-beta/Smad3 signals repress chondrocyte hypertrophic differentiation and are required for maintaining articular cartilage.* J Cell Biol, 2001. **153**(1): p. 35-46.

260. Serra, R., et al., *Expression of a truncated, kinase-defective TGF-beta type II receptor in mouse skeletal tissue promotes terminal chondrocyte differentiation and osteoarthritis.* J Cell Biol, 1997. **139**(2): p. 541-52.

261. Li, T.F., et al., *Smad3-deficient chondrocytes have enhanced BMP signaling and accelerated differentiation.* J Bone Miner Res, 2006. **21**(1): p. 4-16.

262. Kugimiya, F., et al., *Involvement of endogenous bone morphogenetic protein (BMP) 2 and BMP6 in bone formation.* J Biol Chem, 2005. **280**(42): p. 35704-12.

263. Yi, S.E., et al., *The type I BMP receptor BMPRIB is required for chondrogenesis in the mouse limb.* Development, 2000. **127**(3): p. 621-30.

264. Grimsrud, C.D., et al., *BMP signaling stimulates chondrocyte maturation and the expression of Indian hedgehog.* J Orthop Res, 2001. **19**(1): p. 18-25.

265. Yang, Y., et al., *Wnt5a and Wnt5b exhibit distinct activities in coordinating chondrocyte proliferation and differentiation.* Development, 2003. **130**(5): p. 1003-15.

266. Church, V., et al., *Wnt regulation of chondrocyte differentiation.* J Cell Sci, 2002. **115**(Pt 24): p. 4809-18.

267. Lee, H.H. and R.R. Behringer, *Conditional expression of Wnt4 during chondrogenesis leads to dwarfism in mice.* PLoS One, 2007. **2**(5): p. e450.

268. Spater, D., et al., *Wnt9a signaling is required for joint integrity and regulation of Ihh during chondrogenesis.* Development, 2006. **133**(15): p. 3039-49.

269. Enomoto-Iwamoto, M., et al., *The Wnt antagonist Frzb-1 regulates chondrocyte maturation and long bone development during limb skeletogenesis.* Dev Biol, 2002. **251**(1): p. 142-56.

270. Guo, X., et al., *The Wnt/beta-catenin pathway interacts differentially with PTHrP signaling to control chondrocyte hypertrophy and final maturation.* PLoS One, 2009. **4**(6): p. e6067.

271. Hill, T.P., et al., *Canonical Wnt/beta-catenin signaling prevents osteoblasts from differentiating into chondrocytes.* Dev Cell, 2005. **8**(5): p. 727-38.

272. Matsuzaki, E., et al., *Differentiation-inducing factor-1 alters canonical Wnt signaling and suppresses alkaline phosphatase expression in osteoblast-like cell lines.* Journal of Bone and Mineral Research, 2006. **21**(8): p. 1307-1316.

273. Yun, K. and S.-H. Im, *Transcriptional regulation of MMP13 by Lef1 in chondrocytes.* Biochemical and Biophysical Research Communications, 2007. **364**(4): p. 1009-1014.

274. Chen, M., et al., *Inhibition of beta-catenin signaling causes defects in postnatal cartilage development.* Journal of Cell Science, 2008. **121**(9): p. 1455-1465.

275. Mak, K.K., et al., *Indian hedgehog signals independently of PTHrP to promote chondrocyte hypertrophy.* Development, 2008. **135**(11): p. 1947-56.

276. Mak, K.K., et al., *Wnt/beta-catenin signaling interacts differentially with Ihh signaling in controlling endochondral bone and synovial joint formation.* Development, 2006. **133**(18): p. 3695-707.

277. Pritzker, K.P., et al., *Osteoarthritis cartilage histopathology: grading and staging.* Osteoarthritis Cartilage, 2006. **14**(1): p. 13-29.

278. Aigner, T., et al., *Mechanisms of disease: role of chondrocytes in the pathogenesis of osteoarthritis--structure, chaos and senescence.* Nat Clin Pract Rheumatol, 2007. **3**(7): p. 391-9.

279. Kuhn, K., et al., *Cell death in cartilage.* Osteoarthritis Cartilage, 2004. **12**(1): p. 1-16.

280. Kouri, J.B., et al., *Apoptotic chondrocytes from osteoarthrotic human articular cartilage and abnormal calcification of subchondral bone.* J Rheumatol, 2000. **27**(4): p. 1005-19.

281. Brew, C.J., et al., *Gene expression in human chondrocytes in late osteoarthritis is changed in both fibrillated and intact cartilage without evidence of generalised chondrocyte hypertrophy.* Ann Rheum Dis, 2010. **69**(1): p. 234-40.

282. Reboul, P., et al., *The new collagenase, collagenase-3, is expressed and synthesized by human chondrocytes but not by synoviocytes. A role in osteoarthritis.* J Clin Invest, 1996. **97**(9): p. 2011-9.

283. Tchetina, E.V., G. Squires, and A.R. Poole, *Increased type II collagen degradation and very early focal cartilage degeneration is associated with upregulation of chondrocyte differentiation related genes in early human articular cartilage lesions.* J Rheumatol, 2005. **32**(5): p. 876-86.

284. Majumdar, M.K., et al., *Double-knockout of ADAMTS-4 and ADAMTS-5 in mice results in physiologically normal animals and prevents the progression of osteoarthritis.* Arthritis Rheum, 2007. **56**(11): p. 3670-4.

285. Song, R.H., et al., *Aggrecan degradation in human articular cartilage explants is mediated by both ADAMTS-4 and ADAMTS-5.* Arthritis Rheum, 2007. **56**(2): p. 575-85.

286. Glasson, S.S., et al., *Deletion of active ADAMTS5 prevents cartilage degradation in a murine model of osteoarthritis.* Nature, 2005. **434**(7033): p. 644-648.

287. Little, C.B., et al., *Matrix metalloproteinase 13-deficient mice are resistant to osteoarthritic cartilage erosion but not chondrocyte hypertrophy or osteophyte development.* Arthritis Rheum, 2009. **60**(12): p. 3723-33.

288. Neuhold, L.A., et al., *Postnatal expression in hyaline cartilage of constitutively active human collagenase-3 (MMP-13) induces osteoarthritis in mice.* J Clin Invest, 2001. **107**(1): p. 35-44.

289. van der Kraan, P.M. and W.B. van den Berg, *Chondrocyte hypertrophy and osteoarthritis: role in initiation and progression of cartilage degeneration?* Osteoarthritis and Cartilage, 2012. **20**(3): p. 223-232.

290. Pfander, D., B. Swoboda, and T. Kirsch, *Expression of Early and Late Differentiation Markers (Proliferating Cell Nuclear Antigen, Syndecan-3, Annexin VI, and Alkaline Phosphatase) by Human Osteoarthritic Chondrocytes.* The American Journal of Pathology, 2001. **159**(5): p. 1777-1783.

291. Lin, A.C., et al., *Modulating hedgehog signaling can attenuate the severity of osteoarthritis.* Nat Med, 2009. **15**(12): p. 1421-5.

292. Kamekura, S., et al., *Contribution of runt-related transcription factor 2 to the pathogenesis of osteoarthritis in mice after induction of knee joint instability.* Arthritis & Rheumatism, 2006. **54**(8): p. 2462-2470.

293. von der Mark, K., et al., *Type X collagen synthesis in human osteoarthritic cartilage. Indication of chondrocyte hypertrophy.* Arthritis Rheum, 1992. **35**(7): p. 806-11.

294. Roach, H.I., et al., *Association between the abnormal expression of matrix-degrading enzymes by human osteoarthritic chondrocytes and demethylation of specific CpG sites in the promoter regions.* Arthritis Rheum, 2005. **52**(10): p. 3110-24.

295. Tetlow, L.C., D.J. Adlam, and D.E. Woolley, *Matrix metalloproteinase and proinflammatory cytokine production by chondrocytes of human osteoarthritic cartilage: associations with degenerative changes.* Arthritis Rheum, 2001. **44**(3): p. 585-94.

296. Zhu, M., et al., *Activation of beta-catenin signaling in articular chondrocytes leads to osteoarthritis-like phenotype in adult beta-catenin conditional activation mice.* J Bone Miner Res, 2009. **24**(1): p. 12-21.

297. Lories, R.J., et al., *Articular cartilage and biomechanical properties of the long bones in Frzb-knockout mice.* Arthritis Rheum, 2007. **56**(12): p. 4095-103.

298. Kadri, A., et al., *Inhibition of bone resorption blunts osteoarthritis in mice with high bone remodelling.* Annals of the Rheumatic Diseases, 2010. **69**(8): p. 1533-1538.

299. Dodds, R.A., et al., *Expression of mRNA for IL1 beta, IL6 and TGF beta 1 in developing human bone and cartilage.* J Histochem Cytochem, 1994. **42**(6): p. 733-44.

300. Chowdhury, T.T., et al., *Biomechanical modulation of collagen fragment-induced anabolic and catabolic activities in chondrocyte/agarose constructs.* Arthritis Res Ther, 2010. **12**(3): p. R82.

301. Guo, D., L. Ding, and G.A. Homandberg, *Telopeptides of type II collagen upregulate proteinases and damage cartilage but are less effective than highly active fibronectin fragments.* Inflamm Res, 2009. **58**(3): p. 161-9.

302. Yasuda, T., et al., *Peptides of type II collagen can induce the cleavage of type II collagen and aggrecan in articular cartilage.* Matrix Biology, 2006. **25**(7): p. 419-429.

303. Fichter, M., et al., *Collagen degradation products modulate matrix metalloproteinase expression in cultured articular chondrocytes.* J Orthop Res, 2006. **24**(1): p. 63-70.

304. Huang, C.Y., et al., *Advanced glycation end products cause collagen II reduction by activating Janus kinase/signal transducer and activator of transcription 3 pathway in porcine chondrocytes.* Rheumatology (Oxford), 2011. **50**(8): p. 1379-89.

305. Klatt, A.R., et al., *A critical role for collagen II in cartilage matrix degradation: collagen II induces pro-inflammatory cytokines and MMPs in primary human chondrocytes.* J Orthop Res, 2009. **27**(1): p. 65-70.

306. Klatt, A.R., et al., *Discoidin domain receptor 2 mediates the collagen II-dependent release of interleukin-6 in primary human chondrocytes.* J Pathol, 2009. **218**(2): p. 241-7.

307. Woodell-May, J., et al., *Autologous protein solution inhibits MMP-13 production by IL-1beta and TNFalpha-stimulated human articular chondrocytes.* J Orthop Res, 2011. **29**(9): p. 1320-6.

308. Flannery, C.R., et al., *Effects of culture conditions and exposure to catabolic stimulators (IL-1 and retinoic acid) on the expression of matrix metalloproteinases (MMPs) and disintegrin metalloproteinases (ADAMs) by articular cartilage chondrocytes.* Matrix Biol, 1999. **18**(3): p. 225-37.

309. Cortial, D., et al., *Activation by IL-1 of bovine articular chondrocytes in culture within a 3D collagen-based scaffold. An in vitro model to address the effect of compounds with therapeutic potential in osteoarthritis.* Osteoarthritis Cartilage, 2006. **14**(7): p. 631-40.

310. Yuasa, T., et al., *Wnt/beta-catenin signaling stimulates matrix catabolic genes and activity in articular chondrocytes: its possible role in joint degeneration.* Lab Invest, 2008. **88**(3): p. 264-74.

311. Franses, R.E., et al., *Osteochondral angiogenesis and increased protease inhibitor expression in OA.* Osteoarthritis Cartilage, 2010. **18**(4): p. 563-71.

312. Pufe, T., et al., *The splice variants VEGF121 and VEGF189 of the angiogenic peptide vascular endothelial growth factor are expressed in osteoarthritic cartilage.* Arthritis Rheum, 2001. **44**(5): p. 1082-8.

313. Pfander, D., et al., *Vascular endothelial growth factor in articular cartilage of healthy and osteoarthritic human knee joints.* Ann Rheum Dis, 2001. **60**(11): p. 1070-3.

314. Fenwick, S.A., P.J. Gregg, and P. Rooney, *Osteoarthritic cartilage loses its ability to remain avascular.* Osteoarthritis Cartilage, 1999. **7**(5): p. 441-52.

315. Prasadam, I., et al., *ERK-1/2 and p38 in the regulation of hypertrophic changes of normal articular cartilage chondrocytes induced by osteoarthritic subchondral osteoblasts.* Arthritis Rheum, 2010. **62**(5): p. 1349-60.

316. Sanchez, C., et al., *Osteoblasts from the sclerotic subchondral bone downregulate aggrecan but upregulate metalloproteinases expression by chondrocytes. This effect is mimicked by interleukin-6, -1beta and oncostatin M pre-treated non-sclerotic osteoblasts.* Osteoarthritis Cartilage, 2005. **13**(11): p. 979-87.

317. Sanchez, C., et al., *Subchondral bone osteoblasts induce phenotypic changes in human osteoarthritic chondrocytes.* Osteoarthritis and Cartilage, 2005. **13**(11): p. 988-997.

318. Patil, A.S., R.B. Sable, and R.M. Kothari, *An update on transforming growth factor-beta (TGF-beta): sources, types, functions and clinical applicability for cartilage/bone healing.* J Cell Physiol, 2011. **226**(12): p. 3094-103.

319. Trippel, S., et al., *Gene therapy for articular cartilage repair.* Proc Inst Mech Eng H, 2007. **221**(5): p. 451-9.

320. Indrawattana, N., et al., *Growth factor combination for chondrogenic induction from human mesenchymal stem cell.* Biochem Biophys Res Commun, 2004. **320**(3): p. 914-919.

321. Steinert, A.F., et al., *Enhanced in vitro chondrogenesis of primary mesenchymal stem cells by combined gene transfer.* Tissue Eng Part A, 2009. **15**(5): p. 1127-39.

322. Carter, D.R. and M. Wong, *Modelling cartilage mechanobiology.* Philos Trans R Soc Lond B Biol Sci, 2003. **358**(1437): p. 1461-71.

323. Mueller, M.B. and R.S. Tuan, *Functional characterization of hypertrophy in chondrogenesis of human mesenchymal stem cells.* Arthritis Rheum, 2008. **58**(5): p. 1377-88.

324. Zhou, S., K. Eid, and J. Glowacki, *Cooperation between TGF-beta and Wnt pathways during chondrocyte and adipocyte differentiation of human marrow stromal cells.* J Bone Miner Res, 2004. **19**(3): p. 463-70.

325. Taboas, J.M., *Mechanobiologic regulation of skeletal progenitor cell differentiation*2004. 1 v.

326. Mwale, F., et al., *Limitations of using aggrecan and type X collagen as markers of chondrogenesis in mesenchymal stem cell differentiation.* J Orthop Res, 2006. **24**(8): p. 1791-8.

327. Fischer, J., et al., *Human articular chondrocytes secrete parathyroid hormone-related protein and inhibit hypertrophy of mesenchymal stem cells in coculture during chondrogenesis.* Arthritis Rheum, 2010. **62**(9): p. 2696-706.

328. Perrier, E., et al., *Analysis of collagen expression during chondrogenic induction of human bone marrow mesenchymal stem cells.* Biotechnol Lett, 2011. **33**(10): p. 2091-101.

329. Steinert, A.F., et al., *Indian hedgehog gene transfer is a chondrogenic inducer of human mesenchymal stem cells.* Arthritis Res Ther, 2012. **14**(4): p. R168.

330. Fischer, J., et al., *Human articular chondrocytes secrete parathyroid hormone–related protein and inhibit hypertrophy of mesenchymal stem cells in coculture during chondrogenesis.* Arthritis & Rheumatism, 2010. **62**(9): p. 2696-2706.

331. Rodan, G.A. and M. Noda, *Gene expression in osteoblastic cells.* Crit Rev Eukaryot Gene Expr, 1991. **1**(2): p. 85-98.

332. Sawamura, C., et al., *Effect of in ovo immobilization on development of chick hind-limb articular cartilage: An evaluation using micro-MRI measurement of delayed gadolinium uptake.* Magnetic Resonance in Medicine, 2006. **56**(6): p. 1235-1241.

333. Mikic, B., A.L. Isenstein, and A. Chhabra, *Mechanical modulation of cartilage structure and function during embryogenesis in the chick.* Ann Biomed Eng, 2004. **32**(1): p. 18-25.

334. Fisk, N.M., et al., *Normal amniotic pressure throughout gestation.* Br J Obstet Gynaecol, 1992. **99**(1): p. 18-22.

335. Carter, D.R. and M. Wong, *The role of mechanical loading histories in the development of diarthrodial joints.* J Orthop Res, 1988. **6**(6): p. 804-16.

336. Meyer, E.G., et al., *The effect of cyclic hydrostatic pressure on the functional development of cartilaginous tissues engineered using bone marrow derived mesenchymal stem cells.* J Mech Behav Biomed Mater, 2011. **4**(7): p. 1257-65.

337. Vinardell, T., et al., *Hydrostatic pressure acts to stabilise a chondrogenic phenotype in porcine joint tissue derived stem cells.* Eur Cell Mater, 2012. **23**: p. 121-32; discussion 133-4.

338. Steward, A.J., et al., *Cell-matrix interactions regulate mesenchymal stem cell response to hydrostatic pressure.* Acta Biomater, 2012. **8**(6): p. 2153-9.

339. Angele, P., et al., *Cyclic hydrostatic pressure enhances the chondrogenic phenotype of human mesenchymal progenitor cells differentiated in vitro.* J Orthop Res, 2003. **21**(3): p. 451-7.

340. Miyanishi, K., et al., *Effects of hydrostatic pressure and transforming growth factor-beta 3 on adult human mesenchymal stem cell chondrogenesis in vitro.* Tissue Eng, 2006. **12**(6): p. 1419-28.

341. Miyanishi, K., et al., *Dose- and time-dependent effects of cyclic hydrostatic pressure on transforming growth factor-beta3-induced chondrogenesis by adult human mesenchymal stem cells in vitro.* Tissue Eng, 2006. **12**(8): p. 2253-62.

342. Finger, A.R., et al., *Differential effects on messenger ribonucleic acid expression by bone marrow-derived human mesenchymal stem cells seeded in agarose constructs due to ramped and steady applications of cyclic hydrostatic pressure.* Tissue Eng, 2007. **13**(6): p. 1151-8.

343. Wagner, D.R., et al., *Hydrostatic pressure enhances chondrogenic differentiation of human bone marrow stromal cells in osteochondrogenic medium.* Ann Biomed Eng, 2008. **36**(5): p. 813-20.

344. Sakao, K., et al., *Induction of chondrogenic phenotype in synovium-derived progenitor cells by intermittent hydrostatic pressure.* Osteoarthritis Cartilage, 2008. **16**(7): p. 805-14.

345. Elder, S.H., K.S. Fulzele, and W.R. McCulley, *Cyclic hydrostatic compression stimulates chondroinduction of C3H/10T1/2 cells.* Biomech Model Mechanobiol, 2005. **3**(3): p. 141-6.

346. Whitmarsh, A.J. and R.J. Davis, *Transcription factor AP-1 regulation by mitogen-activated protein kinase signal transduction pathways.* J Mol Med (Berl), 1996. **74**(10): p. 589-607.

347. Rao, A., C. Luo, and P.G. Hogan, *Transcription factors of the NFAT family: regulation and function.* Annu Rev Immunol, 1997. **15**: p. 707-47.

348. Vallabhapurapu, S. and M. Karin, *Regulation and function of NF-kappaB transcription factors in the immune system.* Annu Rev Immunol, 2009. **27**: p. 693-733.

349. Arufe, M.C., et al., *Umbilical cord as a mesenchymal stem cell source for treating joint pathologies.* World J Orthop, 2011. **2**(6): p. 43-50.

350. McQueeney, K., R. Soufer, and C.N. Dealy, *Beta-catenin-dependent Wnt signaling in apical ectodermal ridge induction and FGF8 expression in normal and limbless mutant chick limbs.* Dev Growth Differ, 2002. **44**(4): p. 315-25.

351. Hill, T.P., et al., *Multiple roles of mesenchymal beta-catenin during murine limb patterning.* Development, 2006. **133**(7): p. 1219-29.

352. Sargiacomo, M., et al., *Oligomeric structure of caveolin: implications for caveolae membrane organization.* Proc Natl Acad Sci U S A, 1995. **92**(20): p. 9407-11.

353. de Ruijter, A.J., et al., *Histone deacetylases (HDACs): characterization of the classical HDAC family.* Biochem J, 2003. **370**(Pt 3): p. 737-49.

354. Hollins, A.J., et al., *Caveolin expression during chondrogenesis in the avian limb.* Dev Dyn, 2002. **225**(2): p. 205-11.

355. Yano, F., et al., *The canonical Wnt signaling pathway promotes chondrocyte differentiation in a Sox9-dependent manner.* Biochem Biophys Res Commun, 2005. **333**(4): p. 1300-8.

356. Wang, L., Y.Y. Shao, and R.T. Ballock, *Thyroid hormone interacts with the Wnt/beta-catenin signaling pathway in the terminal differentiation of growth plate chondrocytes.* J Bone Miner Res, 2007. **22**(12): p. 1988-95.

357. Huang, Y., et al., *Inhibition of beta-catenin signaling in chondrocytes induces delayed fracture healing in mice.* J Orthop Res, 2012. **30**(2): p. 304-10.

358. Im, G.I., J.M. Lee, and H.J. Kim, *Wnt inhibitors enhance chondrogenesis of human mesenchymal stem cells in a long-term pellet culture.* Biotechnol Lett, 2011. **33**(5): p. 1061-8.

359. Im, G.I. and Z. Quan, *The effects of Wnt inhibitors on the chondrogenesis of human mesenchymal stem cells.* Tissue Eng Part A, 2010. **16**(7): p. 2405-13.

360. Yang, Z., et al., *Temporal Activation of ss-Catenin Signaling in the Chondrogenic Process of Mesenchymal Stem Cells Affects the Phenotype of the Cartilage Generated.* Stem Cells Dev, 2011.

361. Lepourcelet, M., et al., *Small-molecule antagonists of the oncogenic Tcf/beta-catenin protein complex.* Cancer Cell, 2004. **5**(1): p. 91-102.

362. Huang, S.M., et al., *Tankyrase inhibition stabilizes axin and antagonizes Wnt signalling.* Nature, 2009. **461**(7264): p. 614-20.

363. Ring, D.B., et al., *Selective glycogen synthase kinase 3 inhibitors potentiate insulin activation of glucose transport and utilization in vitro and in vivo.* Diabetes, 2003. **52**(3): p. 588-95.

364. Bennett, C.N., et al., *Regulation of Wnt signaling during adipogenesis.* J Biol Chem, 2002. **277**(34): p. 30998-1004.

365. Finlay, D., et al., *Glycogen synthase kinase-3 regulates IGFBP-1 gene transcription through the thymine-rich insulin response element.* BMC Mol Biol, 2004. **5**: p. 15.

366. Lozito, T.P. and R.S. Tuan, *Mesenchymal stem cells inhibit both endogenous and exogenous MMPs via secreted TIMPs.* J Cell Physiol, 2011. **226**(2): p. 385-96.

367. De Bari, C., et al., *A biomarker-based mathematical model to predict bone-forming potency of human synovial and periosteal mesenchymal stem cells.* Arthritis Rheum, 2008. **58**(1): p. 240-50.

368. Duke, J. and W.A. Elmer, *Cell adhesion and chondrogenesis in brachypod mouse limb mesenchyme: fragment fusion studies.* J Embryol Exp Morphol, 1978. **48**: p. 161-8.

369. Savontaus, M., M. Metsranta, and E. Vuorio, *Retarded skeletal development in transgenic mice with a type II collagen mutation.* Am J Pathol, 1996. **149**(6): p. 2169-82.

370. Coffin-Collins, P.A. and B.K. Hall, *Chondrogenesis of mandibular mesenchyme from the embryonic chick is inhibited by mandibular epithelium and by epidermal growth factor.* Int J Dev Biol, 1989. **33**(2): p. 297-311.

371. Renault, J.Y., J.M. Caillaud, and J. Chevalier, *Ultrastructural characterization of normal and abnormal chondrogenesis in micromass rat embryo limb bud cell cultures.* Toxicol Appl Pharmacol, 1995. **130**(2): p. 177-87.

372. Prabhakar, U., et al., *A novel human bone marrow stroma-derived cell line TF274 is highly osteogenic in vitro and in vivo.* Calcif Tissue Int, 1998. **63**(3): p. 214-20.

373. Alvarez, J., et al., *The perichondrium plays an important role in mediating the effects of TGF-beta1 on endochondral bone formation.* Dev Dyn, 2001. **221**(3): p. 311-21.

374. Corr, M., *Wnt-beta-catenin signaling in the pathogenesis of osteoarthritis.* Nat Clin Pract Rheumatol, 2008. **4**(10): p. 550-6.

375. Wang, M., et al., *Recent progress in understanding molecular mechanisms of cartilage degeneration during osteoarthritis.* Ann N Y Acad Sci, 2011. **1240**: p. 61-9.

376. Duke, P.J. and D. Montufar-Solis, *Exposure to altered gravity affects all stages of endochondral cartilage differentiation.* Adv Space Res, 1999. **24**(6): p. 821-7.

377. Bobick, B.E. and W.M. Kulyk, *Regulation of cartilage formation and maturation by mitogen-activated protein kinase signaling.* Birth Defects Res C Embryo Today, 2008. **84**(2): p. 131-54.

378. Kim, H.J. and G.I. Im, *The effects of ERK1/2 inhibitor on the chondrogenesis of bone marrow- and adipose tissue-derived multipotent mesenchymal stromal cells.* Tissue Eng Part A, 2010. **16**(3): p. 851-60.

379. Tuli, R., et al., *Transforming growth factor-beta-mediated chondrogenesis of human mesenchymal progenitor cells involves N-cadherin and mitogen-activated protein kinase and Wnt signaling cross-talk.* J Biol Chem, 2003. **278**(42): p. 41227-36.
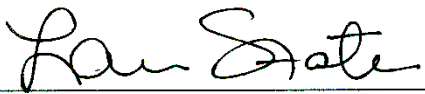
380. Klees, R.F., et al., *Laminin-5 induces osteogenic gene expression in human mesenchymal stem cells through an ERK-dependent pathway.* Mol Biol Cell, 2005. **16**(2): p. 881-90.

381. Pelaez, D., N. Arita, and H.S. Cheung, *Extracellular signal-regulated kinase (ERK) dictates osteogenic and/or chondrogenic lineage commitment of mesenchymal stem cells under dynamic compression.* Biochem Biophys Res Commun, 2012. **417**(4): p. 1286-91.

382. Hens, J.R., et al., *TOPGAL mice show that the canonical Wnt signaling pathway is active during bone development and growth and is activated by mechanical loading in vitro.* J Bone Miner Res, 2005. **20**(7): p. 1103-13.

383. Robinson, J.A., et al., *Wnt/beta-catenin signaling is a normal physiological response to mechanical loading in bone.* J Biol Chem, 2006. **281**(42): p. 31720-8.

384. Armstrong, V.J., et al., *Wnt/beta-catenin signaling is a component of osteoblastic bone cell early responses to load-bearing and requires estrogen receptor alpha.* J Biol Chem, 2007. **282**(28): p. 20715-27.

385. Case, N., et al., *Beta-catenin levels influence rapid mechanical responses in osteoblasts.* J Biol Chem, 2008. **283**(43): p. 29196-205.

386. Arnsdorf, E.J., P. Tummala, and C.R. Jacobs, *Non-canonical Wnt signaling and N-cadherin related beta-catenin signaling play a role in mechanically induced osteogenic cell fate.* PLoS One, 2009. **4**(4): p. e5388.

387. Jansen, J.H., et al., *Stretch-induced inhibition of Wnt/beta-catenin signaling in mineralizing osteoblasts.* J Orthop Res, 2010. **28**(3): p. 390-6.

388. Sen, B., et al., *Mechanical loading regulates NFATc1 and beta-catenin signaling through a GSK3beta control node.* J Biol Chem, 2009. **284**(50): p. 34607-17.

389. Premaraj, S., I. Souza, and T. Premaraj, *Mechanical loading activates beta-catenin signaling in periodontal ligament cells.* Angle Orthod, 2011. **81**(4): p. 592-9.

390. Kawano, Y. and R. Kypta, *Secreted antagonists of the Wnt signalling pathway.* J Cell Sci, 2003. **116**(Pt 13): p. 2627-34.

391. Zhang, M., et al., *Smad3 prevents beta-catenin degradation and facilitates beta-catenin nuclear translocation in chondrocytes.* J Biol Chem, 2010. **285**(12): p. 8703-10.

392. Zimmermann, P., et al., *Correlation of COL10A1 induction during chondrogenesis of mesenchymal stem cells with demethylation of two CpG sites in the COL10A1 promoter.* Arthritis Rheum, 2008. **58**(9): p. 2743-53.

393. Jorgensen, C., et al., *Multipotent mesenchymal stromal cells in articular diseases.* Best Pract Res Clin Rheumatol, 2008. **22**(2): p. 269-84.

394. Villemure, I. and I.A. Stokes, *Growth plate mechanics and mechanobiology. A survey of present understanding.* J Biomech, 2009. **42**(12): p. 1793-803.

395. Brown, T.D. and R.J. Singerman, *Experimental determination of the linear biphasic constitutive coefficients of human fetal proximal femoral chondroepiphysis.* J Biomech, 1986. **19**(8): p. 597-605.

396. Labrador, J.P., et al., *The collagen receptor DDR2 regulates proliferation and its elimination leads to dwarfism.* EMBO Rep, 2001. **2**(5): p. 446-52.

397. Leitinger, B. and A.P. Kwan, *The discoidin domain receptor DDR2 is a receptor for type X collagen.* Matrix Biol, 2006. **25**(6): p. 355-64.

398. Xu, L., et al., *Activation of the discoidin domain receptor 2 induces expression of matrix metalloproteinase 13 associated with osteoarthritis in mice.* J Biol Chem, 2005. **280**(1): p. 548-55.

399. Zhang, Y., et al., *An essential role of discoidin domain receptor 2 (DDR2) in osteoblast differentiation and chondrocyte maturation via modulation of Runx2 activation.* J Bone Miner Res, 2011. **26**(3): p. 604-17.

400. Kevorkian, L., et al., *Expression profiling of metalloproteinases and their inhibitors in cartilage.* Arthritis Rheum, 2004. **50**(1): p. 131-41.

401. Flannelly, J., et al., *Metalloproteinase and tissue inhibitor of metalloproteinase expression in the murine STR/ort model of osteoarthritis.* Osteoarthritis Cartilage, 2002. **10**(9): p. 722-33.

402. Kuo, C.K. and R.S. Tuan, *Mechanoactive tenogenic differentiation of human mesenchymal stem cells.* Tissue Eng Part A, 2008. **14**(10): p. 1615-27.

403. Jenkins, G., *The role of proteases in transforming growth factor-beta activation.* Int J Biochem Cell Biol, 2008. **40**(6-7): p. 1068-78.

404. Bauvois, B., *New facets of matrix metalloproteinases MMP-2 and MMP-9 as cell surface transducers: outside-in signaling and relationship to tumor progression.* Biochim Biophys Acta, 2012. **1825**(1): p. 29-36.

405. Scotti, C., et al., *Recapitulation of endochondral bone formation using human adult mesenchymal stem cells as a paradigm for developmental engineering.* Proc Natl Acad Sci U S A, 2010. **107**(16): p. 7251-6.

406. Jamieson, C., M. Sharma, and B.R. Henderson, *Wnt signaling from membrane to nucleus: beta-catenin caught in a loop.* Int J Biochem Cell Biol, 2012. **44**(6): p. 847-50.

Publishing Agreement

It is the policy of the University to encourage the distribution of all theses, dissertations, and manuscripts. Copies of all UCSF theses, dissertations, and manuscripts will be routed to the library via the Graduate Division. The library will make all theses, dissertations, and manuscripts accessible to the public and will preserve these to the best of their abilities, in perpetuity.

I hereby grant permission to the Graduate Division of the University of California, San Francisco to release copies of my thesis, dissertation, or manuscript to the Campus Library to provide access and preservation, in whole or in part, in perpetuity.

9|5|2012

Author Signature   Date

188